

Communications in Asteroseismology

Volume 152
January, 2008

Proceedings of the
First BRITE Workshop
Vienna, May 22 & 23, 2007

Edited by
Konstanze Zwintz & Alexander Kaiser

Austrian Academy
of Sciences Press



Vienna 2008

OAW

Communications in Asteroseismology

Editor-in-Chief: **Michel Breger**, michel.breger@univie.ac.at

Editorial Assistant: **Daniela Klotz**, klotz@astro.univie.ac.at

Layout & Production Manager: **Paul Beck**, paul.beck@univie.ac.at

Institut für Astronomie der Universität Wien
Türkenschanzstraße 17, A - 1180 Wien, Austria
<http://www.univie.ac.at/tops/CoAst/>
Comm.Astro@univie.ac.at

Editorial Board: Connie Aerts, Gerald Handler,
Don Kurtz, Jaymie Matthews, Ennio Poretti

Cover Illustration

Artist's impression of a BRITE satellite in orbit. The Orion belt in the background symbolizes the richest target field for BRITE-Constellation.

British Library Cataloguing in Publication data.

A Catalogue record for this book is available from the British Library.

All rights reserved
ISBN 978-3-7001-6062-5
ISSN 1021-2043
Copyright © 2008 by
Austrian Academy of Sciences
Vienna

Austrian Academy of Sciences Press
A-1011 Wien, Postfach 471, Postgasse 7/4
Tel. +43-1-515 81/DW 3402-3406, +43-1-512 9050
Fax +43-1-515 81/DW 3400
<http://verlag.oeaw.ac.at>, e-mail: verlag@oeaw.ac.at

Contents

Preface	
by Werner W. Weiss	5
BRITE-Constellation: Astrophysical Concept	
by W. Weiss	6
BRITE-Austria/TUG Sat1: Project Overview	
by O. Koudelka	11
From MOST to BRITE: With a Stopover at CanX-2	
by C. Grant and R. Zee	21
BRITE-Austria/TUG Sat1: System Design and Simulation Results	
by M. Unterberger	26
BRITE-Constellation: Science Operations Concept	
by R. Kuschnig	34
BRITE-Constellation: Simulation of Photometric Performance	
by A. Kaiser, S. Mochnecki and W. W. Weiss	43
BRITE Orbits - Visibility and Feature Plots	
by C. Lhotka and B. Funk	51
BRITE-Constellation: Observation Planning	
by A. Kaiser and R. Kuschnig	55
BRITE-Austria/TUG Sat1: Ground Station Technology	
by O. Koudelka	60
BRITE-Austria/TUG Sat1: Launch Opportunities	
by B. Josseck	65
A MOST open-field data reduction software and its applications to BRITE	
by D. Huber and P. Reegen	77
BRITE-Constellation: Input Catalogue	
by A. Kaiser, K. Zwintz and W. W. Weiss	89
The BRITE satellite and Delta Scuti Stars: The Magnificent Seven	
by M. Breger	97

CP Stars - probing stellar surface structure with BRITE Constellation by T. Lüftinger, W. W. Weiss,	106
Observing γ Doradus Stars with BRITE - an Outlook by M. Gruberbauer, R. Neuteufel and W.W. Weiss	116
β Pictoris: Planets and Pulsations by K. Zwintz	121
Stellar Activity with BRITE: the “Aurigae” field by K. G. Strassmeier	124
Exploring solar-type pulsation with BRITE by T. Kallinger	131
Identifying pulsation modes from two-passband photometry by J. Daszyńska-Daszkiewicz	140
Theoretical Aspects of Massive Stars by E. A. Dorfi and A. Stökl	154
β Cephei and Slowly Pulsating B stars as targets for BRITE-Constellation by G. Handler	160
The search for extrasolar planets with BRITE by R. Dvorak and Á. Bazsó	166
Cluster and Association Members by E. Paunzen	175
BRITE stars on the AGB by T. Lebzelter and J. Hron	178
List of Participants	183

Preface

Werner W. Weiss¹

¹ Institut für Astronomie, Universität Wien, Türkenschanzstrasse 17, 1180 Vienna, Austria

With UniBRITE and BRITE-Austria (TUG-SAT 1) progressing smoothly according to a scheduled launch at the end of 2008 or early 2009, time was right to bring together all involved parties for an intensive exchange of information: instrument developers as well as the potential user community. It was possible to use the facilities of the *Haus der Forschung* thanks to the hospitality of the *Austrian Research Promotion Agency* (Forschungsförderungsgesellschaft, Agentur für Luft- und Raumfahrt), FFG-ALR.

This first BRITE Workshop while intentionally focused on an information exchange within the Austrian community, also greatly benefited from a participation of our canadian colleagues representing the other main community involved in the BRITE-Constellation Project. Presently, UniBRITE and BRITE-Austria are the first fully funded components with the prospect of additional units funded by Canada.

Originally, there was no commitment to produce workshop proceedings given the fact that most of the meeting participants are already under pressure to write manuscripts for other conference publications. In the end these proceedings were compiled to provide reference information for the workshop participants and the BRITE Science and Engineering Teams as a guide to the ongoing instrument development and mission planning activities. To reduce the strain on authors we accepted reasonably well commented Powerpoint presentations (or similar). This new approach is an experiment and we hope that the current proceedings will serve as an appropriate recollection of what was presented and discussed during the two days in May 2007, despite its non-classical format.

A follow-up workshop is planned for the first week of July 2008 with the intention to attract further attention for the BRITE-Constellation mission in the international science community.

Finally, I want to thank all participants, my team and in particular the editors of this volume, Konstanze Zwintz and Alexander Kaiser, for all their efforts and devotion. We all are looking forward to meet you and others again in summer 2008 offering another enjoyable closing dinner at our observatory.

Werner W. Weiss

BRITE-Constellation: Astrophysical Concept

W. Weiss¹

¹ Institut für Astronomie, Türkenschanzstrasse 17, 1180 Vienna, Austria

Abstract

This proceeding paper was generated using a Power-Point presentation from the workshop.

Presentation Slides

Many technical and scientific details of BRITE-Constellation will be discussed during this workshop. Hence, I can limit myself to briefly summarize the arguments leading to the concept of BRITE-Constellation.

4 “elements” of BRITE-Constellation

1. **Science case:** Variability of (massive) bright stars in time scale of hours and more & extensive additional science
2. **Feasibility:** Nano-sat CanX program at UTIAS, miniaturized nanoHPAC stabilisation system (based on MOST experience) - the Canadian connection
3. **Funding in Austria:**
 1. UNIBRITE by U-Vienna (2005), built by UTIAS-SFL
 2. BRITE-Austria (TUG Sat-1) by ASAP3 (2005) and ASAP4 (2006) as first Austrian Satellite, built in and operated from Austria by TU-Graz
 3. Canadian counterpart (tbc) BRITE-Canada 1 & 2
4. **Innovation:** Operating a system of nanosats on a national level: **BRITE-Constellation** proposed by IfA

HPAC: High Precision Attitude Control (system); UTIAS: University of Toronto, Institute for Aerospace Studies; SFL: Space Flight Laboratory; ASAP: Austrian Space & Aeronautic Program.

Why from space?

- High photometric precision for **bright** stars not realistic from ground
- Complementary to **MOST & COROT**
- FOV of $25 \times 25^\circ \rightarrow$ average 4 stars $+3.5^m$
in Milky Way \sim 6-16 stars (1/3 sky with >2 stars)
- Potentially strong public interest
- Amateurs & schools (ground support).

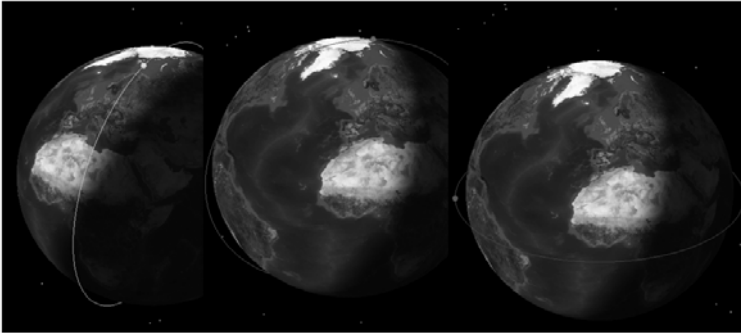
and parallel spectroscopy is realistic !!!

To be kept in mind during this workshop

- **Low budget space project** (Mission requirements)
 - ▶ equivalent of typically 1/10 VLT back-instruments or 1/400 ESA Medium Size Mission
- **Limits in science potential** (importance of optimization)
- **Yet not fully decided**
 - ▶ Launch date
 - ▶ Orbit
 - ▶ 1 or 2 pairs (Canada / Spain / Russia)

The next slide illustrates three extreme LEOs (Low Earth Orbits) with distinct advantages and disadvantages for spacecraft operation and observing programs. From the polar orbits with continuous viewing zones (CVZs) along the celestial equator we show a dusk-dawn orbit (realized for MOST) with the advantage of a rather constant thermal load and stray light situation. This

Dusk-Dawn, Midnight-Noon, Aequatorial

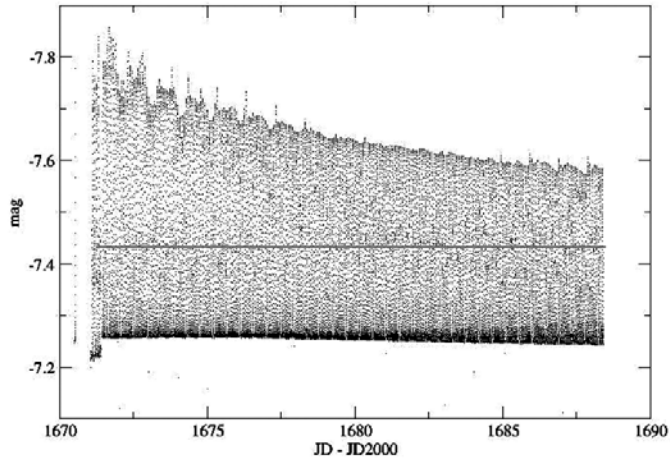


will be certainly not the case for a midnight-noon orbit. However, as can be seen from the next figure, stray light variations for a dusk-dawn orbit still can be strong. Good baffling will therefore be a requirement for BRITE, but sophisticated data reduction can reduce the stray light component significantly (next-but-one figure).

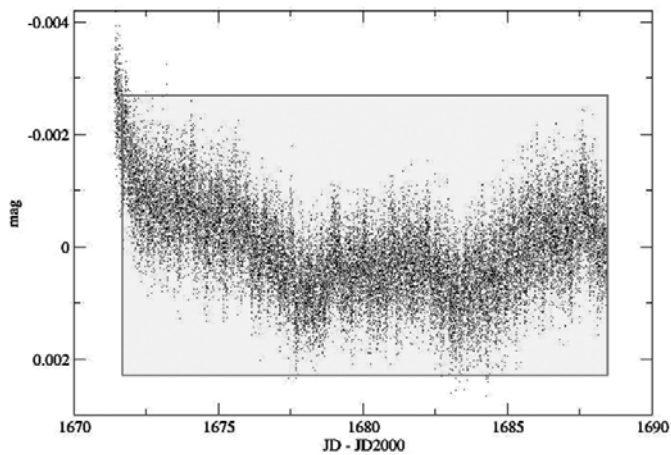
The CoRoT orbit is sun-synchronous and changing during about 3 months from dusk-dawn to midnight-noon.

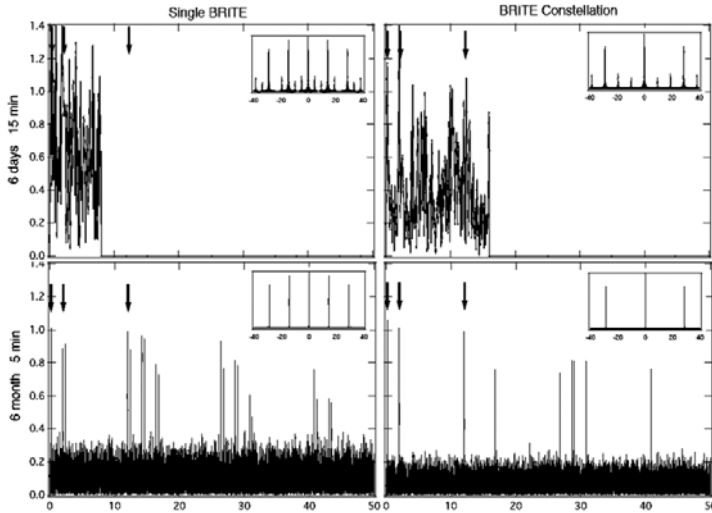
The equatorial orbit provides CVZs at the celestial poles, but for a low orbit the satellite would not be visible from Vienna preventing telecommunication. The MOST orbit is a dusk-dawn orbit.

MOST stray light



MOST stray light corrected





This figure illustrates the advantage of uninterrupted observations (from space). It shows Fourier spectra of simulated data containing white noise with an amplitude of 1 and three sinusoidal signals with same amplitude of 1 (vertical arrows). The inserted figure in the upper right corner indicates the Spectral Window of the simulated data set.

For a single BRITE satellite and one data point per orbit (of typically 90 min orbit period) integrated during 15 minutes one would not be able to detect the input signal due to the high noise level. The highest frequency signal could not be detected as it is beyond the Nyquist frequency.

The noise level in the Fourier domain can be drastically reduced, if the observations can be extended from only 6 days to 6 months (lower left panel). An increased sensitivity by a factor of three allows to reduce the integration time of 15 min to only 5 min, allowing to obtain 3 consecutive data points which push the Nyquist frequency well beyond the highest frequency of the three input signals. However, due to the poor spectral window an unquestionable identification of the 3 input signals will still be difficult. The two right hand side panels repeat the mentioned simulations, but assume that a second satellite will be able to observe the target while it is invisible for the other BRITE. This is the situation we are aiming for with two pairs of BRITE satellites, observing each in the red and blue spectral range. Status as of January 2007.

BRITE-Austria/TUG Sat1: Project Overview

O. Koudelka¹

¹ Institut für Kommunikationsnetze und Satellitenkommunikation, Universität Graz,
Inffeldgasse 12, 8010 Graz, Austria

Abstract

This proceeding paper was generated using a Power-Point presentation from the workshop.

Presentation Slides

PLANNED SATELLITE PROJECTS (1)

- GRAZIJA:
 - Small scientific sub-satellite to be released from MIR Space Station during AUSTROMIR mission 1991
 - nicht realised to due time constraints

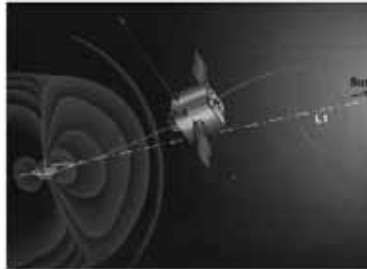


Quelle: ESA

PLANNED SATELLITE PROJECTS (2)

- **ALPSAT:**

- Cooperation Switzerland / Austria
- Very challenging mission, satellite positioned at Lagrange-Point
- Not realised due to budget constraints



PROJECT IDEAS

- Workshops for potential small satellite missions
- Indication by FFG/ALR for support of a small satellite project
- CUBESAT studies by TU Graz
- BRITE proposal by UTIAS and Univ. of Vienna
- Joint proposal by TUG, UV, TUW submitted to FFG/ALR in September 2005

TUG SAT-1 /BRITE AUSTRIA

- Design, Development, Construction, Test, Launch and Operations of the first Austrian Satellite
- Financed within framework of Austrian National Space Program by Austrian Science Promotion Agency (FFG)
- Training of students
 - Hands-on experience in conduct of a challenging space projects
- Synergies between several scientific fields
 - Electrical engineering and telematics
 - Astronomy
 - Mechanical engineering and thermodynamics
 - Satellite geodesy

BRITE AUSTRIA – The Partners

- Ministry of Transport, Innovation and Transport
 - National Space Programm
- Science Promotion Agency FFG/ALR
 - Initiator of the project
 - Operations of the national Space Program
- TU Graz (Prof.O.Koudelka)
 - Project Management TUGSAT-1/BRITE-AUSTRIA
 - System studies, building/testing of TUGSAT-1/BRITE-AUSTRIA
 - Launch, operations of Graz station
- University of Vienna Wien (Prof.W.Weiss)
 - Astronomy, Science Cooperation
- TU Wien (Prof.A.Scholtz)
 - Operations of Vienna Ground Station
- Space Flight Laboratory, University of Toronto
 - Design
 - Delivery of key components

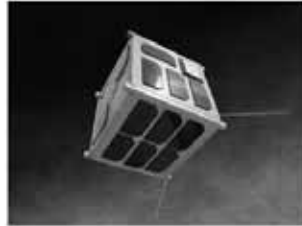


universität
wien



TUG SAT-1 / BRITE AUSTRIA Bright Target Explorer

- Scientific Goal: Investigation of massive luminous stars with precise star camera
- Opens up new dimension for astronomers
- Observation of stars without interference of earth atmosphere
- With small low-cost spacecraft



SCIENTIFIC GOAL

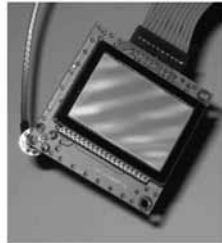
- Measurement of oscillation of luminous stars (magnitude +3.5)
- Recording of time-series (minutes to months)

SATELLITE CONSTELLATION

- Pair of satellites:
 - Different spectral filters (red and blue)
 - Colour information in addition to brightness
 - No moving parts
 - Longer observation times
 - Minimisation of risk
 - Reduction of development costs

INSTRUMENT

- Telescope with CCD sensors
- Simultaneous observation of several stars
- Differential photometry
- Nominal exposure time 15 Minuten (orbit duration 100 minutes)
- Sequences of > 100 days



TUG SAT-1 / BRITE-AUSTRIA

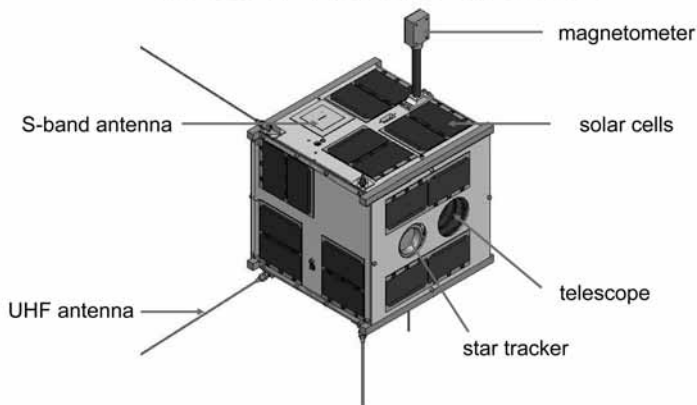
- „Nanosatellite“
- Mass: approx. 6 kg
- Innovation: precise three-axis stabilisation
 - Arcminute level
 - Nano momentum wheels
 - Attitude control computer
 - Coarse and fine sun sensors
 - Magnetometer
 - Magnetorquer



TECHNICAL DATA

- Power supply: 6 W (solar cells)
- Data rate: 32 kbit/s (min.), 256 kbit/s (max.)
- Data volume/ day: typ. 2 MByte
- Frequencies:
 - 2234.4 MHz (S-Band downlink)
 - 437.365 MHz (UHF uplink)
 - 145.89 MHz (VHF beacon)
- Transmit power:
 - 0.5 W (for S-band downlink)
 - 0.1 W (for VHF beacon)

TUGSAT-1 /BRITE-AUSTRIA



ORBIT

- Sun-synchronous or polar orbit
- Approx. 800 km

COSTS / TIME PLAN

- Development and testing: 2 years
- Costs for development: 450 k€ (FFG/ALR) + 50 k€ for ground station Graz (TUG)
- First part of Phase 2: 250 k€
 - Launch opportunities
 - Software development (ground support and science software)
- Mission duration: min. 2 years

STATUS

- PDR in October 2007
- CDR before summer 2007
- Building starts in summer
- Completion of spacecraft by Q3/2008
- Launch planned for end 2008 / begin 2009

SUMMARY

- Challenging scientific and technological mission
- Sustainability: development of a cost-efficient satellite platform for future missions
- Added value for education:
 - Training for students
 - Young engineers and scientists
- Raising interest of the public for space research and technology

INFORMATION

www.iks.tugraz.at www.tugsat.at

Kontakt: tugsat1@iks.tugraz.at



O. Koudelka and W. W. Weiss inaugurating the workshop dinner at the Institute of Astronomy.

Engineering

From MOST to BRITE: With a Stopover at CanX-2

C. Grant¹, R. Zee¹

¹ Space Flight Laboratory, University of Toronto, Institute for Aerospace Studies,
4925 Dufferin Street, Toronto, Ontario, Canada, M3H 5T6

Abstract

This proceeding paper was generated using a Power-Point presentation from the workshop.

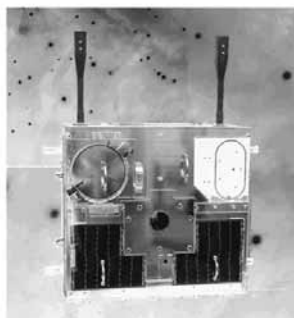
Presentation Slides

Who Are We?

- Unique university lab in Canada focusing on **microspace** systems.
- “Microspace” = disciplined small team approach to using commercial technologies in space.
- Developed key subsystems for the **MOST** microsatellite and supported integration, test and operations.
- Canadian Advanced Nanospace eXperiment (**CanX**) nanosatellite program provides low cost access to space.



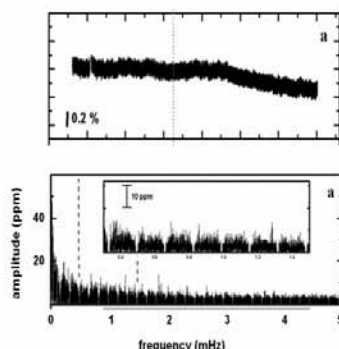
MOST



- Microvariability & Oscillations of STars
- Mission goals: Use photometry to characterize stellar behavior, determine age of universe, discover planets
- Canada's First Space Telescope, first microsat for CSA, first Canadian-built satellite in 35 years, and the world's first precision-pointed microsat
- Launched June 30, 2003 and currently operating in space and exceeding performance expectations

MOST Impressive

- Setting the new standard for microsatellites by far exceeding its required performance
- Currently completing its 4th year in operation
- Achieving performance some believed impossible for such a small spacecraft
- Numerous scientific discoveries that added to, refined and even rewrote existing theories



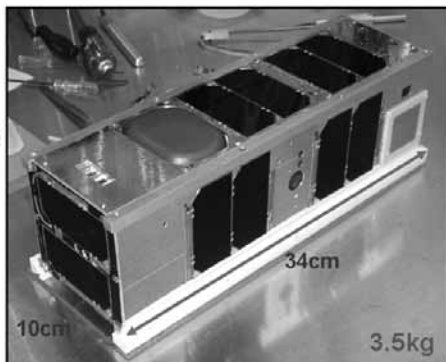
CanX Program



- Canadian Advanced Nanospace eXperiment
- Established at SFL in 2001 to:
 - Provide inexpensive and rapid access to space
 - Train students to build real satellites
 - Exploit staff knowledge and lab resources gained through MOST
- CanX-1 launched in 2003
- CanX-2 to be launched this year

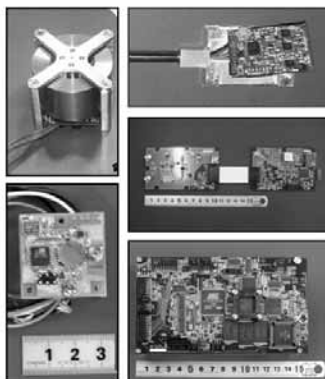
CanX-2

- First CanX nanosatellite to follow the development approach used for MOST
- CanX-2 will be:
 - Launched from India on a PSLV in September
 - Three-axis stabilized
 - Carry three science payloads (one optical)
 - Carry numerous technologies demos



CanX-2

- CanX-2 will qualify technologies needed for upcoming missions including BRITE
- Key technologies include:
 - Reaction wheel
 - Sun sensors
 - Magnetometer
 - UHF receiver
 - S-band transmitter
 - On-board computer
- CanX-2 reduces risk on the BRITE mission



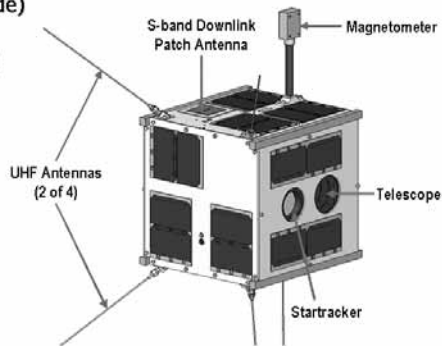
BRITE



- Mission is similar to MOST but also complementary
- Focus is on the most luminous and massive stars
- Observe fields for 15 minutes each orbit for up to 100 days
- Uses a nanosat bus ($\approx 6\text{kg}$) instead of a microsat bus
- Reuse technologies tested and proven on CanX-2
- Use knowledge and lessons learned from MOST (science & engineering)

BRITE

- Cubic form factor (20cm/side) with mass < 7kg
- Pre-deployed antennas and booms
- Telescope (Blue and Red):
 - 11 Megapixel CCD
 - Aperture = 3cm
 - FOV = 24°
- Three-axis attitude control (≈ 1.5 arcminute stability)



Conclusion

- MOST was a groundbreaking mission for microsatellites
- BRITE has the potential to be just as revolutionary for nanosatellites



BRITE-Austria/TUG Sat1: System Design and Simulation Results

M. Unterberger¹

¹ Institut für Kommunikationsnetze und Satellitenkommunikation, Universität Graz,
Inffeldgasse 12, 8010 Graz, Austria

Abstract

This proceeding paper was generated using a Power-Point presentation from the workshop.

Presentation Slides

PLANNED SATELLITE PROJECTS (1)

- GRAZIJA:
 - Small scientific sub-satellite to be released from MIR Space Station during AUSTROMIR mission 1991
 - nicht realised to due time constraints

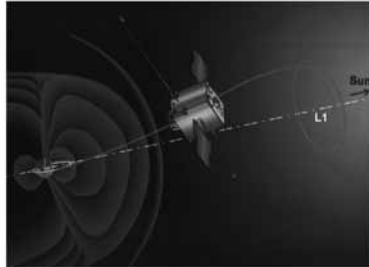


Quelle: ESA

PLANNED SATELLITE PROJECTS (2)

- ALPSAT:

- Cooperation Switzerland / Austria
- Very challenging mission, satellite positioned at Lagrange-Point
- Not realised due to budget constraints



PROJECT IDEAS

- Workshops for potential small satellite missions
- Indication by FFG/ALR for support of a small satellite project
- CUBESAT studies by TU Graz
- BRITE proposal by UTIAS and Univ. of Vienna
- Joint proposal by TUG, UV, TUW submitted to FFG/ALR in September 2005

TUG SAT-1 /BRITE AUSTRIA

- Design, Development, Construction, Test, Launch and Operations of the first Austrian Satellite
- Financed within framework of Austrian National Space Program by Austrian Science Promotion Agency (FFG)
- Training of students
 - Hands-on experience in conduct of a challenging space projects
- Synergies between several scientific fields
 - Electrical engineering and telematics
 - Astronomy
 - Mechanical engineering and thermodynamics
 - Satellite geodesy

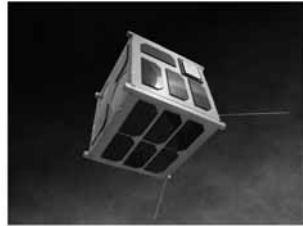
BRITE AUSTRIA – The Partners

- Ministry of Transport, Innovation and Transport
 - National Space Programm
- Science Promotion Agency FFG/ALR
 - Initiator of the project
 - Operations of the national Space Program
- TU Graz (Prof.O.Koudelka)
 - Project Management TUGSAT-1/BRITE-AUSTRIA
 - System studies, building/testing of TUGSAT-1/BRITE-AUSTRIA
 - Launch, operations of Graz station
- University of Vienna Wien (Prof.W.Weiss)
 - Astronomy, Science Cooperation
- TU Wien (Prof.A.Scholtz)
 - Operations of Vienna Ground Station
- Space Flight Labortory, University of Toronto
 - Design
 - Delivery of key components



TUG SAT-1 / BRITE AUSTRIA Bright Target Explorer

- Scientific Goal: Investigation of massive luminous stars with precise star camera
- Opens up new dimension for astronomers
- Observation of stars without interference of earth atmosphere
- With small low-cost spacecraft

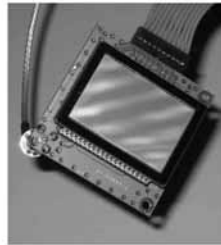


SCIENTIFIC GOAL

- Measurement of oscillation of luminous stars (magnitude +3.5)
- Recording of time-series (minutes to months)

INSTRUMENT

- Telescope with CCD sensors
- Simultaneous observation of several stars
- Differential photometry
- Nominal exposure time 15 Minuten (orbit duration 100 minutes)
- Sequences of > 100 days



SATELLITE CONSTELLATION

- **Pair of satellites:**
 - Different spectral filters (red and blue)
 - Colour information in addition to brightness
 - No moving parts
 - Longer observation times
 - Minimisation of risk
 - Reduction of development costs

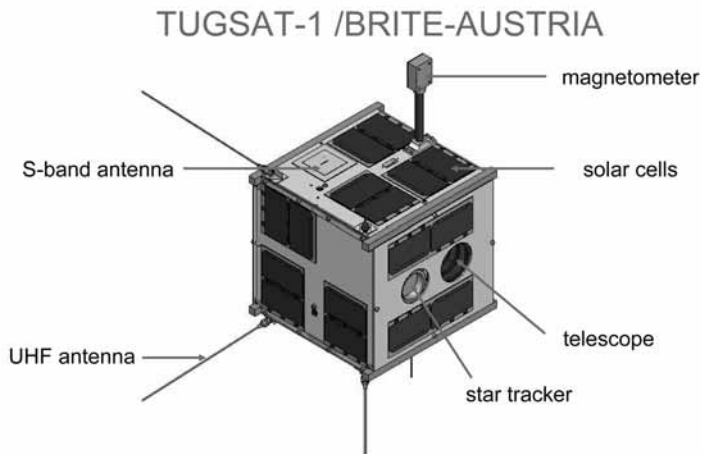
TUG SAT-1 / BRITE-AUSTRIA

- „Nanosatellite“
- Mass: approx. 6 kg
- Innovation: precise three-axis stabilisation
 - Arcminute level
 - Nano momentum wheels
 - Attitude control computer
 - Coarse and fine sun sensors
 - Magnetometer
 - Magnetorquer



TECHNICAL DATA

- Power supply: 6 W (solar cells)
- Data rate: 32 kbit/s (min.), 256 kbit/s (max.)
- Data volume/ day: typ. 2 MByte
- Frequencies:
 - 2234.4 MHz (S-Band downlink)
 - 437.365 MHz (UHF uplink)
 - 145.89 MHz (VHF beacon)
- Transmit power:
 - 0.5 W (for S-band downlink)
 - 0.1 W (for VHF beacon)



ORBIT

- Sun-synchronous or polar orbit
- Approx. 800 km

COSTS / TIME PLAN

- Development and testing: 2 years
- Costs for development: 450 k€ (FFG/ALR) + 50 k€ for ground station Graz (TUG)
- First part of Phase 2: 250 k€
 - Launch opportunities
 - Software development (ground support and science software)
- Mission duration: min. 2 years

STATUS

- PDR in October 2007
- CDR before summer 2007
- Building starts in summer
- Completion of spacecraft by Q3/2008
- Launch planned for end 2008 / begin 2009

SUMMARY

- Challenging scientific and technological mission
- Sustainability: development of a cost-efficient satellite platform for future missions
- Added value for education:
 - Training for students
 - Young engineers and scientists
- Raising interest of the public for space research and technology

INFORMATION

www.iks.tugraz.at

www.tugsat.at

Kontakt: tugsat1@iks.tugraz.at

BRITE-Constellation: Science Operations Concept

R. Kuschnig^{1,2}

¹ Univ. of British Columbia, 6224 Agricultural Road, Vancouver V6T 1Z1, Canada

² Institut für Astronomie, Türkenschanzstrasse 17, A-1180 Wien, Austria

Abstract

The BRITE-Constellation currently consists of two nano-satellites: BRITE-AUSTRIA and Uni-BRITE. Both are in principle of identical build with one exception, the respective telescopes will be designed for two different band-passes one constrained to RED (555-690nm) and the other to BLUE (400-450nm) wavelengths. In general both satellites will collect data from the same stars during any particular observing run. A proposal to build and launch an additional pair of spacecrafts to complement the constellation is currently under review. This article describes the organization structure, the main operations tasks and the software tools to conduct the mission.

BRITE-Constellation Management

The BRITE-Constellation mission will be governed by essentially three main entities working in concert. The Science Consortium is the deciding body for the instalment of observing plans by proposals from local Science Teams. Mission Control is responsible for evaluating the Observing Plan, detailed scheduling, instruments setups, daily data quality assessment, data reformatting, first-look science analysis, internal data release and data archiving. Satellite Control will aid the verification process of the observing plan, operate the satellites, control the ground stations, asses the health of the spacecrafts and their subsystems. Figure 1 depicts the organizational chart.

In baseline configuration the BRITE-Constellation will operate two satellites: BRITE-AUSTRIA and Uni-BRITE. Both shall, simultaneously, be in low earth orbit (in the same or different orbits is yet to be decided) for the main mission phase. It is possible that two more satellites will join the mission funded in Canada. In such a scenario it is planned that the BRITE-Constellation management will still rely on a single Science Consortium with full program authority but will have likely establish two collaborating Mission Control and Satellite Control teams located in the respective countries.

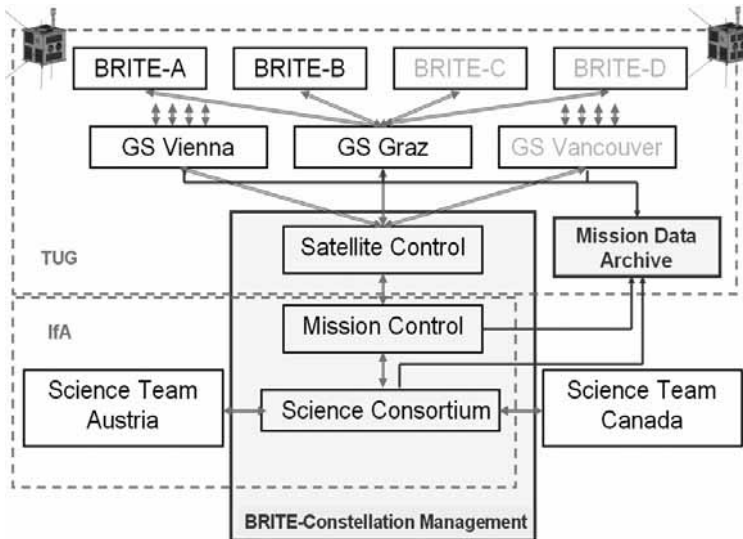


Figure 1: BRITE-Constellation Management Scheme.

BRITE Operations Overview

The primary input for the BRITE-Constellation operations will be an actual observing plan, to be released in bi-annual intervals by the Science Consortium. It will contain lists of primary targets with start and end observing dates. This plan will be subject to verification and optimization by Mission Control and Satellite Control personnel prior to enactment. For each observing run the field orientation and camera setup parameters will be defined and submitted to the Satellite Control team for subsequent transmission to satellites contributing to a specific observing run. Science data will be gathered during the specified observing period. During each ground station contact a satellite health diagnostic shall be performed and recorded. After data transmission the downloaded raw science data files (a.k.a. whole orbit data files or WOD) will be uncompressed and dissected into individual science records. Their contents will be displayed graphically as time series plots with automated checks for data quality and integrity. Then all valid data records from a finished observing run will be transformed into astronomy standard FITS files. Finally, data products like: setup parameters, the originally transmitted files, individual Science Data Records, satellite telemetry files, all log files, diagnostic information and finally the FITS files are moved to the Mission Data Archive.

BRITE On-board Science Data Generation

Prior to the description of ground software packages the core BRITE science data contents, generated on-board the satellites, are described.

Image Data Generation

The BRITE telescopes (3cm aperture, 5 lens plus filter, system) will each feed a KODAK KA11002 interline transfer progressive scan CCD. The light sensitive area is a 4008x2672 pixels array and with its plate scale of about 30 arcsec/pixel a wide field ($\sim 33 \times 22$ deg) is covered in a full frame. Given a baseline time sampling of 1/min for a typical set of 7-15 target stars per field and the downlink bandwidth limits a sub-raster scheme with stacking of individual exposures are required to operate the camera. Figure 2 presents an example of how bright Orion stars could be exposed in the focal plane with 7 sub-rasters, each typically 32x32 pixels large (the FWHM of the image PSF is ~ 6 pixels) covering the primary objects of interest.

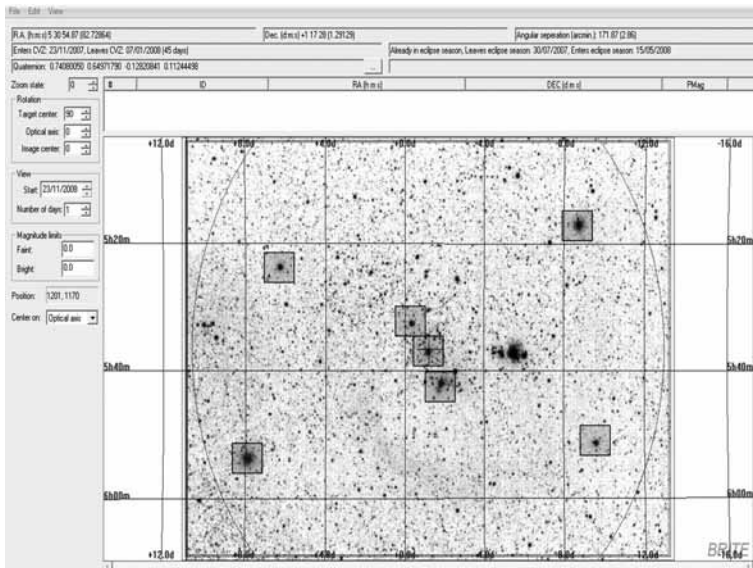


Figure 2: Virtual display of the BRITE FOV/CCD, placed to render the Orion field.

With exposures times of typically 1sec and even shorter depending on the brightness of the primary target star, image data from consecutive exposure will be co-added 'stacked' on-board. This scheme is illustrated in figure 2.

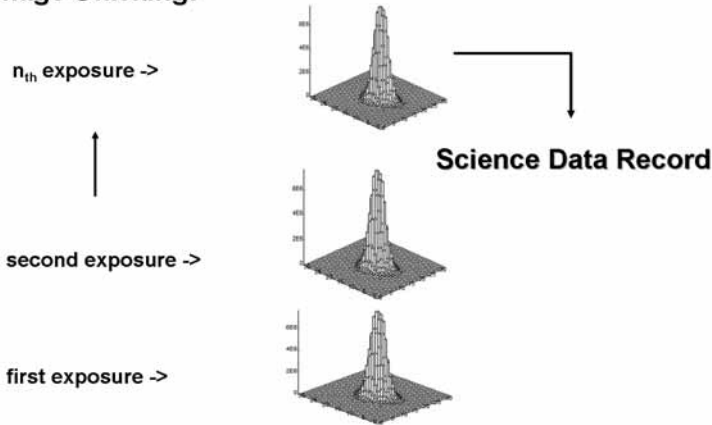
Image Stacking:

Figure 3: An illustration of on-board image stacking.

On-board Data Processing

The main target stars of the BRITE mission will be between 0 and 4 mag and in general for all those objects in any given field, image data will be obtained. However performance simulations reveal that even fainter objects down to 6 mag could provide useful signal levels respectively scientifically relevant photometry. Considering that the number of sub-rasters (the total amount of pixel resolved image data) is limited, photometric values from those stars have to be obtained by means of on-board data processing. This will reduce the bulky image data manageable amounts of background and star signal values. The details of on-board data treatment collected from fainter stars are still under investigation but are all based on customized aperture photometry schemes.

Complete Data Record

Beyond gathering image data and processed photometry a Science Data Record (SDR) will also contain auxiliary information acquired from the instrument and the other satellite sub-systems. Among those are: timing information, pointing errors, various temperatures, heater voltages and local magnetic field strength, all sampled with a typically a 1Hz rate. The Science Data Generation Code (SDGC) executed by the instrument on-board computer (a DSP type micro-processor) will handle those tasks and produce the SDRs. Individual SDRs will

be compressed and bundled into larger files for on-board storage and subsequent ground transmission. Figure 4 shows the schematic processing and information collection by the SDGC.

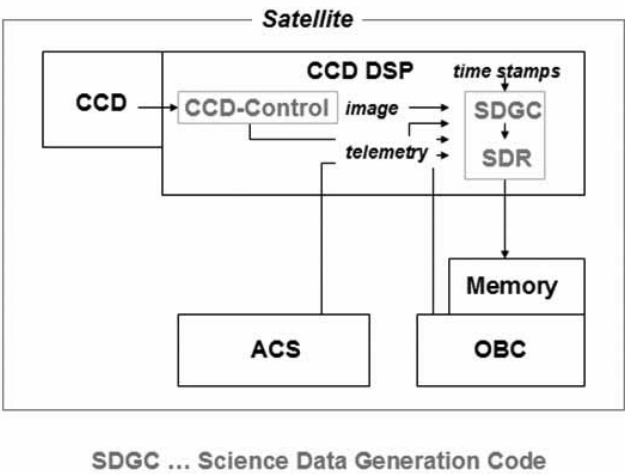


Figure 4: On-board Science Data Generation Scheme.

BRITE Ground Software Modules

In figure 5 the main software modules are schematically placed in relation to the operations teams, Mission Control and Satellite Control as well as the Science Consortium. On the left side (arrow up) utilities are listed that will help to: prepare the observing plan, setup the camera, control the spacecraft subsystems, operate the ground stations and regulate data transmission. On the right are programs that will diagnose the satellites health, separate individual data records from raw download files, check and display science data and related telemetry, reformat data and perform first cut science data analysis.

In the following part individual programs and software packages are described in abstract form. The reader shall be aware that currently working titles are used and that final names and definitions will emerge out of the ongoing design and specification phase.

BRITE-MAP: This is the main tool to investigate the observing constraints of star fields in a global perspective. This program has a rich graphics user interface as well as analytical routines to support the Science Teams and the

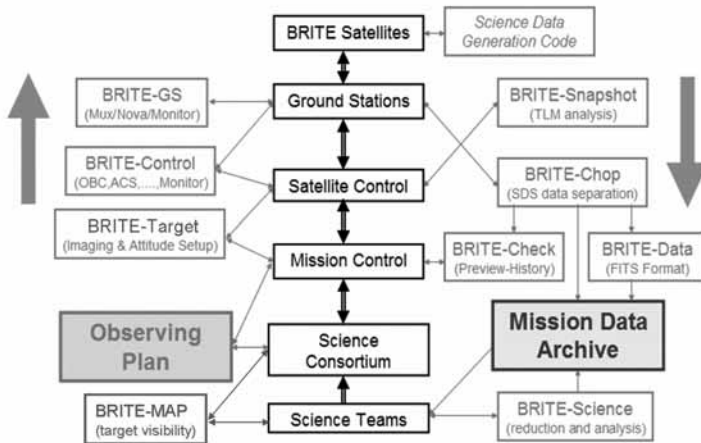


Figure 5: BRITE-Constellation software modules overview in context with operation teams

Science Consortium to contemplate observing scenarios and finally to assemble observing plans. Applications examples are found in this volume ('Observing Strategies' Kaiser, A.).

BRITE-Target: Displays selected target fields as a virtual projection on the instrument FOV/CCD (see Figure 2). It allows the precise placement a reference star onto any pixel on the detector and the selection of an instrument bore sight roll angle. This program enables the definition of sub-rasters covering target stars, sky areas as well as dark and bias regions. To each sub-raster a processing code can be assigned which specifies what kind of on-board procedures shall be applied. The output is a unique set of setup and processing parameters.

BRITE-Control: This is group of programs will allow Satellite Control teams to instruct and operate all spacecraft subsystems most notably the Camera Control System to conduct science data collection and the Attitude Control System responsible for pointing the instrument precise and stable in a specified direction.

BRITE-GS: Software modules to operate a ground station like satellite tracking, pass scheduling, rotor/antennae control, data transfer and emergency shut-down.

BRITE-Snapshot: A routine that automatically investigates the most vital spacecraft telemetry information during contact times (ground station passes). It will send instantaneous feedback (via e-mail) information to Satellite Control and Mission Control team members. Alarm conditions can be specified and

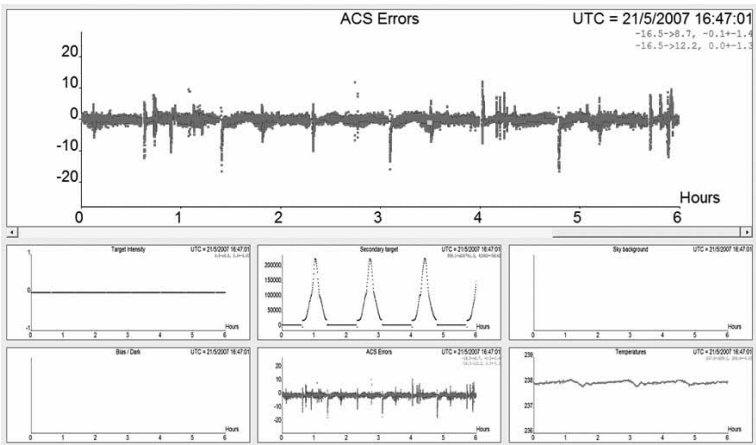


Figure 6: Time series display of science data records and spacecraft telemetry. Top panel: pointing errors.

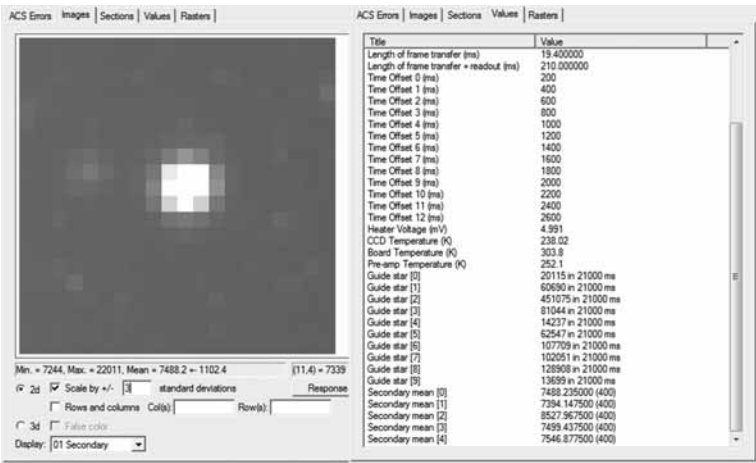


Figure 7: Preview display of a particular Science Data Record. Left: sub-raster image. Right: time offsets and processed photometry values

violations are listed at the top of the reports.

BRITE-Chop: Is a program that dissects 'chops' whole orbit data files that are originally transmitted to ground into individual science records/files which are subsequently sent to data repositories of the instrument monitoring system (BRITE-Check) and also forwarded to the Mission Data Archive.

BRITE-Check: This software package displays the contents of selected sets of Science Data Records as time series (history) and provides access to individual records (preview). This enables Mission Control to get a comprehensive and quick look at the instrument performance. Figure 6 and 7 are screenshots from development versions of history and preview displays.

BRITE-Data: A program to transform Science Data Records into FITS files. BRITE FITS files will contain not only information generated on-board the satellites. This software also calculates auxiliary values such as positions of the instrument with respect to Sun, Earth and Moon, ground corrected times and more. Essentially everything possibly needed to reduce and analyze the obtained photometry. FITS files will be the sole source for the BRITE Science Analysis.

BRITE-Science: This program package will comprise all optimized science data reduction and time series analysis routines. The core shall be a properly developed and tested data reduction pipeline. Ideally this software suite will be distributed among all science teams as an application to derive scientific results.

BRITE Mission Data Archive

All collected data and information will be sent to and organized within the Mission Data Archive.

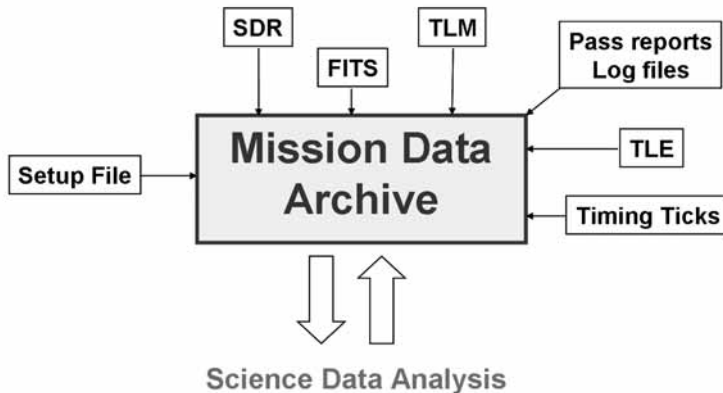


Figure 8: Mission Data Archive input: setup information, SDR Science Data Record, FITS files, TLM Telemetry files, Pass reports and log files, TLE Two Line Elements, Timing Ticks, Science analysis results.

Figure 8 lists the main input data products to the archive. Observing plans, setup information, science data files, telemetry data from all satellites, operations logs from all ground stations including pass reports, time reference data, FITS files, reduced photometry data and finally analysis results will be included. While many data products are just stored the FITS files will be made available for mission internal use as soon as possible. Furthermore, it is planned to sequentially open the Mission Data Archive to the wider science community after the elapse of a proprietary period (length yet to be decided).

Acknowledgments. Financial support was received from the Austrian Research Promotion Agency (FFG)



A. Kaiser, M. Unterberger, K. Zwintz and R. Kuschnig in front of the BRITE nanosatellite model.

BRITE-Constellation: Simulation of Photometric Performance

A. Kaiser¹, S. Mochnacki², W.W. Weiss¹

¹ Institut für Astronomie, Türkenschanzstrasse 17, 1180 Vienna, Austria

² University of Toronto, 50 St. George Street, Toronto M5S 3H4, Canada

Abstract

BRITE (BRiGht Target Explorer) is a satellite mission dedicated to survey the sky, measuring the brightness and temperature variations of the brightest stars. In order to evaluate the expected performance of the science payload, a detailed simulation of the camera and the optical system has been performed. The results confirm that the SNR specified in the mission requirements can be achieved.

Science Instrument

The science payload of the satellite (Figure 1) consists of a five-lens telescope with an aperture of 30 mm and the interline CCD detector KAI 11002-M (Table 1) from Kodak with 11 megapixels, in combination with a baffle to reduce stray light. The photometer has a resolution of 26.52 arcseconds per pixel and a field-of-view of 24 degrees. The mechanical designs of the blue and the red instrument are nearly identical; only the dimensions of the lenses are slightly different (Figure 2).

Filters

The red edge of the effective wavelength range of the instrument is determined by the sensitivity of the detector and the blue edge by the transmission properties of the lens material. The filter design aims to generate the same number of electrons on the detector for a star of 10 000 K (average temperature for all BRITE target stars) for both systems. The blue and the red filters cover wavelength ranges of 390–460 nm and 550–700 nm respectively, both are assumed to have a maximum transmission of 95% (Figure 3).

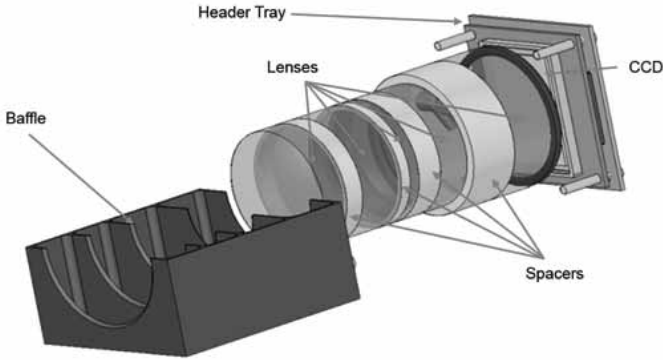


Figure 1: BRITE science instrument layout (optical cell and part of baffle removed for clarity).

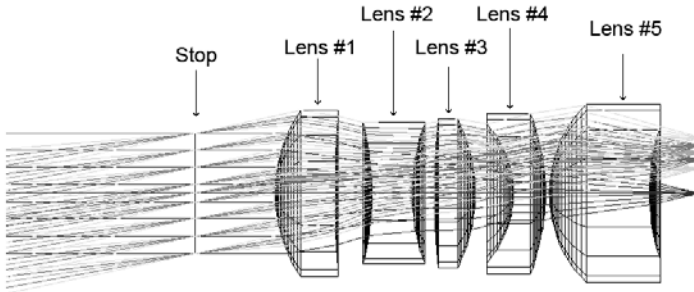


Figure 2: Optical design with external aperture stop configuration for the blue system.

Synthetic Fluxes

For the simulation of stellar fluxes, different model atmosphere codes were employed in order to compute a grid of fluxes for temperatures from 4000 K to 40000 K and for $\log g$ (cgs) from ≈ 1 to 5: MARCS (www.astro.uu.se/marcs) for cool stars, NEMO for intermediate-temperature stars and LLM for hot stars (ams.astro.univie.ac.at/nemo).

Figure 4 displays the flux distribution for a star with 10000 K, $\log g = 4$ and an apparent visual magnitude of 4^m . The thick solid line indicates the stellar flux scaled to the aperture size of the telescope; the dashed line shows the quantum efficiency (QE) of the CCD detector. The solid lines represent the

Kodak KAI 11002-M CCD	
Imager size	37.25×25.70 mm
Number of pixels	4008×2672 (effective)
Pixel size	$9 \times 9 \mu\text{m}$
Peak quantum efficiency	50%
Saturation signal	60000 e^-
Dark current	$4 \text{ e}^-/\text{s}/\text{pixel}$
Read out noise	$13 \text{ e}^-/\text{pixel}$
Power consumption	1 W

Table 1: CCD detector specifications.

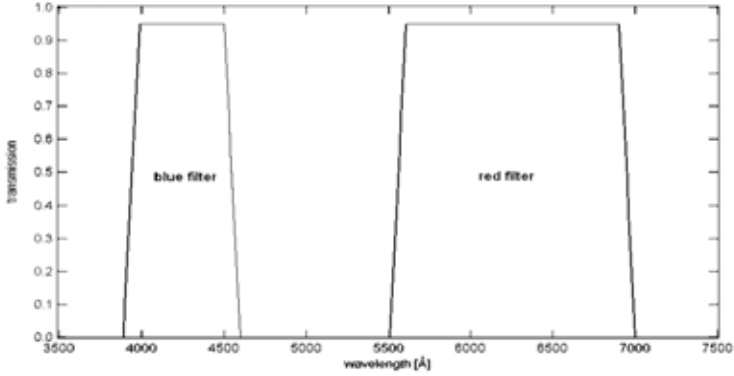


Figure 3: Transmission properties of the red and blue BRITE filters.

flux after folding with the transmission properties of the lenses, the QE and the filter functions.

Optical System Properties

The optical system of the science instrument was designed by Ceravolo Optics (www.ceravolo.com). To calculate the distribution of the stellar point-spread-function (PSF) on the detector plane, a grid of computed spot diagrams for different wavelengths and angles of incidence was used (Figure 5). Figure 6 shows a 32×32 pixel subframe with the PSF for the blue and the red system referring to a star with the flux distribution shown in Figure 4 and an angle of incidence of 7° . The total number of electrons is equal in both filters.

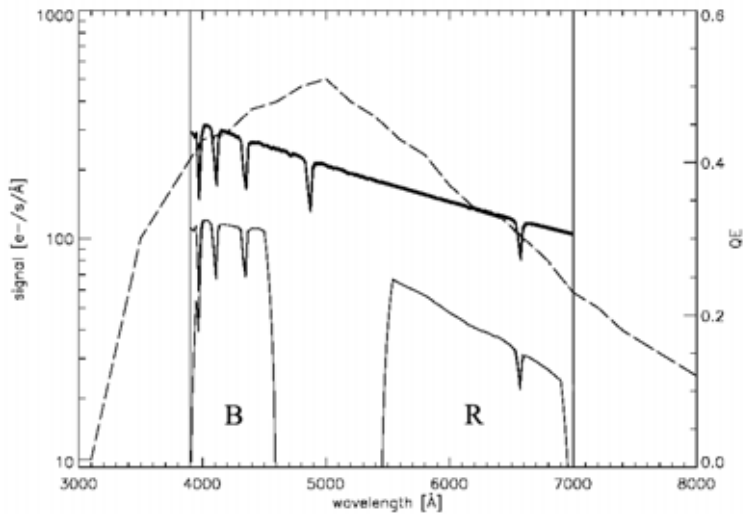


Figure 4: Flux distribution for a star with 10 000 K, $\log g = 4$ and a visual apparent magnitude of 4^m . The dashed line shows the QE of the detector.

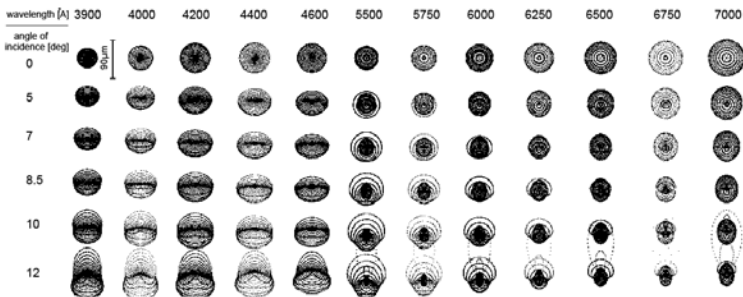


Figure 5: Spot diagram matrix for the blue and red filter system.

Synthetic Photometry

In order to perform a simulation of a time series, one has to account for errors in the pointing accuracy of the attitude control system (ACS) of the spacecraft. The mission requirement for the pointing error is 2–3 pixel rms with the goal of 1 pixel. Figure 7 shows a time-resolved simulation for the pitch and yaw error sampled in one-second steps for a 15-minute subset employing two different reaction wheel models developed by the University of Toronto, Space Flight

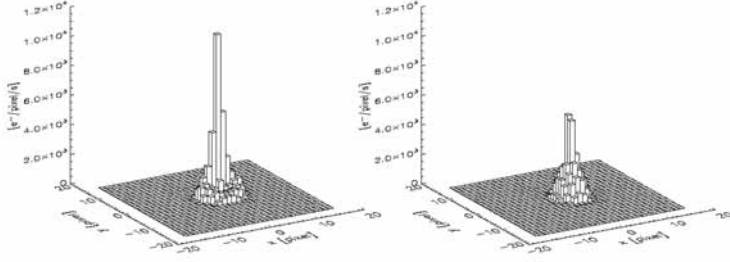


Figure 6: PSF of the blue (left panel) and the red (right panel) filter system for a star with 10 000 K, $\log g = 4$ and a visual apparent magnitude of 4^m , without jitter and a 7° angle of incidence for the optical system.

Labs (UTIAS/SFL). The resulting pointing accuracy is one and two pixels, respectively.

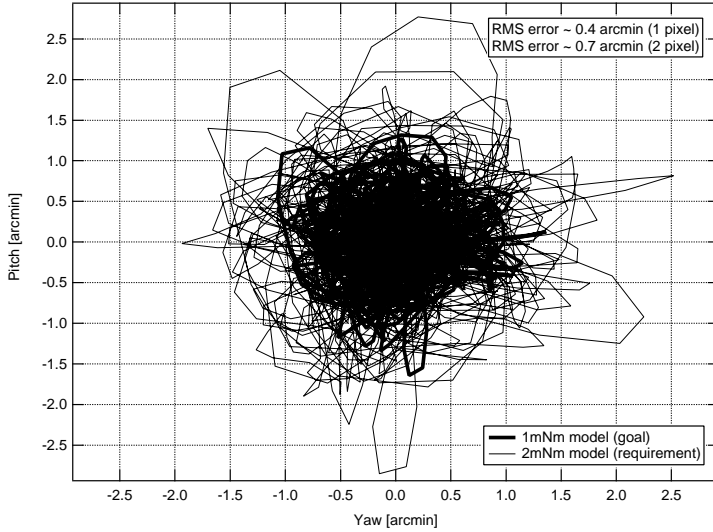


Figure 7: Pitch and yaw pointing errors (satellite jitter) simulated for 15 minutes in one second steps.

To avoid saturation of the CCD, the maximum exposure time for a star is limited by the intensity of the brightest pixel of the PSF. Figure 8 shows

the maximum exposure times for the blue and the red filter system for a grid of stars with a 7° angle of incidence for the optical system. The black dots correspond to the main BRITE-Constellation targets with $V < 4^m$. It shows that a majority of the stars saturates at exposure times larger than one second.

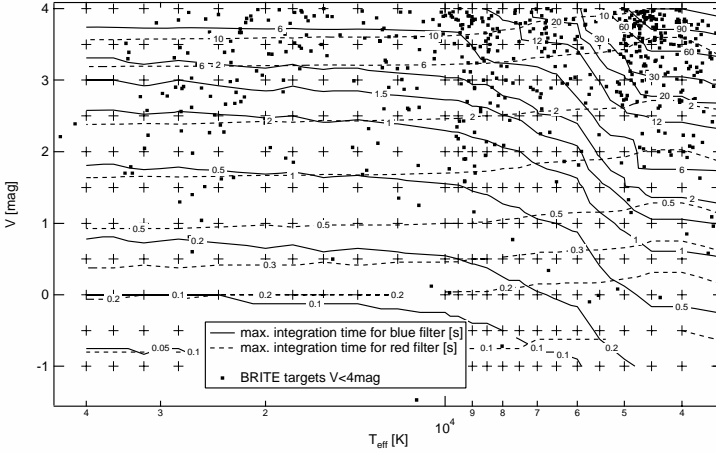


Figure 8: Maximum exposure times in seconds for the brightest pixel in the PSF for a grid of stars (black crosses) for the blue and the red filter with a 7° angle of incidence for the optical system. The dots correspond to the stars from the BRITE-Constellation input catalog.

The simulation of the expected SNR assumes a dark current of $4 e^-/\text{pixel}/s$, a readout noise of $13 e^-/\text{pixel}$ and a sky background of $18 \text{ mag}/\text{arcsec}^2$ corresponding to $141 e^-/\text{pixel}/s$ for the red system and $99 e^-/\text{pixel}/s$ for the blue system. For each grid point, the maximum possible exposure time (5/6 of the saturation level) was used, and a readout gap of one second between consecutive exposures was assumed. Figures 9 and 10 show the resulting SNR for different spectral types. The thin black line is a histogram of the stars from the BRITE-Constellation input catalog.

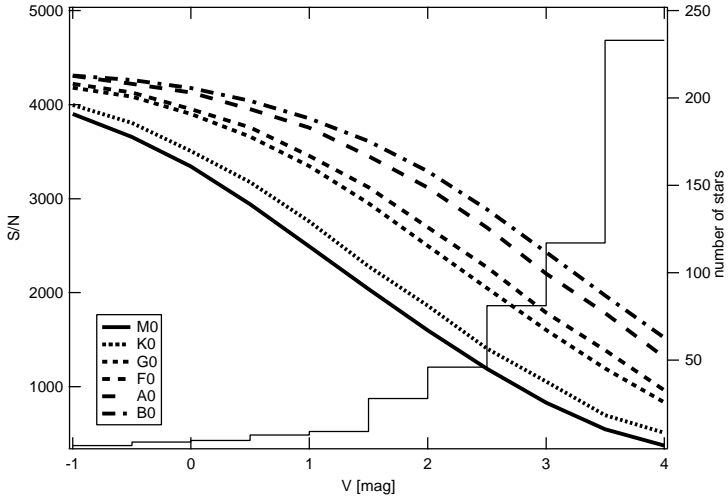


Figure 9: Estimated SNR for one minute of stacked frames with optimum exposure times for the blue system. The thin black line refers to a histogram of the stars from the BRITE-Constellation input catalog.

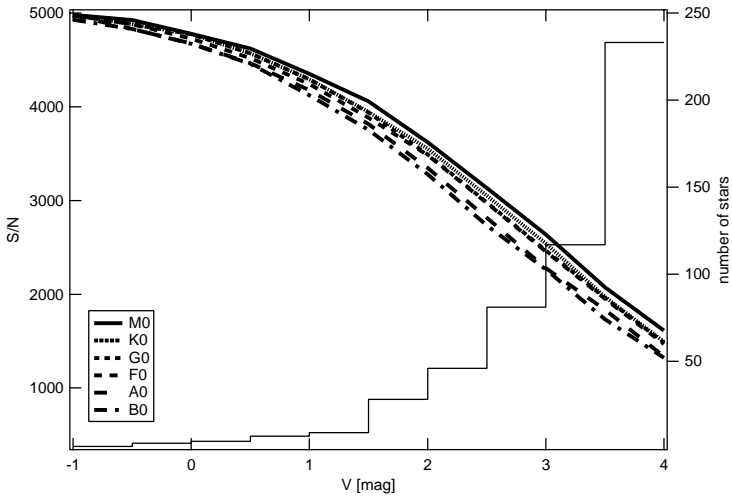


Figure 10: Same as Figure 10 for the red system.

Conclusion

In order to simulate the expected performance of the science instrument and to validate the specified mission requirements, a simulation has been performed. It shows that the mission requirement of an S/N of 1000 for a star of 3.5^m can be reached for 15 minutes of observation during one orbit.

Acknowledgments. This research is supported by the Austrian Science Promotion Agency (BRITE-Austria) and the University of Vienna (Uni-BRITE). This research made use of the MARCS model atmosphere code developed at the Department of Astronomy and Space Physics at the Uppsala University and the NEMO model atmosphere code developed by the SAPS research group at the Department of Astronomy, University Vienna.

References

- Gustafsson, B., Edvardsson, B., Eriksson, K., et al. 2003, ASP Conf. Ser. 288, 331
- Kaiser, A., Zwintz, K., Weiss, W.W. 2007, CoAst 152 (these proceedings)
- Moffat, A.F.J., Weiss, W.W., Rucinski, S.M., et al. 2006, ASTRO 2006 - 13th CASI Canadian Astronautics Conference
- Nendwich, J., Heiter, U., Kupka, F., et al. 2004, CoAst 144, 43-78

BRITE Orbits - Visibility and Feature Plots

C. Lhotka¹, B. Funk¹

¹ Institut für Astronomie, Türkenschanzstrasse 17, 1180 Vienna, Austria

Abstract

The goal of this investigation was the development of analysis tools in form of a software bundle to investigate the opportunities of feasibility during the BRITE mission, before the mission itself takes place. The simulation software and analysis tools will help to make critical mission decisions on the one hand, and on the other hand will help the observer to plan their observing strategies, thus to answer two fundamental questions:

- 1) Which orbit should be chosen for BRITE?
- 2) Which stars may be observed during mission time best, depending on the scientific purpose?

BRITE Visibility

To calculate the possible observation times for BRITE-stars during a defined time interval, we have to check their visibility, e.g. if and when they are occulted by the sun, moon, earth or other planets during this time period. We define a discrete time step Δt , which is the minimum time interval between two consecutive simulation states of the BRITE mission. The whole simulation starts at mission time $t=0$ and ends up at time T , which is a multiple of Δt . In the next simulation step we check, if the stars of interest from a given database are visible or not:

We define *True*/1 (light blocks in Fig. 1 for visible and *False*/0 (dark in Fig. 1) for invisible. If we do so for each star at each time step we end up in a set of multivariate dimensional time series (one time series for each star, dimension depending on the number of BRITE satellites), with only two possible states: visible or not.

The results of the simulation are stored in a global database and can be accessed via filter functions, leading to a report for explicit objects or a visibility plot for the whole set of stars defined in the database. A report returns

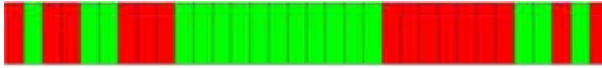


Figure 1: Binary time series example for a BRITE star. Light gray means visible, dark gray not visible.

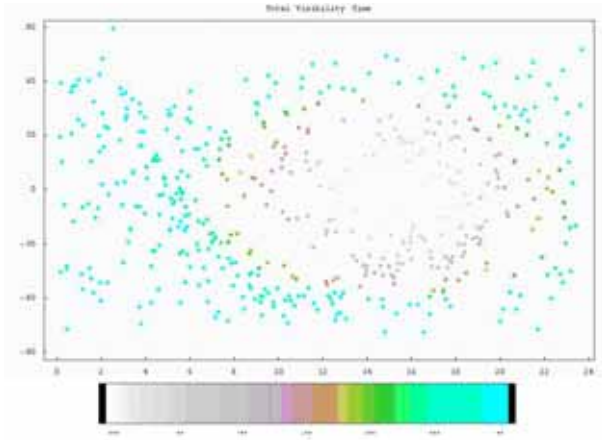


Figure 2: Total visibility time of the BRITE-sky during a simulated mission of 1 month.

the information associated with a single object in the database, the physical characteristics and its possible observation times.

A visibility plot shows the whole sky with all BRITE-stars, defined in the database, color-coded according to a qualitative or quantitative feature, the observer or mission planner wants to know. The features can be accessed and calculated via filter functions: Fig. 2 e.g. shows the total amount of visible time steps during the simulation at all or the size of the longest consecutive visibility time. Other characteristics may be plotted as well, like the min., mean or max observation time, or the number of fragments during a specific mission period. A report for a specific star defined in the database delivering all necessary information the observer wants to know is shown in Fig. 3.

To clarify the way of calculating the visibility we use Fig. 1 as an example:

The simulation time T is $32 \times \Delta t$, where Δt is, say, 60 seconds, thus we did the simulation for 32 minutes or 1920 seconds. The total possible observation time for a star, with this time series would be $17 \times \Delta t = 17$ minutes, the longest consecutive possible observation is $11 \times \Delta t = 11$ minutes, the mean observation time would be $17/32$ therefore 53% of the simulation time, the smallest window of observation is $1 \times \Delta t = 1$ minute. If we want to observe this star more than


```

In[51]: Report[Star[33]]

RA              7.28571
DE             -37.0975
magB            4.353
magV            2.729
Spectraltype    K
subtype        3
lunclass       Ib
HD             HD 56855
Teff           3830.14
e(Teff)
logg           NA
e(logg)
VISAT
object type     Double or multiple star
# stars with relevant shaded star type 5
int.flux[%]     739.1
filename        BRITE_ID0421.csv

#      start      end      duration
1      60        6900      6840
2     7020      7560       540
3     7680     16980      9300
4    17100     17640       540
5    17760     18300       540
6    18420     27720      9300
7    27840     28380       540
8    28500     37800      9300
9    37920     38460       540
10   38580     39120       540
11   39240     44700      5460

Out[51]: (Fragments → 11, Observation Time → 43440)

```

Figure 3: Report for a specific BRITE star defined in the database of BRITE star objects.

one time, we may need information about the amount of fragmentation, which is for our example 5 (consecutive visibility times shown in green).

A general filter function may return a plot (or report) according to the sentence:

Show me all stars with physical parameters X (spectral type, brightness, etc...) during mission time T (modelled in time steps Δt), showing visibility times similar to the distribution D color-coded according to other features K , resulting from the visibility time series.

Free parameters during the simulation are the mission length T , the discrete time steps Δt , number and orbit of the BRITE satellites and the regions around occulting objects like the earth, moon and the sun (called exclusion angles). The number of observers (number of BRITE satellites) and the number of occulting objects (sun, moon, planets) is arbitrary in the calculation and only limited due to computational and therefore memory limits.

For our study we used the well known NORAD satellite propagator particularly the SGP4 propagator, which was developed by Ken Cranford in 1970 and is used for near-Earth satellites. To compare the results of the Norad program with the STK program we used the two line elements of different orbits, e.g. the ISS and the MOST mission, and integrated the orbits with both programmes for one and two months. Therefore we used the SGP4 Model, implemented in

the STK (Satellite Toolkit) as well as in the Norad Package. First tests showed that the orbits, calculated with the two programs, fit quite well. In a second step we compare the results of numerical and analytical propagators. In the STK Program one can choose one numerical integrator (hpop), which is the most precise one we have up to this moment. Therefore we have investigated the differences between this propagator and the analytical propagators (SGP4, SGP8) and found good agreement for less than 24 days to give accurate results. For longer time scales statistical properties still can be deduced from the simulation done so far.

Acknowledgments. The authors wish to thank the SAPS (Stellar Atmospheres and Pulsating Stars) and the ADG (Astro Dynamics Group) for the resources and fruitful discussions.

BRITE-Constellation: Observation Planning

A. Kaiser¹, R. Kuschnig^{1,2}

¹ Institut für Astronomie, Türkenschanzstrasse 17, 1180 Vienna, Austria

² Univ. of British Columbia, 6224 Agricultural Road, Vancouver V6T 1Z1, Canada

Abstract

This proceeding paper was generated using a Power-Point presentation from the workshop.

Presentation Slides

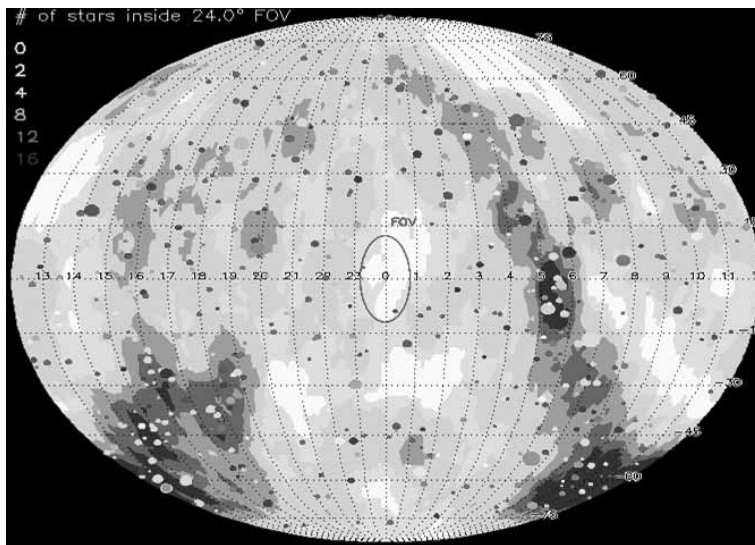


Figure 1: Plot of the whole sky for all 534 stars with a visual apparent magnitude brighter than 4^m . Coded in levels of grey is the number of stars inside a field of view of 24° .

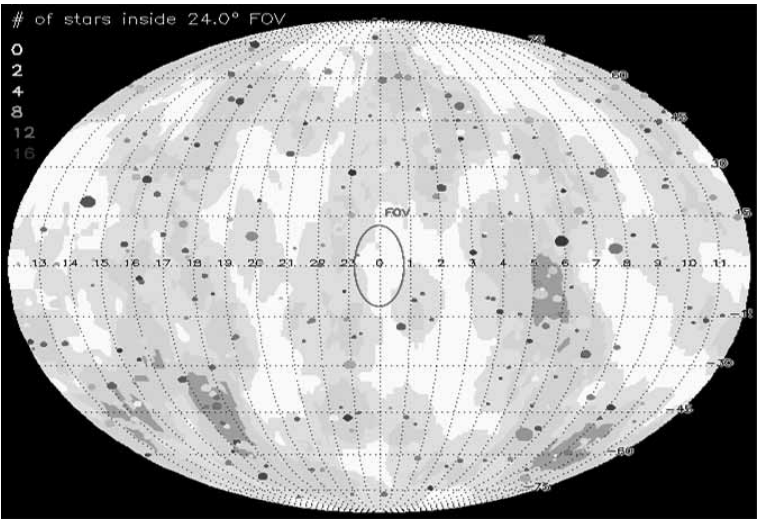


Figure 2: Same as Figure 1 but only for the 274 stars with less than 0.1% flux from polluting background objects.

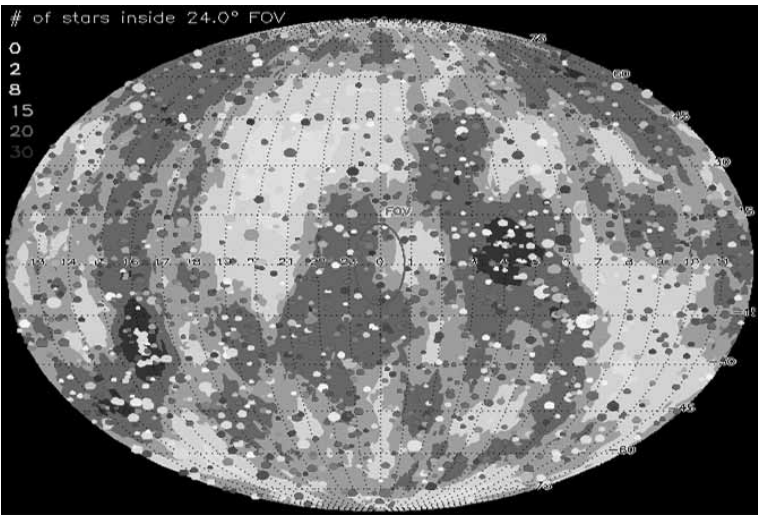


Figure 3: Same as Figure 2 but for stars with with a visual apparent magnitude brighter than 6^m .

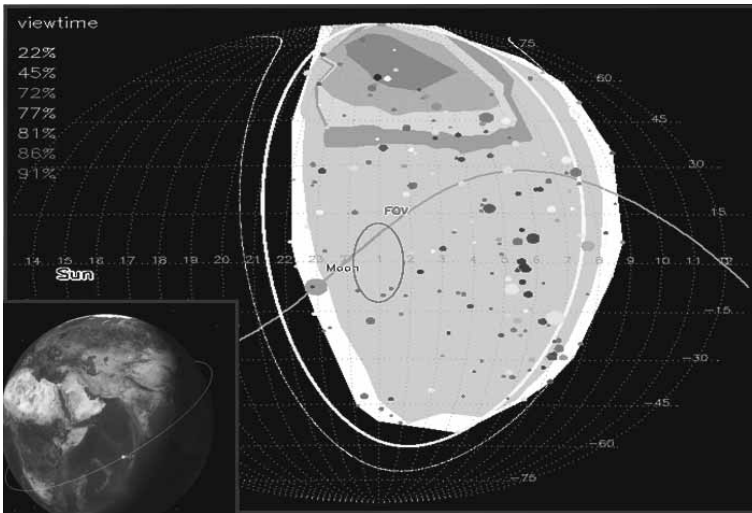


Figure 4: Unobstructed sky coverage for the Hubble Space Telescope for October 2008 coded in levels of grey.

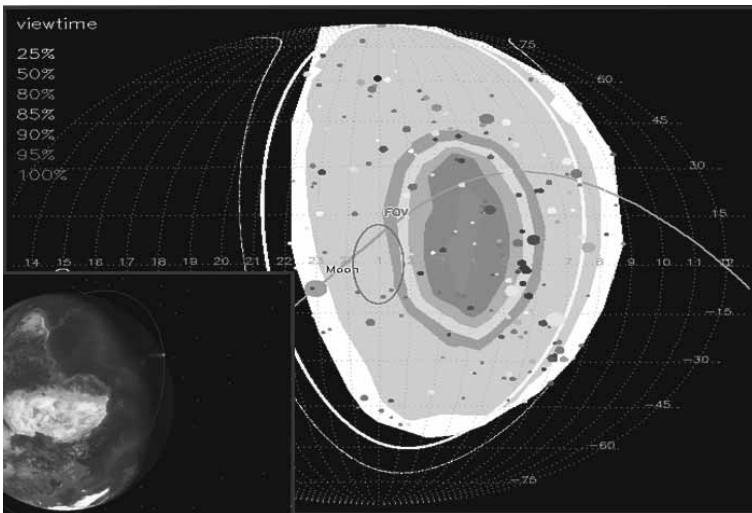


Figure 5: Same as Figure 4 but for the MOST Space Telescope.

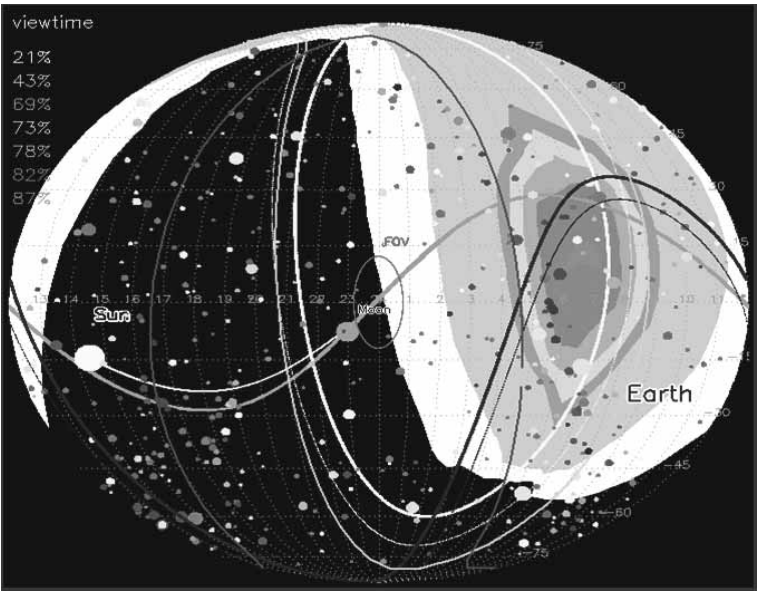


Figure 6: Same as Figure 5 but for 4 month.

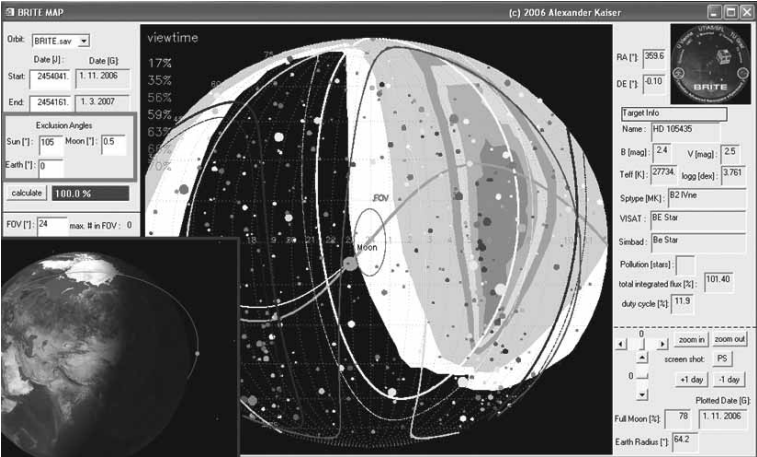


Figure 7: Same as Figure 6 but for a noon-midnight orbit.

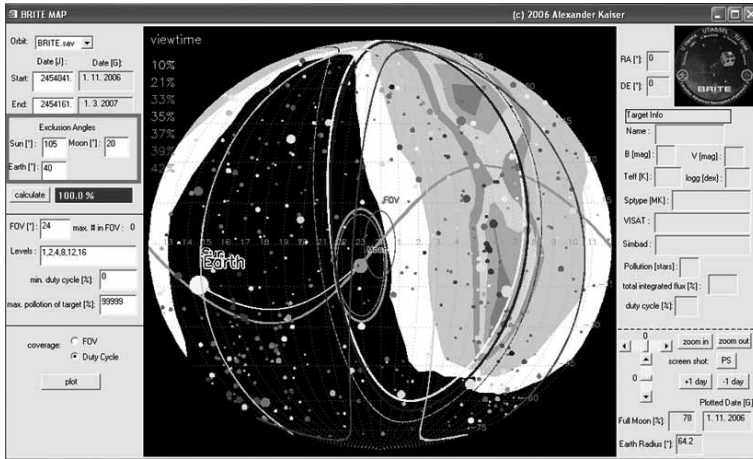


Figure 8: Same as Figure 7 but for larger earth and moon exclusion angles.

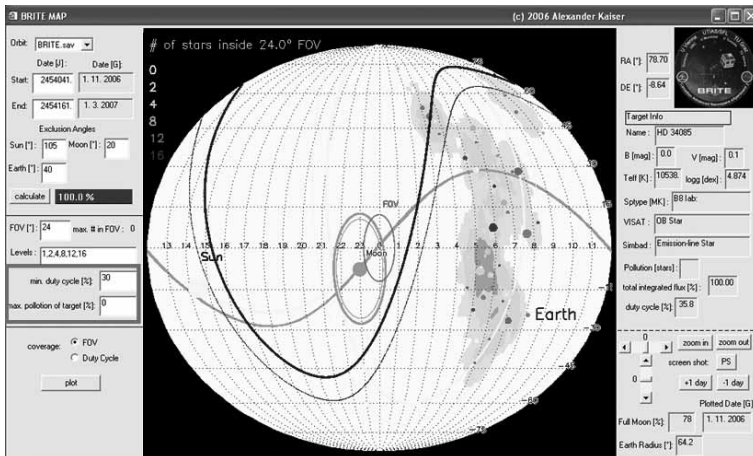


Figure 9: Plot of the whole sky coverage coded in levels of grey for targets with more than 30% viewtime and less than 0.1% flux from polluting background objects.

BRITE-Austria/TUG Sat1: Ground Station Technology

O. Koudelka¹

¹ Institut für Kommunikationsnetze und Satellitenkommunikation, Universität Graz,
Inffeldgasse 12, 8010 Graz, Austria

Abstract

This proceeding paper was generated using a Power-Point presentation from the workshop.

Presentation Slides

COMMUNICATIONS SPECS (1)

- Downlink (S Band)
 - Science data
 - Housekeeping data
- Uplink (UHF Band)
 - Sending commands
- Beacon (VHF Band)
 - Essential housekeeping data
 - Locating satellite

FREQUENCIES

- S-Band: 2234.4 MHz
 - Scientific band
- UHF-Band: 437.365 MHz
 - Amateur radio
- VHF Band: 145.89 MHz
 - Amateur radio

POWER

- S-Band Uplink: 0.5 W
- UHF Uplink: 100 W
- Beacon: 100 mW

DATA RATES

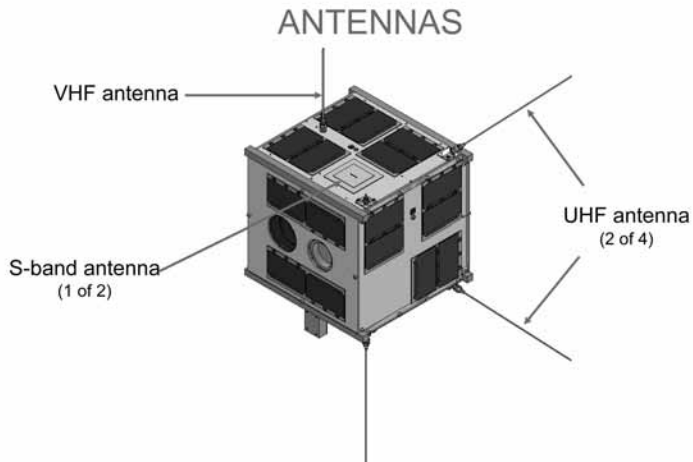
- S-Band: 32 kbit/s min. (link budget supports up to 512 kbit/s)
- Downlink protected by forward error-correction (convolutional encoding/Viterbi decoding)
- Modulation: BPSK (QPSK)
- UHF Uplink: 4 kbit/s
- Modulation GMSK (simple, robust)
- No coding
- Beacon: slow-speed Morse code

LINK BUDGETS

- Orbit: 900 km (worst case)
- Free-space loss:
 - 145 dB (VHF)
 - 155 dB (UHF)
 - 169 dB (S-Band)
- Margins:
 - 9 dB (VHF)
 - 14.3 dB (UHF)
 - 8.7 dB (S-Band)

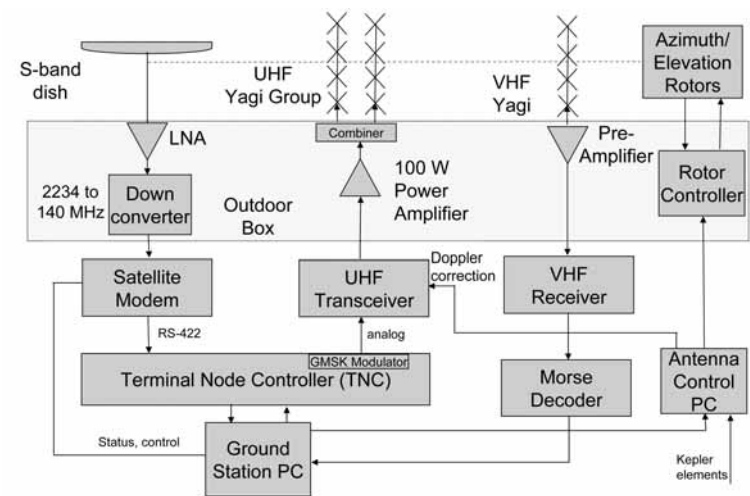
ANTENNAS

- Satellite:
 - S-Band: 2 patch antennas on opposite sides
 - UHF: 4 canted $\lambda/4$ monopoles, generating circular polarisation
 - VHF: monopole (shortened antenna)
- Ground stations:
 - 3 m parabolic dish for S-band
 - Cross-Yagi group for UHF
 - Cross-Yagi antenna for VHF



TRACKING

- Satellite moves relative to ground station
- Antennas need to track spacecraft
- Program track
 - Computer calculates orbits
 - Based on Kepler elements provided by NORAD
 - Azimuth/elevation rotor driven by computer
 - Doppler correction calculated -> UHF uplink frequency modified
 - Downlink modem tracks automatically frequency



O. Koudelka, W. W. Weiss and C. Grant during the workshop dinner at the Institute of Astronomy.

BRITE-Austria/TUG Sat1: Launch Opportunities

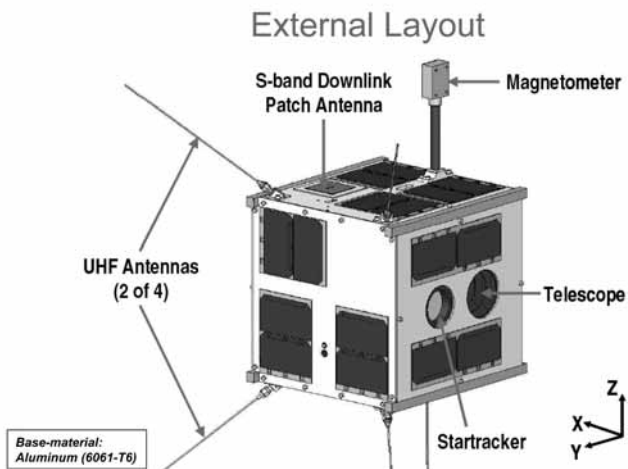
B. Josseck¹

¹ Institut für Kommunikationsnetze und Satellitenkommunikation, Universität Graz,
Inffeldgasse 12, 8010 Graz, Austria

Abstract

This proceeding paper was generated using a Power-Point presentation from the workshop.

Presentation Slides



BRITE-Austria - Baseline Orbits

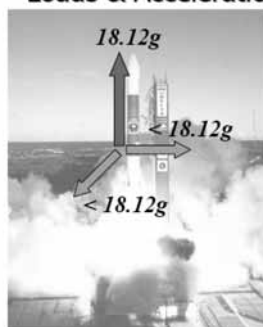
BRITE is designed for any low earth orbit in view of the ground stations to maximize launch flexibility. Typically, the following orbits are used for analysis:

- Dawn-Dusk Sun-Synchronous (minimum eclipse): hot case for thermal analysis
- Noon-Midnight Sun-Synchronous (maximum eclipse): cold case for thermal analysis, worst power conditions
- 900 km altitude orbit for link budgets
- 550 km altitude orbit for atmospheric drag and Doppler

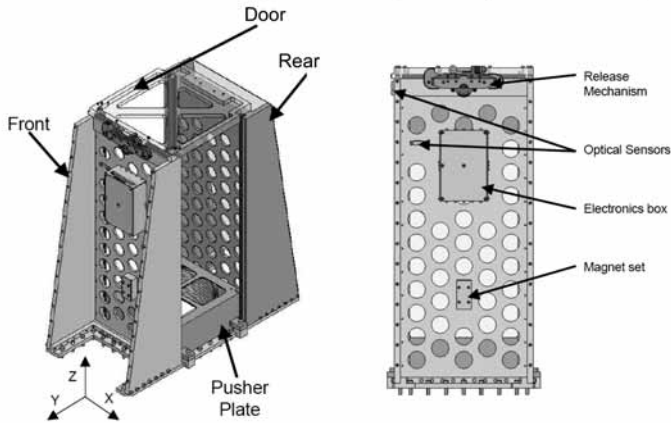
The launch (and consequently the orbit) of BRITE is unknown at this time. The spacecraft will be launched as a secondary or tertiary payload, hopefully in late 2008.

Boundary Conditions

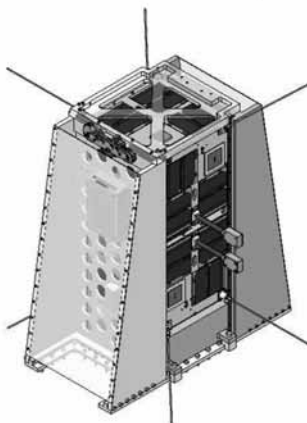
Loads & Accelerations



Nanosatellite Separation System (XPOD Duo)

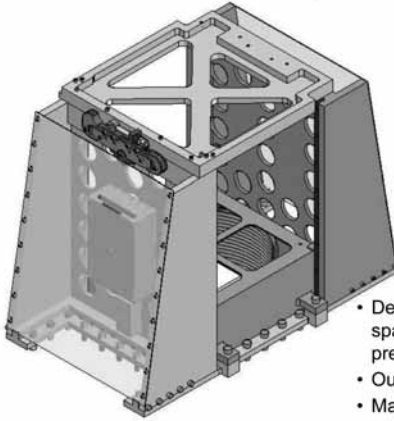


Nanosatellite Separation System (XPOD Duo)



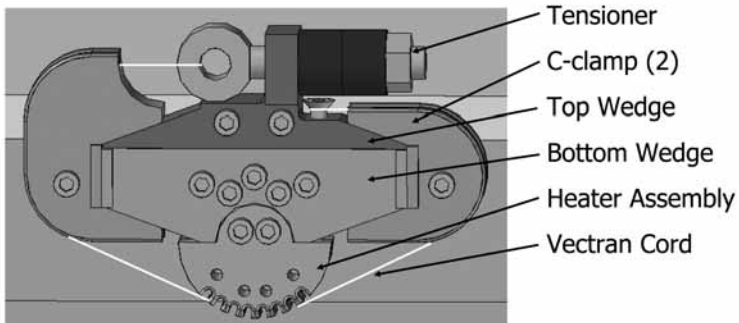
- Is designed to accommodate two 6 kg, 20 x 20 x 22 cm spacecrafts (antennas, booms etc. pre-deployed)
- Outer dimensions: ~ 24 x 49 x 55 cm
- Mass: + 12 kg

XPOD GNB Separation System

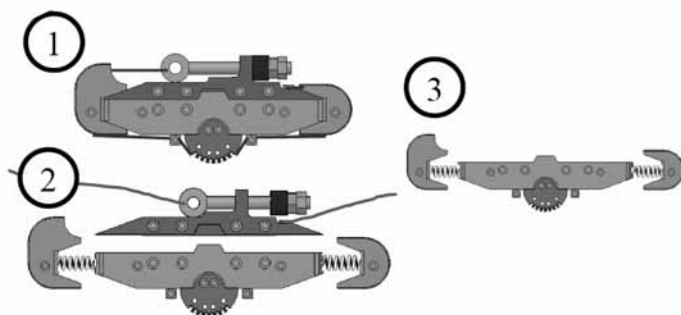


- Designed for 20 x 20 x 22 cm spacecraft (antennas, booms etc. pre-deployed)
- Outer dimensions: ~ 24 x 38 x 33 cm
- Mass: ~ 9 kg

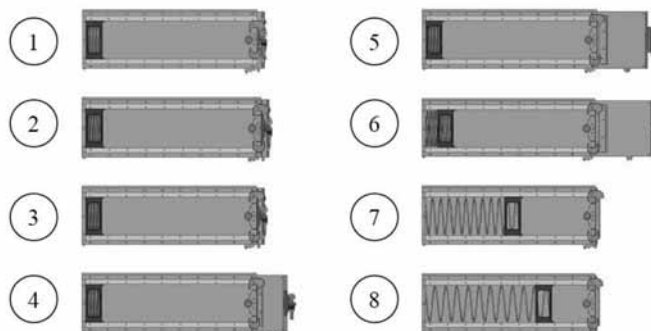
Release Mechanism



Mechanism Release Sequence

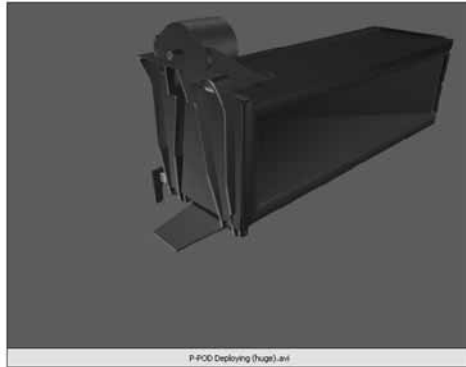


Release Sequence



Deployment Principle

(Quelle: The CubeSat Program / Cal Poly State University)



Launch Opportunities

Launcher:

- DNEPR
- ROKOT
- KOSMOS
- ARIANE V

Launch Sites:

- Plesetsk (Ru)
- Baikonur (Kas)
- Kourou (F)

Launch Costs:

- ca. € 10.000,- bis 20.000,- / kg



ROKOT (Khrunichev)

Launch Opportunities

- AGIIF, Vienna, April 23, 2007: Signing of a MOU between the Russian and the Austrian side (article 7 - providing support with launch of TUGSAT-1)
- In our first contacts, Roscosmos suggested a *Dnepr* launch.
- Kazakhstan, July 26, 2006: 18 Russian and foreign-made micro-satellites were destroyed when a civilian version of the heavy R-36M2 crashed shortly after liftoff, due to a first stage engine shutdown.
- On April 17 Russia has successfully launched a *Dnepr* carrier rocket. 16 foreign (Egyptian, Saudi satellites) and additional P-Pod and Cube-Sat micro-satellites were delivered and successfully deployed into 640 km sun-synchronous orbit (being the 8th commercial launch).
- Currently the reliability factor for the rocket (160 launches in SS-18 and Dnepr configuration) is 0,97

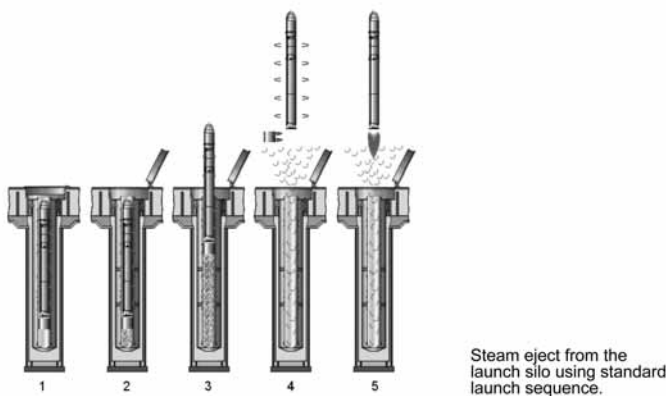
Russian rocket fails (July 26, 2006)

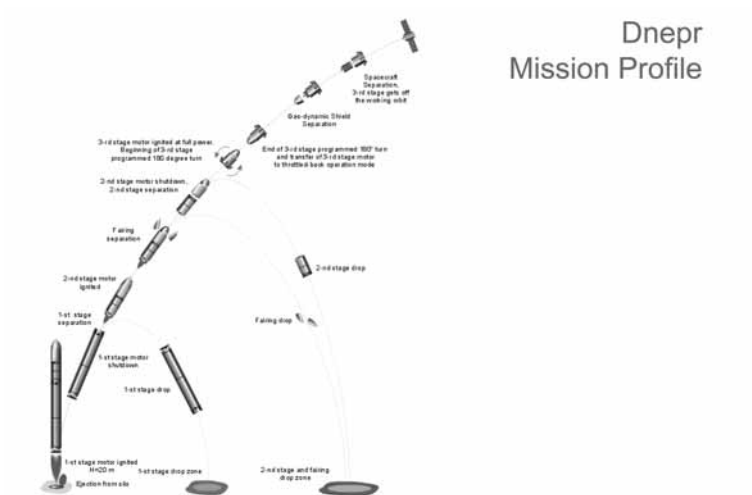
Kazakhstan: The Dnepr's wreckage was discovered 150 km's from the space center, due to a first stage engine shutdown. Russia has agreed to pay more than \$1 mio. in compensation for the July crash.





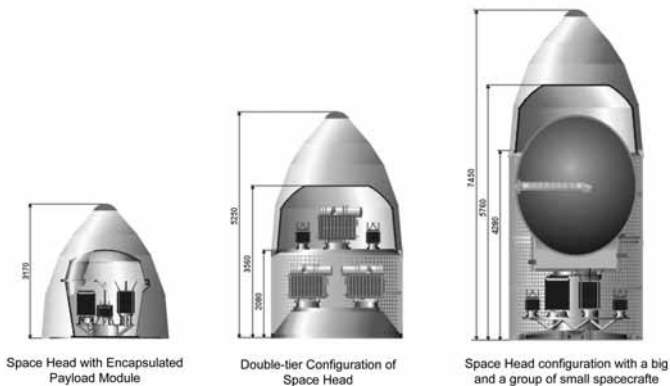
Dnepr – Liftoff Diagram





Dnepr Application for Space Missions

Dnepr Cluster Launch Capability for Small and Microsatellites

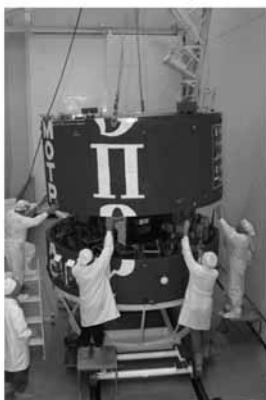


DNEPR – Integration



Quelle:
Kosmotras

Dnepr - Launch Preparation



Quelle:
Kosmotras



DNEPR - Launch Preparation



Earth Transportation Facility: Launcher in horizontal position



DNEPR - Deployment Simulation



(Quelle: The CubeSat Program / Cal Poly State University)

Informations

www.tugsat.at oder www.tugsat.com

www.iks.tugraz.at

Contact TUGSAT-Team:

tugsat@tugraz.at

A MOST open-field data reduction software and its applications to BRITE

D. Huber¹, P. Reegen¹

¹ Institut für Astronomie, Türkenschanzstrasse 17, 1180 Vienna, Austria

Abstract

A data reduction pipeline specifically developed for space-based open-field photometry obtained with the MOST satellite is presented. The reduction steps include correction of cosmic ray events, identification and rejection of exposures showing distorted images due to pointing instabilities and efficient correction of stray light influences on the CCD. Considering the planned instrumentation for the BRITE mission, suggestions for an efficient data reduction based on the experiences with MOST are made. It is concluded that under the current specifications for the mission many of the developed techniques might be directly applicable for the development of a BRITE data reduction pipeline.

Introduction

The MOST (Microvariability and Oscillations of STars) space mission (Walker et al. 2003) was launched in June 2003 to perform high-precision space photometry of bright stars. Equipped with a 15 cm Rumak-Maksutov telescope and a custom broadband filter (350 – 700 nm), MOST is positioned in a polar, sun-synchronous orbit, enabling the satellite to monitor the same star for up to 2 months without interruptions.

In the original design MOST was equipped with two CCDs, one for science and one for tracking, the latter however being disfunctional due to a particle hit since early 2006. The primary observing mode makes use of a Fabry microlens array. Entering a field stop of 1 arcmin diameter, an extended defocused image of the telescope's entrance pupil is projected on the science CCD. This image is very insensitive to pointing instabilities, hence provides a high photometric quality. Secondary science is performed on the remaining areas of the CCD, corresponding to conventional CCD photometry as will be performed in the BRITE mission. Figure 1 shows a typical point-spread function (PSF) of the MOST open field photometry. The typical FWHM of the MOST PSF is about 2-3 pixels, with one pixel corresponding to 0.3 arcsec.

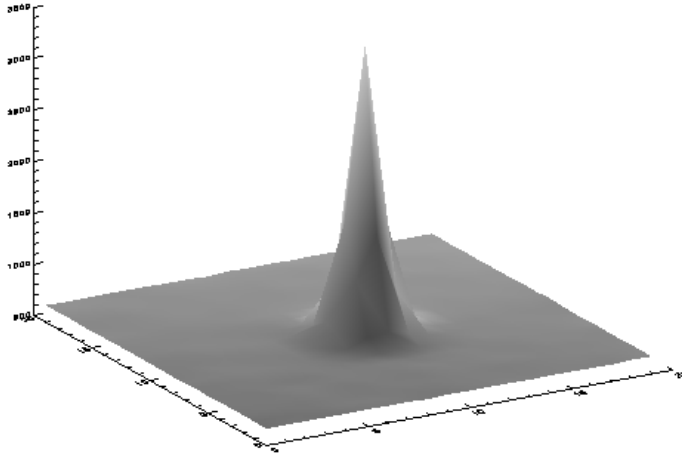


Figure 1: Typical PSF of MOST open field photometry. The FWHM is about 2-3 pixels.

The main data reduction pipeline for the primary Fabry Imaging observing mode is fully described in Reegen et al. (2006). Based on the techniques used for this pipeline, we developed a reduction software for processing open-field photometry which will be presented in detail in the following sections. An independent reduction for this observing mode was also developed by Rowe et al. (2006).

Aperture determination

Since possible satellite jitter due to pointing instabilities sometimes causes the PSF to wander over the CCD, it is not a priori possible to set a fixed aperture for all exposures of the same observing run. Many reduction steps however are based on a fixed identification of pixels illuminated by starlight (hereafter target pixels) and sky signal (hereafter background pixels) in order to analyze and correct instrumental influences over time rather than locally on one exposure. To realize an aperture determination, a gaussian function of the form

$$F(x, y) = A_0 + A_1 e^{-\frac{U}{2}} \quad (1)$$

with the elliptical function

$$U = \left(\frac{x'}{a}\right)^2 + \left(\frac{y'}{b}\right)^2 \quad (2)$$

is fitted to each exposure. The ellipse with semi-major axis a and semi-minor axis b is allowed to rotate in the coordinate system $(x, y) \rightarrow (x', y')$ by applying a rotation matrix in cartesian coordinates, yielding

$$x' = (x - h) \cos T - (y - k) \sin T \quad (3)$$

$$y' = (x - h) \sin T + (y - k) \cos T \quad (4)$$

with T being the rotation angle in clockwise direction of a and b with respect to the x - and y -axis, and (h, k) denoting the center position of the ellipse. A_0 denotes a constant offset of the function from the zero point, and A_1 a scaling factor to unity. A least-squares fit yields the 7 parameters $(A_0, A_1, a, b, h, k, T)$ which completely describe the airy disk of the star exposure. In the most straightforward approach, this procedure allows to define target pixels simply as all pixels showing larger intensities than the surface constant A_0 .

Cosmics Correction

The automatic identification and correction of cosmic ray events constitutes an important part of the data reduction of space based imaging. Especially during the crossing of the South Atlantic Anomaly, cosmic hits can severely influence the count rates and deteriorate the derived results from the data. For MOST open-field photometry, a two step strategy has been developed to identify cosmics in target and background pixels, respectively.

Background Pixels

As a first step a determination of target and background pixels as described in the previous section is performed for each exposure. In the case of background pixels, the identification of cosmics is then based on a simple sigma-clipping procedure. The standard deviation σ is computed for all background pixels and every pixel intensity I fulfilling the condition

$$I > k\sigma \quad (5)$$

is flagged as a cosmic candidate (k being an integer value, usually set to 4). The cosmic candidate is then replaced by the mean value of all surrounding background pixels which were not flagged. Additionally, a limit for the maximum number of cosmic candidates per frame is set. In the default mode this

limit is set to 10, i.e. if 10 out of all pixels of the 20×20 subraster are flagged as cosmic candidates, the exposure is rejected.

Target Pixels

On the contrary to background pixels, the cosmic identification for target pixels is based on comparing pixel intensities over time rather than locally on the same image. To achieve this, a distant-weighted average (DWA) of the form

$$F_\nu(t) = \frac{\sum_{n=1, t_n \neq t}^N |t - t_n|^{-\nu} I_n}{\sum_{n=1, t_n \neq t}^N |t - t_n|^{-\nu}} \quad (6)$$

where N is the number of frames used to average, I_n the mean intensity of all target pixels of the frame n and ν a weighting parameter ($\nu=0$ corresponds to a normal arithmetic mean) is computed. Essentially, a DWA returns a value averaged and weighted over time, e.g. a datapoint further apart from the value of interest is weighted less. The range over which the DWA is calculated is a free parameter, usually set to 10-20 frames. Since an anomalous value due to a cosmic ray event does sometimes persist over a couple of images this method is appropriate for detecting such an event. Considering a datapoint at times n , with a mean intensity I_n , a distant weighted average $F_\nu(t_n)$ and a standard deviation of the mean intensities of the DWA range σ , a cosmic hit is identified if

$$I_n - F_\nu(t_n) > k\sigma \quad (7)$$

is fulfilled, i.e. the deviation of a mean intensity of a frame is large with respect to the distant weighted average mean intensity. The value of k is a free parameter, with a default value of $k = 4$. Since all these calculations are based on mean intensities of the stellar image, the only conclusion to be drawn from equation (7) is that there are anomalous pixel values in the target area. Since there is no clean way to recover the actual stellar intensity, each frame showing such a feature is automatically rejected. An example for the application of this procedure to MOST data is shown in Figure 2.

Image Geometry

In some rare cases, severe pointing instabilities can cause the starlight to enter the telescope aperture with an extreme angle. This results in images showing

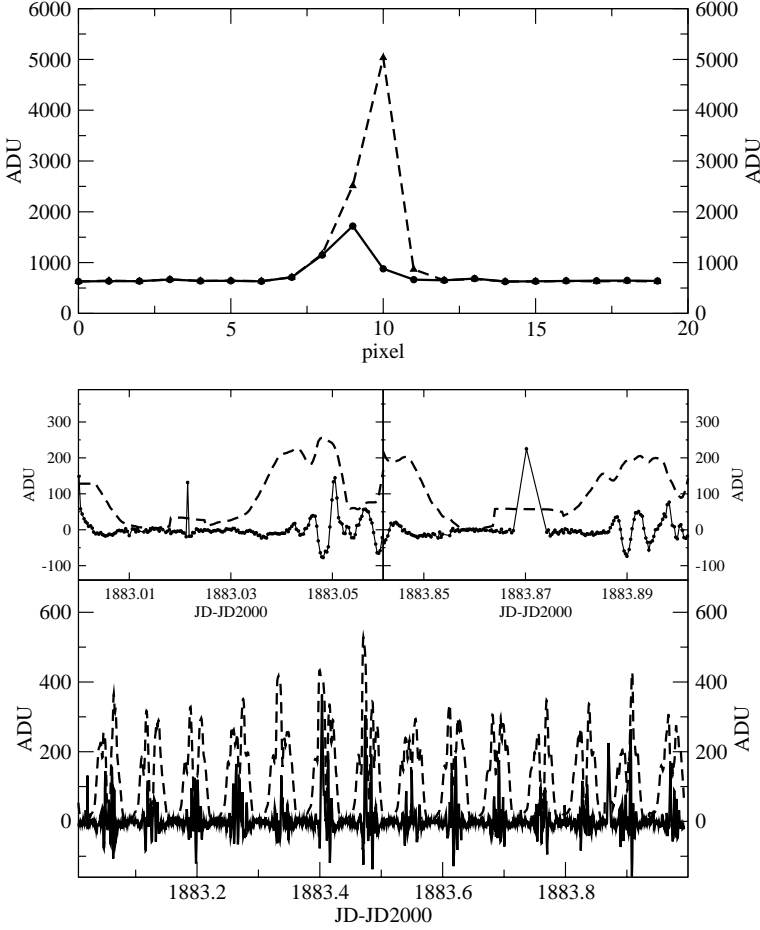


Figure 2: Examples of cosmic ray impacts in the target area of MOST observations. The bottom panel shows the left side of equation (7) (i.e. the deviation of the mean intensity from the calculated DWA, solid line) and a 4σ curve of the frames in the DWA range (i.e. right side of equation (7) with $k = 4$, dashed line). Two outliers, one at the beginning and one at the end of the one day dataset, can clearly be identified. The smaller panels show these two areas zoomed in. In the top panel, the dashed line shows the intensity over a row of the 20×20 subraster (containing the star) for the example of the earlier outlier (JD-JD2000 ~ 1883.02). The solid line shows the same plot for the exposure right before the affected image. Clearly, a cosmic ray event has altered the stellar intensity.

a deformed PSF shape which naturally would lead to disturbed count rates. Figure 3 shows examples for such images in the MOST data. Since there is no way to reconstruct the original count rate, such exposures have to be automatically identified and rejected by the pipeline.

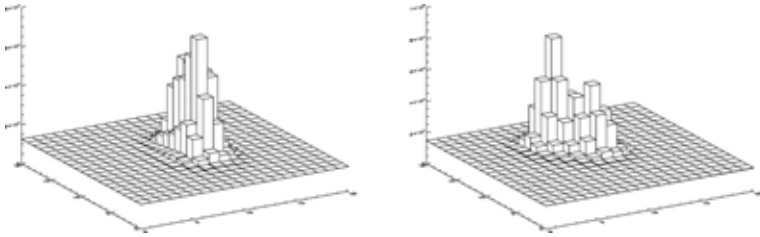


Figure 3: Examples for deformed image geometry due to severe pointing instabilities in MOST data.

To do so, the PSF fitting procedure described is again evaluated. Possible rejection criteria include:

- The fit does not converge.
- The number of target pixels exceeds a certain limit (for a 20×20 subraster ~ 150).
- The PSF center coordinates deviate more than a certain limit from the most common center position.

The last criterium is imposed as a preparation for the stray light reduction module, which will be the subject of the following section.

Stray Light Correction

General Concept and Implementation

Various influences which are beforehand hard to estimate might cause scattered light from other sources than the star illuminating the CCD. Most prominent examples for this are light from the illuminated side of the Earth or moonshine. As BRITE will most likely not be launched in a sun-synchronous orbit, it is expected that the observations will also be affected by this influence to some extent.

A proper reduction of stray light has been the major challenge in MOST data processing. The technique which was finally developed is based on calculating correlations of target with background intensities over time. An example for

such an intensity-intensity correlation is shown in Figure 4. Since the influences from stray light are the same for target and background pixels, a correction of this correlation (i.e., a decorrelation) using a linear regression will correct the instrumental signal in the data.

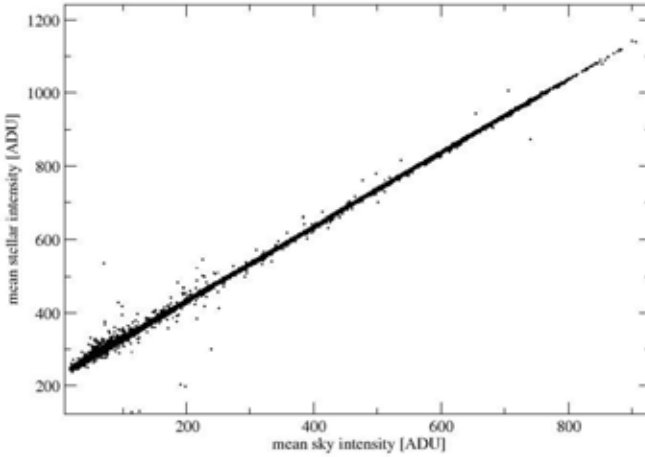


Figure 4: Example for an intensity-intensity correlation diagram for a timespan of several MOST orbital periods used for correcting stray light influences. In this case, mean stellar and sky intensities are plotted.

In the most simple approach, the decorrelation can be performed for mean intensities of target and background pixels, respectively. In reality, however, the stray light pattern across the CCD might not be uniform and show a much more complex structure. For this case, a stepwise pixel-to-pixel decorrelation has been developed (originally for Fabry Imaging, see Reegen et al. 2006). In this procedure, the background pixel showing the best correlation with the mean target intensity is calculated. Consequently, all pixels on the CCD are decorrelated with this pixel. This procedure is repeated with different background pixels until all stray light influences are reduced to a satisfactory extent.

While in the Fabry Imaging mode the extended defocused stellar image remains stable on the CCD, considerable PSF wander can occur in the open-field photometry due to minor pointing instabilities. It is obvious that such a variation of the PSF position will prevent a pixel-to-pixel decorrelation, since

one pixel can change over time from being identified as target or background pixel. To still be able to make use of this powerful technique, an additional routine which aligns the PSF positions had to be implemented to circumvent this problem.

The first difficulty is to be able to define a symmetric aperture around the stellar signal on an individual frame. It is not (or almost never) given that the PSF fits symmetrically within these physical restrictions. Instead, stellar intensity will occupy different amounts of pixel space at each edge. One way to solve this problem is to define a circular aperture on non-integer coordinates and estimate the intensity on a subpixel scale. This can however not be applied here, since the decorrelation method demands whole pixel intensity values to be correlated. Another method therefore is to simply transform the point of the PSF defining the symmetry center, i.e. the centroid position, from its original (non-integer) position to the exact center of its pixel. By applying this transformation to all surrounding pixels as well, the PSF will align much better on integer pixel coordinates, and hence an aperture based on integer pixels will fit more symmetrically. The transformation is done by a bilinear subpixel intensity interpolation applied to all pixels with respect to the centroid position. Having all intensities aligned to a common pixel grid, the final shifting procedure is implemented. Using the centroid position calculated in the step before (using only pixels within the PSF), the integer part of this value is taken and the difference to the mean position (already calculated in an earlier step of the reduction) is determined. This is done in x- and y-axis and all intensities are subsequently shifted by this amount of integer pixel numbers. This results in images which are aligned to the most common PSF position (therefore minimizing the amount of shifting). With these two steps combined, it is now possible to define an aperture symmetrically surrounding the PSF which at the same time fits all images due to their aligned position. It is noted that due to the fact that the shifting can occur for different images in different directions, the overlapping common image area will be smaller than before the shifting procedure. Hence, the final image size will be shrunk. An example for the image shifting process for consecutive exposures is shown in Figure 5.

With all images aligned, decorrelation can be applied. Since the stray light is also modulated on long timescales, the correction is performed in subsets considerably smaller than the total observation time. Moreover, to prevent intensity differences between consecutive parts of the light curve, the decorrelation is calculated for a larger subset (typically 5 MOST orbits or ~ 0.3 days), but applied only to a smaller subset (typically 0.005 days). The next subset step is then shifted by the small subset size until the end of the dataset is reached.

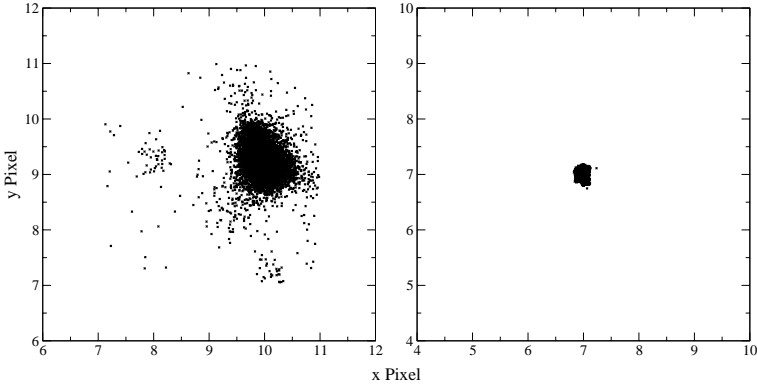


Figure 5: Demonstration of image shifting routine for about 9000 consecutive frames of a MOST run. Each point shows the center coordinates of the calculated PSF for a single exposure. *Left*: raw images before alignment; *Right*: processed images after shifting routine. Note that in both cases the axis scales are the same (6x6 pixels).

Restrictions

There are restrictions in open field photometry which limit the performance of the decorrelation technique compared MOSTs Fabry Imaging mode. Generally, the correlation between pixel intensities seems to be poorer due to the fact that the star light is focused on only a few pixels rather than spread out evenly over the CCD as is the case for Fabry Imaging. If a considerable stray light gradient over the CCD subraster of interest is present, this significantly limits the efficiency of pixel-to-pixel decorrelation. Therefore in some cases, this approach can introduce significant scatter in the reduced light curve. The reduction software therefore allows to choose between using mean intensities and/or pixel intensities for decorrelation.

Another important aspect concerning observation strategy is image stacking, which has been implemented for the MOST mission after the loss of the startracker CCD in early 2006. It has been found that stacking intensities over longer timescales significantly worsens correlations of star and background intensities. This is most likely due to the fact that the stray light is variable on timescales shorter than the total exposure time of the combined subexposures, which smears out the stray light effects over time. Hence, stray light influences appearing in target and background pixels will deviate and cause non-linearities in the intensity-intensity diagrams. To compensate for this problem, higher order fits have been implemented to correct the correlation. Additionally, an outlier rejection routine was included to improve the correlations. Nevertheless,

image stacking is still a persistent problem and slightly limits the effectiveness of the stray light correction technique.

Dark & Flatfield Calibration

Due to the limited budget of small space telescope missions such as MOST or BRITE, no or few moveable parts can be realized when building the satellite. This prevents the ability to perform standard CCD reduction procedures such as dark current measurements or flatfield calibrations.

For the reduction of MOST photometry, however, Rowe et al. 2006 proposed an alternative approach to obtain such measurements without using a mechanical shutter. Using exposures during high stray light phases, CCD sub-raster regions which are free of light from surrounding stars are recovered. After removing the gradient caused by the stray light with a polynomial fit, the resulting images can be used as flatfield and dark frames, respectively. Due to lack of testing time, this routine has not yet been implemented in the reduction software presented here. For more information, we refer to Rowe et al. (2006).

An Example

Figure 6 shows an example of the application of the data reduction to MOST photometry. The top panel, showing the raw data extracted by simple aperture photometry, demonstrates the complexity of the stray light behavior. Besides the main intensity peaks reappearing with the orbital period of the satellite (~ 101 min), a longer modulation trend of the stray light can be identified. The bottom panel of the same plot shows the light curve after the reduction has been completed. The running average indicated by the solid line shows the clear intrinsic variability of the star which could only be guessed in the raw light curve. Indeed, this star is a δ Scuti pulsator discovered by MOST.

Applications for BRITE

Almost all techniques described above do not depend specifically on the characteristics of MOST and should therefore be easily applicable for other high-duty cycle CCD photometry. An important aspect however is the combination of PSF fitting and aperture photometry used which naturally critically depends on the shape of the PSF.

For BRITE, the current design foresees a largely defocused PSF (4.5 pixels FWHM) which actually favors the application of the decorrelation technique for stray light correction. However, the defocused PSF is currently planned to

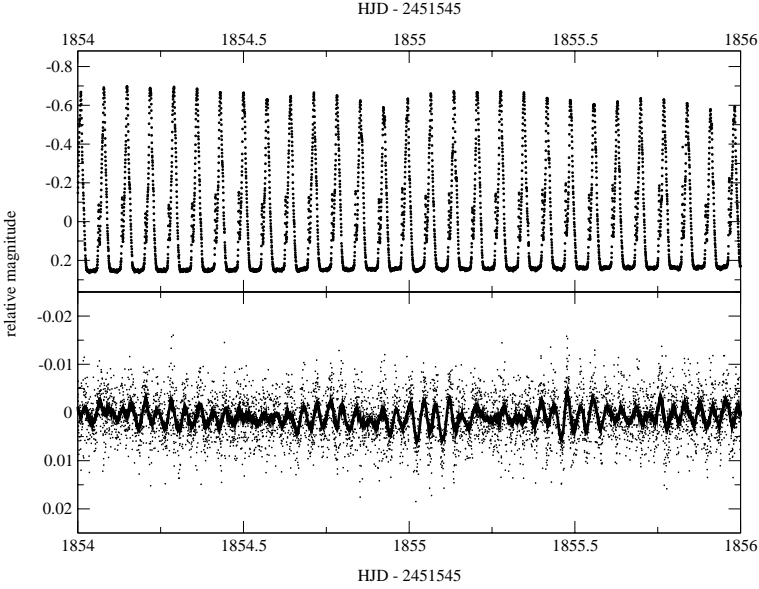


Figure 6: Subset of MOST photometry of a δ Scuti pulsator spanning over two days. The top panel shows the raw data, the bottom panel the reduced light curve using the techniques described above. The solid line in the bottom panel shows a running average of the data, clearly revealing the light variations of the star. Note the difference in y-axis scaling between the two panels.

be realized by combining subexposures which due to satellite jitter would cause the stellar light to be distributed more evenly over the CCD. If such an image stacking is realized this way, it will, based on the current experience with MOST data, be extremely important to save information of the background readings in the subexposures at some point. Although the mission is concipated to only observe very bright stars, the exposure times will still most likely be large compared to the variation timescales of possible stray light. Therefore, if no background information is saved it will be very difficult to recover the stray light pattern and therefore the correlation of instrumental artefacts polluting both target and background pixels.

The application of the routines described will largely depend on the ability to model the PSF in the manner it is possible for MOST using a simple 3D gaussian function. The use of a distance weighted average routine to identify outliers based on a temporal rather than a local comparison is a powerful tool for space missions which show regular sampling for a long time of observations. In any case, the principles and lessons learned from MOST for handling the major

difficulties in space based CCD photometry such as cosmic ray events, influences of pointing instabilities and stray light will most likely be applicable to BRITE in some sense. The development of a detailed application will certainly only become possible when real data become available and the specific characteristics of the photometry are known.

Conclusions

We conclude that most of the procedures developed for the reduction of space-based photometry by MOST will most likely be applicable to the BRITE mission. However, important differences will have to be taken into account, especially the differences in the shape of the PSF. Recent MOST photometry has shown that although image stacking does significantly enhance S/N, its consequences for correcting possible stray light influences can be quite severe. If possible, a largely defocused PSF spreading the star light as evenly as possible over the CCD without having to resort to image stacking would be the best option for the BRITE mission if a large amount of complex stray light influences is expected. If image stacking is applied, saving information about the background level of the subexposures will be an important option for correcting instrumental influences. In any case, the experience gathered with the wealth of data obtained by MOST will positively enhance (and hopefully speed up) the development of a reduction pipeline for BRITE.

Acknowledgments. The authors thank Thomas Kallinger, Denis Frast, Werner Weiss and the rest of the Vienna MOST data reduction team for their pioneering work on developing the Fabry Imaging reduction pipeline which served as the base for many applications implemented in the MOST open-field data reduction.

References

- Reegen, P., Kallinger, T., Frast, D., et al. 2006, MNRAS 367, 1417
 Rowe, J.F., Matthews, J.M., Kuschnig, R., et al. 2006, Mem.S.A.It. 77, 282
 Walker, G.A.H., Matthews, J.M., Kuschnig, R., et al. 2003, PASP 115, 1023

BRITE-Constellation: Input Catalogue

A. Kaiser¹, K. Zwintz¹, W.W. Weiss¹

¹ Institut für Astronomie, Türkenschanzstrasse 17, 1180 Vienna, Austria

Abstract

BRITE (BRiGht Target Explorer) is a satellite mission that will survey the sky, measuring the brightness and temperature variations of the brightest stars. In order to compile a mission target catalogue fundamental information of these stars was retrieved and a Hertzsprung-Russell (HR) was diagram compiled. Furthermore the feasibility of the targets was investigated by checking the surroundings for nearby bright contaminating stars.

Introduction

The BRITE-Constellation satellite mission (Moffat et al., 2006) will measure the brightness and temperature variations on timescales ranging from hours to months for the 534 brightest stars in the sky. Amongst others, BRITE-Constellation will investigate the role stellar winds play in setting up future stellar life cycles, and reveal pulsations that will allow astronomers to probe luminous star histories and ages through asteroseismology.

Target Inventory

The Simbad astronomical database (<http://simbad.u-strasbg.fr/>) was searched for objects brighter than $V=4$ mag and coordinates (RA, DE), color information (UBVRI, uvby $H\beta$, 2MASS), object types, spectral types and parallaxes were retrieved for a total number of 534 stars. Using the VISAT database (<http://ams.astro.univie.ac.at/visat>) a cross identification for star types was done. The determination of the fundamental parameters (T_{eff} , $\log g$, Fe/H , mass, radius, ...) was done with the TempLogG TNG software (<http://ams.astro.univie.ac.at>). The absolute magnitude M_V was derived from Hipparcos astrometric satellite parallaxes.

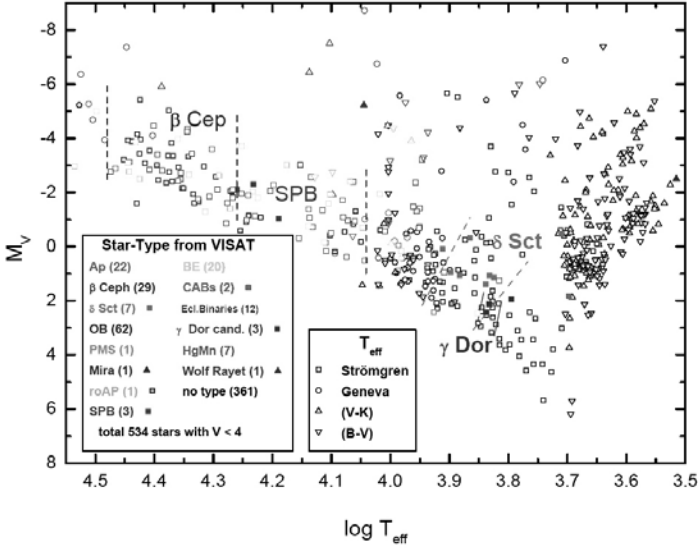


Figure 1: HR diagram of the 534 BRITE target stars with $V < 4^m$. Temperatures have been derived from various color systems, while M_V was derived from Hipparcos astrometric satellite parallaxes.

Target Contamination

As the science instrument of BRITE will produce a quite defocused image of the target stars the surroundings of the potential BRITE targets were checked for close-by bright stars in order to assess the existence of enough feasible (i.e. uncontaminated) targets are existing. Background objects down to an apparent brightness of 15 mag were considered. The additional background flux was then computed with the assumption of a Gaussian like PSF of different full width at half maximum (FWHM). Figure 2 shows the additional flux in percent of the flux of the target star introduced by background objects for a FWHM of 5, 6 and pixels.

It shows that between 190 and 260 stars out of the total sample have contaminations lower than 0.2% and therefore are ideal main target candidates. Figure 3 and Figure 4 show the distribution of star types extracted from VISAT and Simbad for all targets with an additional flux of less than 0.2%.

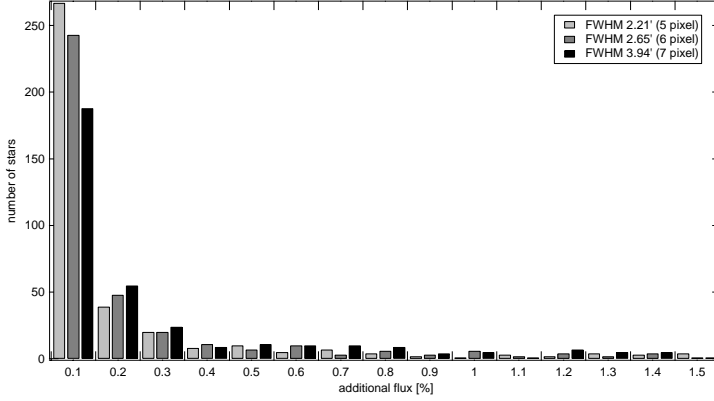


Figure 2: Additional flux in percent of the target star flux introduced by background objects.

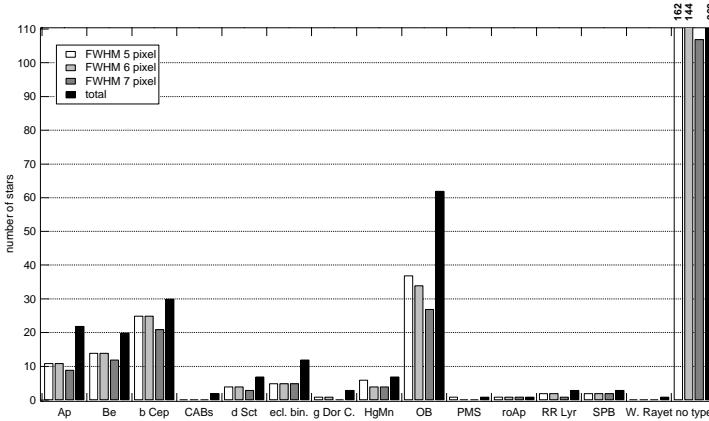


Figure 3: Stars with less than 0.2% additional flux with according star types from the VISAT database.

Catalog Extension

Extended simulations of the science instrument showed that a limiting magnitude of 4 is quite a conservative assumption. Therefore an extension of the input catalog including all stars with $4^m \leq V < 6^m$ has been proposed by the BRITE Science Team (Figure 5).

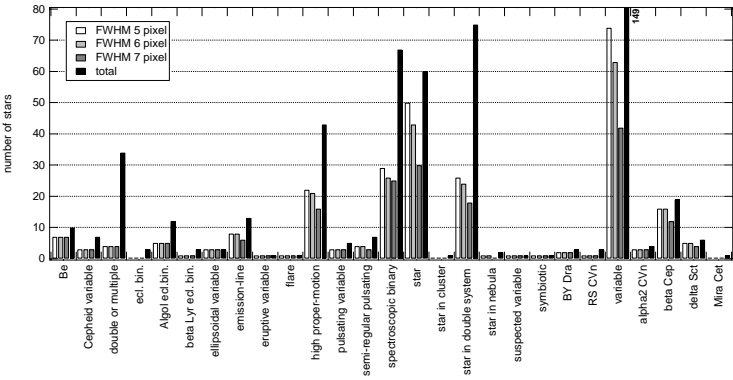


Figure 4: Stars with less than 0.2% additional flux with according star types from the SIMBAD database.

Conclusions

The BRITE-Constellation input catalogue consisting of 534 stars brighter than $V = 4$ mag has been compiled. Simulations have been performed in order to assess the optimal amount of defocusing of the camera system. Based on these simulations it was decided to aim for a PSF of 6 pixels FWHM.

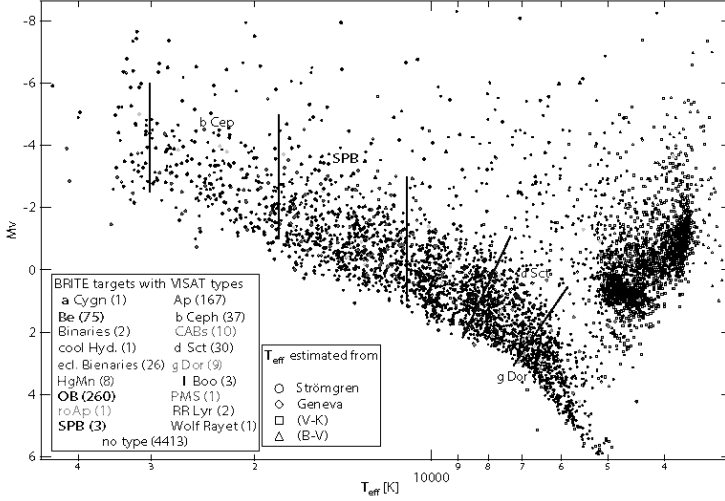


Figure 5: Same as Figure 1 but including the 4935 stars from the BRITE input catalog extension with $4^m \leq V < 6^m$.

Acknowledgments. This research made use of the SIMBAD database, operated at CDS, Strasbourg, France and the VISAT database, operated by the SAPS research group at the Department of Astronomy, University Vienna. This research is supported by the Austrian Science Promotion Agency (BRITE-Austria) and the University of Vienna (Uni-BRITE). Konstanze Zwintz acknowledges funding through the Austrian Science Funds (FWF) project T335-N16.

References

- Kaiser, A. 2006, ASPC, 349, 257
 Kaiser, A., Weiss, W.W. 2007, CoAst, in preparation
 Moffat, A.F.J., Weiss, W.W., Rucinski, S.M. et al. 2006, ASTRO 2006 - 13th CASI Canadian Astronautics Conference

Science

The BRITE satellite and Delta Scuti Stars: The Magnificent Seven

M. Breger

Institut für Astronomie, Türkenschanzstrasse 17, 1180 Vienna, Austria

Abstract

This paper examines the prospect of observing δ Scuti variables with BRITE. In particular, some of the astrophysical questions, which can be investigated, are discussed together with the methods to be applied. Finally, the seven bright stars suitable for BRITE are presented.

Introduction

The δ Scuti stars are pulsators situated in the classical cepheid instability strip on the main sequence or moving from the main sequence to the giant branch. In general, the period range is limited to between 0.02d and 0.25d. This limit provides a good separation from the neighboring or overlapping groups of pulsators in the Hertzsprung–Russell Diagram, such as roAp, γ Dor and RR Lyrae stars.

Regrettably, one should not regard this simple definition and description to be complete. We must consider two additional astrophysical situations: (i) the evolved Pop. II stars inside the classical instability strip with δ Scuti-like periods (SX Phe stars, unobservable with BRITE), and (ii) the massive stars evolving through the instability strip.

The massive ($M > 2M_{\odot}$) stars evolving from the blue main sequence towards the giant region cross the instability strip on nearly horizontal tracks in the Hertzsprung–Russell Diagram. The evolutionary state identifies them as δ Scuti stars. But due to their high mass and luminosity, the periods are longer than those of an average δ Scuti star and may get as large as 1 d. Consequently, in period they overlap the RR Lyrae stars, which are in the post-giant stage of evolution and have low masses below $1M_{\odot}$. It has been proposed (Breger 2000) that these long-period δ Scuti stars be distinguished from RR Lyrae stars by considering the size of stellar rotation. The suggestion is based on the observation by Petersen, Carney & Latham (1996), who point out that RR Lyrae stars show no detectable rotation ($v \sin i \leq 10 \text{ km s}^{-1}$).

δ Scuti stars can also be found among pre-main sequence stars. Examples are the pulsators in the young clusters NGC 2264 (Breger 1972), IC 4996 and NGC 6530 (Zwintz & Weiss 2006).

Some δ Scuti stars are (pure) radial pulsators, while the majority pulsate with a large number of nonradial p modes simultaneously. The nonradial pulsations of δ Scuti stars found photometrically are low-degree ($\ell \leq 3$) and low-order ($n = 0$ to 7) p modes, while spectroscopic studies have confirmed the presence of high-degree nonradial modes with ℓ up to 20 (e. g., for the star τ Peg, Kennelly et al. 1998).

The δ Scuti stars represent a transition between the cepheid-like large-amplitude radial pulsation of the classical instability strip and the ocean of nonradial pulsation occurring in the hot half of the Hertzsprung–Russell Diagram. Many excited modes show photometric amplitudes in excess of 0.001 mag, which makes it possible to study these stars photometrically. The position of δ Scuti stars on and slightly above the main sequence permits the asteroseismological comparison between oscillation data and stellar models in a region where the basic stellar structure is regarded as relatively well known.

Some reasons for the expected success of BRITE data

The BRITE project cannot be in the same league as large satellite missions such as COROT or GAIA. However, this situation could lead to some important advantages as well:

(i) BRITE can focus on a few specific astrophysical questions and objects. For large missions, a number of scientific compromises have to be accepted to ensure a return of the investment and to satisfy a large, sometimes diverse, community.

(ii) Since BRITE has to measure bright stars, the stellar parameters are known. This makes astrophysical interpretations of the results much easier and more reliable.

(iii) Because of the relative 'smallness' of the mission, data reduction and the scientific analyses can be very fast.

(iv) Huge quantities of data require special methods of data analysis including application of 'blind' methods. The BRITE data can avoid these blind methods and can be analyzed by experienced astronomers examining the data in detail at all stages of the reduction process. I regard this as very important: BRITE might lead to data unparalleled in their excellence.

Why study Delta Scuti stars with BRITE?

Asteroseismology relies on the comparison between observed and model frequencies. To achieve this aim, extensive and high-quality observational data are required. Let us illustrate this general statement with three out of many possible examples.

Frequency range of excited regions: direct implications for realistic models

The range of excited frequencies of a star is an important tool for modeling since these limits are very sensitive to effects such as convection and abundance.

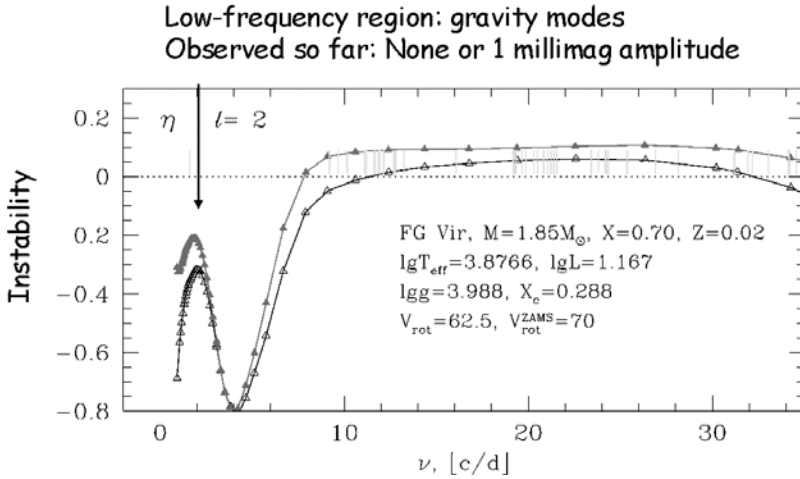


Figure 1: A pulsation excitation model computed by A. A. Pamyatnykh for a typical evolved δ Scuti star. The parameter, η , denotes the amount of instability. Note the low-frequency peak, still situated in the stable region. However, some change in model parameters could shift the peak beyond the instability line in order to match observed low-frequency pulsation.

Fig. 1 shows a pulsation excitation model for FG Vir. We note that there exists a low-frequency peak near 2 c/d. In this model, the peak is still in the stable (unexcited) region. However, some changes in the model can push the peak to instability. This would then become an observable g-mode. There exists some evidence that these have already been detected at low amplitude in a few δ Scuti stars.

The main pulsation of the star FG Vir occurs around 20 c/d. However, the star also shows a number of high-frequency pulsation modes at frequencies

above 40 c/d with small, statistically significant amplitudes of pulsation below one millimag. The observed high-frequency cutoff allows the models to be fine-tuned, especially with respect to the convection treatment. The high-frequency amplitudes are very low, requiring extensive observations, as could be provided by BRITE.

Photometric mode identification: the case for two filters

Let us turn to the identification of individual pulsation modes. For most asteroseismic applications, the frequency information of a particular pulsation mode is not sufficient: the quantum numbers of pulsation (n , ℓ , and m) need to be known. Pulsation mode identification can be very complex. A powerful tool is provided by the phase differences and amplitude ratios between the measurements made through different passbands. For δ Scuti stars, the two Strömgren filters, v and y , are often used. Here the phase differences (i.e., time shifts) between the two passbands are a strong indicator of the ℓ values, the number of node lines on the stellar surface.

Fig. 2 illustrates the method for the star 44 Tau. Since BRITE is planned to measure with two filters, the photometric mode identification method can be applied to δ Scuti stars.

Amplitude variability and close frequencies

Amplitude variability is a common property of pulsating stars. For RR Lyrae stars, this phenomenon is known as the Blazhko Effect since it was noticed by Blazhko (1907) in the RR Lyrae star RW Dra. However, a large number of different types of pulsators in different stages of evolution also show amplitude and phase variability on non-evolutionary time scales. Examples are classical cepheids (e.g., Breger 1981), sdB stars (e.g., Kilkenney et al. 1999), β Cephei stars (Lehmann et al. 2001), White Dwarfs (e.g., Handler et al. 2003), and δ Scuti stars (Breger & Bischof 2002).

Regrettably, the physical origin of these variations is not yet known. One of the reasons is the lack of extensive observational data to distinguish between different hypotheses. The excellent observational coverage, which can be provided by BRITE, makes these stars an excellent tool to study amplitude variability: In the Fourier spectrum of short data sets, two close frequencies beating with each other appear as a single frequency with variable amplitude and phase. For long data sets with sufficient frequency resolution, two peaks will be shown. In the case of a single frequency with a real variable amplitude and/or phase, two (or more) peaks also occur. Consequently, the appearance of two peaks in the Fourier spectrum does not prove the existence of two separate

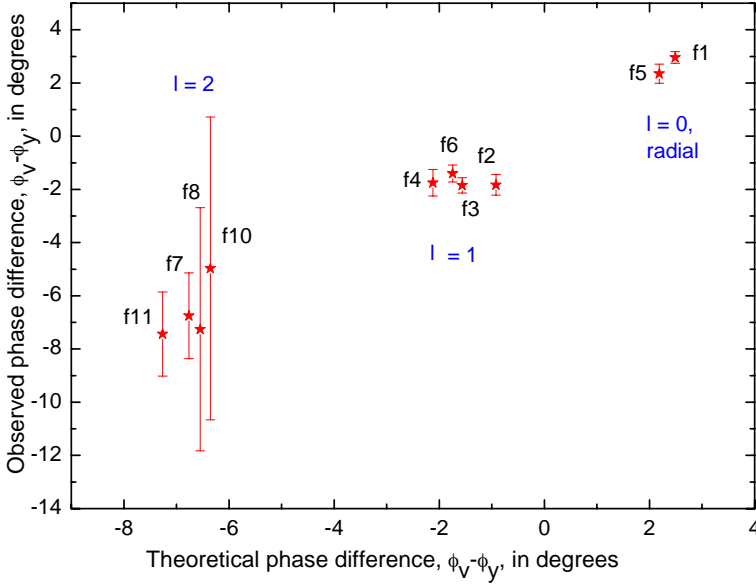


Figure 2: The diagram shows that the observed phase differences between the v and y passbands can successfully identify the pulsational ℓ values by comparing the observations with phase differences predicted from models. The star selected is 44 Tau. The observational error bars are very small for $\ell = 0$ and 1 modes, while the identification of the $\ell = 2$ modes is less certain due to their small photometric amplitudes. The model for 44 Tau is taken from Lenz et al. (2007).

modes, while the absence of a double peak does not exclude the possibility. This is a fact well recognized in the literature.

Fortunately, beating between two (or more) frequencies produces amplitude and phase variations which are mathematically related. The most extreme and easily recognizable situation occurs when two close frequencies have the same amplitude: this leads to a half a cycle phase shift at the time of minimum amplitude of the visible (single) frequency. Even when the amplitudes differ, beating has a specific signature in the amplitude of phase shifts of an assumed single frequency. In particular, the largest phase change (of an assumed single frequency) occurs at the time of minimum amplitude.

Therefore, it is possible to separate beating from true amplitude variability by studying the relationship between the amplitude and phase variations of an assumed single frequency. In practice, large differences in the amplitudes of the frequencies beating with each other, observational noise, as well as short

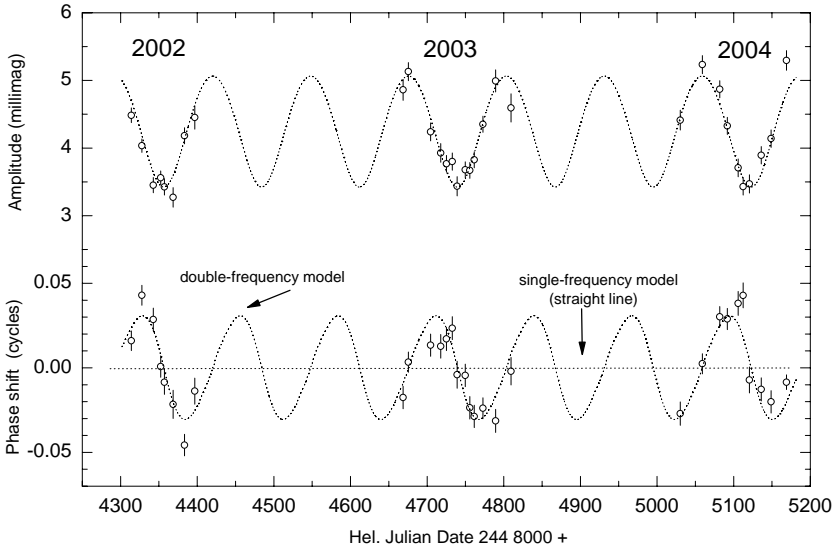


Figure 3: This diagram shows that the observed amplitude and phase variations of the 12.154 c/d frequency in FG Vir are caused by beating between two close frequencies. The open circles represent the observations, while the dotted line is the two-frequency fit. The variations can be explained by two independent frequencies separated by 0.0078 c/d and an amplitude ratio of 0.19. Note the excellent agreement between the different years.

(relative to the beat period) data sets may make the recognition difficult.

The method consists of obtaining an extensive photometric data base, subdividing the data into short time bins and calculating the amplitude and phase of the assumed optimum single frequency for each time bin. Furthermore, if other pulsation frequencies are also present, they need to be corrected for.

The test between true amplitude variability and beating between close frequencies has already been applied by us to three δ Scuti variables. The variability occurs in radial as well nonradial modes. Let us examine a radial mode at 12.154 c/d in the star FG Vir, for which extensive photometric data are available (Breger et al. 2005). Fig. 3 shows the variations in amplitude and phase for the three years.

The variations are similar in all three years with a beat period of 128d. Another important result is that the phase changes are coupled to the amplitude changes. In particular, minimum amplitude occurs at the time of ‘average’ phase and the time of most rapid phase change. As already mentioned earlier, this is an important signature of beating between two close frequencies. The visual

result is confirmed by a two-frequency model with the optimum parameters of frequency, amplitude and phase determined by PERIOD04 (Lenz & Breger 2005). An excellent agreement is obtained for both the amplitude and phase changes with the two-frequency model. It should be noted that the test was successful even with a second mode of small amplitude and phase shifts under 0.05 cycles. If we extend the analysis to include the 1995 data, we also find an excellent agreement between the predicted and observed amplitudes and phases of the earlier measurements.

We conclude that in FG Vir the amplitude and phase variations of the mode at 12.154 c/d can be explained by the beating of two close frequencies. The analysis has been repeated for a number of other pulsation modes in FG Vir and BI CMi. The results are the same: the amplitude and phase variability is caused by beating of close frequencies.

It has, therefore, been shown that beating between close frequencies is responsible for at least some of the observed amplitude and phase variability. However, can it explain all observed cases? Our presently unpublished data for 4 CVn suggests that an additional effect may be evolved, especially for long-term variations just short of the evolutionary time scales. The accurate measurements with BRITE should provide important new results to help decide whether two or more effects are responsible.

The Magnificent Seven

Seven known δ Scuti stars are bright enough to be observed with BRITE. Due to the brightness (!) their photometric variations have not in all cases been well-studied from the ground and the pulsation information given in the table below may not be reliable.

Acknowledgments. This investigation has been supported by the Austrian Fonds zur Förderung der wissenschaftlichen Forschung.

References

- Blazhko, S. 1907, *Astron. Nachr.*, 175, 325
- Breger, M. 1972, *ApJ*, 171, 539
- Breger, M. 1981, *ApJ*, 249, 666
- Breger, M. 2000, *ASP Conf. Ser.*, 210, 3
- Breger, M., & Bischof, K. M. 2002, *A&A*, 385, 537
- Breger, M., Lenz, P., Antoci, V., et al. 2005, *A&A*, 435, 955
- Handler, G., O'Donoghue, D., Müller, M., et al. 2003, *MNRAS*, 340, 1031

Table 1: Seven Delta Scuti stars that can be studied with BRITE

Star	Rotation $v \sin i$	Comments, periods, amplitudes
β Cas	70 km s ⁻¹	Monoperiodic radial? near TAMS, 2.5h, 0.03 mag
ρ Pup	15 km/s	Look for solar-type oscillation, cool, convection radial pulsation: 4h, 0.09 mag single mode or more small-amplitude modes?
γ Boo	115 km/s	$V = 3.0$, High-degree NRP, 1h Needs photometric work, doubtful situation, 0.05 mag?
θ^2 Tau	77 km/s	Delta Scuti Network, WIRE well-studied binary (giant and main-sequence) narrow frequency region - fascinating!
δ Ser	88 km/s	λ Boo-type spectrum, 4h, 0.05 mag
ν UMa	110 km/s	High-degree NRP, $m = 2$ to 11, 1.6 to 2.1h Photometry: maybe 3h period
ρ^1 Sgr	82 km/s	~ 1 hour, 0.02 mag, F0III-IV

- Kennelly, E. J., Brown, T. M., Kotak, R., et al. 1998, *ApJ*, 495, 440
Kilkenny, D., Koen, C., O'Donoghue, D., et al. 1999, *MNRAS* 303, 525
Lehmann, H., Harmanec, P., Aerts, C., et al. 2001, *A&A*, 367, 236
Lenz, P., & Breger, M. 2005, *CoAst* 146, 53
Lenz, P., Pamyatnykh, A. A., Breger, M., & Antoci, V. 2007, *A&A*, in press
Petersen, R. C., Carney, B. W., & Latham, D. W. 1996, *ApJ*, 465, L47
Zwintz, K., & Weiss, W. W. 2006, *A&A*, 457, 237



Lunch with J. Daszynska-Daszkiewicz and M. Breger.

CP Stars - probing stellar surface structure with BRITE Constellation

T. Lüftinger¹, W.W. Weiss¹

¹ Institut für Astronomie, Türkenschanzstrasse 17, 1180 Vienna, Austria

Abstract

More than 170 chemically peculiar (CP) stars will be observable by BRITE Constellation. These stars host a complex interplay of phenomena like strong magnetic fields, chemical diffusion, pulsation and rotation in the same object. Thus they serve as unique stellar laboratories where we can observe the correlation and interaction of these fundamental physical processes.

We present here a summary of the unique potentials BRITE Constellation offers to obtain new insights in the atmospheric structure formation and the complex interplay of abundance variations, pulsation and magnetic fields under conditions that could never be reproduced on Earth.

Introduction

About 10 – 20% of the stars found on or close to the mid-main sequence, covering effective temperatures T_{eff} of about 6500 K up to 30 000 K, reveal stunning anomalies in their spectra and light curves, which translate into remarkable differences in the stellar atmospheric composition from the sun's photosphere and from stars of similar spectral type and luminosity.

Modelling interior structures of these F-, A- and B-type stars was originally expected to be simple as they do not exhibit extensive surface convection zones, hydrogen is their primary source of opacity, and they do not reveal turbulent line broadening or irregular short-period variability. Luminosity and colour variations are sometimes seen to vary periodically at timescales of hours or days to decades, with the same period as their magnetic fields and the shapes and strengths of their spectral line profiles.

However, a wide variety of spectroscopic peculiarities has been observed and classified for these stars and they are generally referred to as chemically peculiar (CP) stars. Preston (1974) divided the CP stars into four main subclasses. We would like to focus on the CP2 (magnetic chemically peculiar, described in the following) and the CP3 stars, the mercury-manganese (HgMn) stars, in which

Hg and Mn are enhanced. Recent investigations by Kochukhov et al. (2007) revealed evidence for dynamical structure formation on their surface.

The CP2 stars, the *magnetic* chemically peculiar A and B (ApBp) stars, exhibit depleted abundances of light elements and normal to strongly enhanced iron-peak elements. The heavy elements and especially the rare earths (REEs) can be overabundant by orders of magnitudes over the solar composition.

A very important subgroup of the CP2 stars are the rapidly oscillating Ap (roAp) stars, which were discovered by Kurtz in 1982. Exhibiting effective temperatures between about 6400 K and 8100 K (Ryabchikova et al. 2004) they occur at the cool end of the ApBp range and show moderate to (sometimes) very strong magnetic fields and various outstanding abundance peculiarities. They pulsate with periods of about 6 to 21 min, consistent with nonradial acoustic (p-mode) pulsations of low degree and high radial order. As the observed pulsational amplitude of a roAp star is modulated with the magnetic (thus, rotation) period, such that the maximum coincides with the peak field strength, there is likely a close connection between the geometries of the magnetic field and the pulsation modes.

Thus Ap and Bp stars with their subgroup of roAp stars serve as unique stellar laboratories where we can observe the correlation and interaction of rotation, strong magnetic fields, chemical diffusion, and pulsation in the same object and explore the origins and the evolution of these fundamental physical processes with conditions that could never be reproduced on Earth.

The oblique rotator model

The hitherto most successful model to explain the extreme abundance anomalies observed for Ap and Bp stars is the so-called oblique rotator concept, which was first proposed by Michaud in 1970. In a stellar atmosphere stabilised by a global magnetic field with only weak turbulent motion, convection or rotational mixing, a sensitive interplay between gravitational settling and radiatively driven diffusion is possible. Atoms and ions can be lifted higher into the atmosphere or sink, causing enhanced or depleted chemical abundances. As these processes are not homogeneous over the stellar surface (influenced by magnetic field geometries, winds, and other processes) the star can develop vertical and horizontal chemical inhomogeneities. The chemical diffusion concept is discussed in detail by Babel (1992) and Vauclair et al. (1991), also considering the possible influence of weak, magnetically confined winds.

The resulting inhomogeneous stellar surface structures lead to variable opacities, temperatures and fluxes, resulting in modulated light curves and spectral line signatures linked to the rotation of the star.

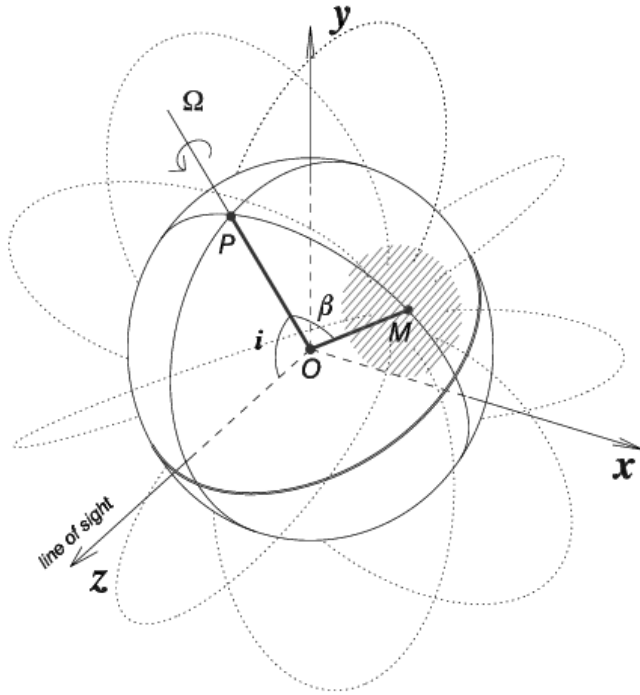


Figure 1: Geometry of an oblique rotator: the line of sight (z -axis) and the stellar rotational axis OP enclose the inclination angle i . OM , the axis of the dipolar magnetic field is inclined by an angle β with respect to the stellar rotation axis OP . The rotational equator is presented by a thick line. In such a configuration, chemical elements may diffuse upwards through the stellar atmosphere and e.g. accumulate in the area around the magnetic pole M . Figure taken from Kochukhov (2003).

Spot Modelling

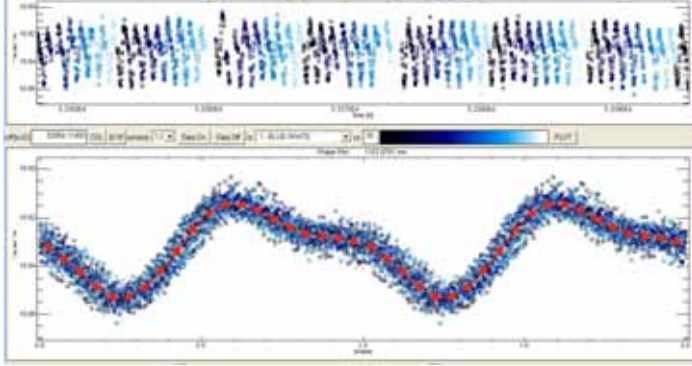


Figure 2: MOST light curve and phase diagram of an Ap star, showing rotational modulation with a period of 0.8 d.

A very successful tool for gaining information on inhomogeneities on the surface of a rotating star caused by changing temperature, abundance and/or magnetic field structure is the technique of Doppler imaging (DI), where time series of photometric, spectroscopic and/or spectropolarimetric observations of rotating stars based on complex mathematical procedures are inverted into temperature structures (cool, active stars) or elemental surface abundances (ApBp stars).

With the MOST space photometer (Walker, Matthews et al. 2003; Matthews et al. 2004) it was already possible to monitor the rotationally modulated light curves of a number of ApBp stars, as presented in Figure 2. For the cool active star κ^1 Ceti photometric observations from different observing seasons could even be used to trace the differential rotation of various spots (see Figure 3) on the surface of this star using StarSpotz (Croll 2006), a program developed specifically to analyse space photometry.

With BRITE Constellation we will be able to obtain space-quality *light* and *color curve variations* of more than 100 CP2 (and CP3 stars) and thus have the possibility to derive surface abundance inhomogeneities (in combination with ground-based spectroscopy) of numerous stars. This will considerably increase the sample of mapped ApBp and HgMn stars, which is indispensable when trying to explore and understand the physics and interaction of diffusion, magnetic fields and rotation.

According to recent investigations (Kaiser et al. 2007, this workshop), we will have access to more than 170 ApBp and HgMn stars spanning the whole

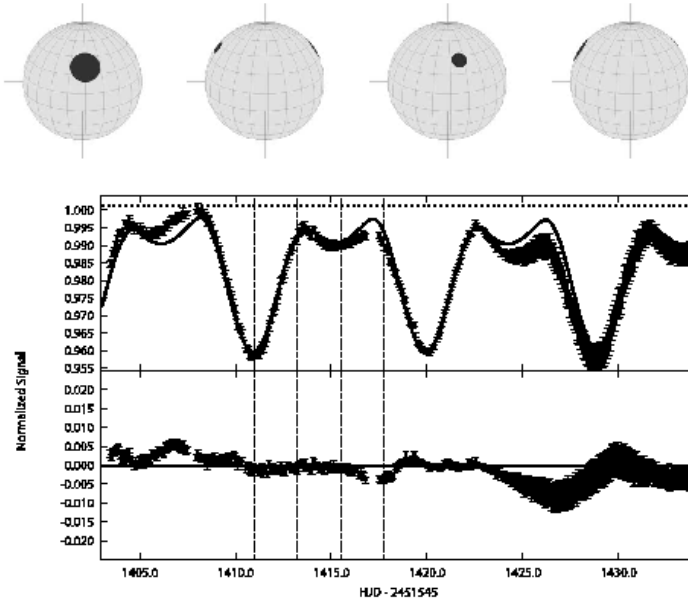


Figure 3: The best fitting two-spot solution for κ^1 Ceti in 2003, seen at phase 0.00, 0.25, 0.50, and 0.75, rotating counterclockwise from left (top panel). In the middle, the corresponding MOST light curve (with errors) is presented and below, the residuals from the model on the same scale are plotted. Figure taken from Walker et al. 2007;

temperature range from 6500 K (and below) up to 30 000 K. Apart from the possibility to cover this huge temperature domain, the region around 6500 K and cooler will be of special interest as exactly there the global magnetic fields of ApBp stars 'switch' into locally strong fields of cool, active stars, resulting in temperature (rather than abundance) inhomogeneities, as e.g. observed for the sun.

Outstanding candidates

At this stage we would like to mention already a few by now outstandingly interesting candidates for our investigations:

CU Virginis

CU Vir (HD 124224, HR 5313) is a bright ($V=5.01$ mag), very fast rotating B9pSi star ($v_e \sin i=160 \text{ km s}^{-1}$) exhibiting photometric, spectrum and magnetic variations. CU Vir shows also one of the shortest known rotational periods for Ap stars and Pyper et al. (1998) found evidence for an abrupt period decrease from 0.5206778 d to 0.5207031 d, most likely due to a breaking mechanism associated with the star's magnetic field ('magnetic breaking').

In Figure 4 O-C diagrams (U+u and B+b light curves) for CU Vir are presented, where panels a and b present the data plotted with *one* constant period of $P_1=0.5206778$ d, which best fits the observations before 1985 (2446000), and in b and c two constant periods, P_1 and $P_2=0.5206778$ d, were applied. It is obvious from the graphs, that with the combination of two different values the observational data obtained over a time span of more than 40 y can be fit best.

In addition, CU Vir was detected as a radio source in 1994 (Leone et al. 1994) and recent investigations give evidence (Kellet et al. 2007) for pulsar-like emission of a highly collimated coherent polarised radiation from one of the stellar magnetic poles.

Observations with BRITe Constellation will facilitate to enable crucial investigations, if the change of the rotational period of CU Vir continues. Spectroscopic DI studies of CU Vir have already been carried out by Kuschnig et al. (1999) and we will be able to test and calibrate our photometric investigations on the necessary (already obtained) ground based spectroscopic results.

Moreover it will be possible to carry out similar, pioneering investigations of potential rotational period changes for numerous other ApBp stars. So far only two more stars of this type, 56 Ari (Adelman et al. 2001) and HD 37776, were detected to show a period decrease linked to the stellar magnetic field.

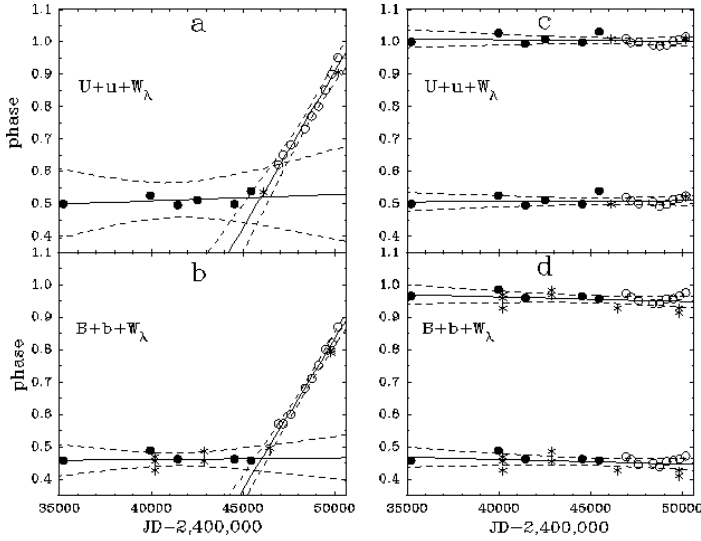


Figure 4: O-C diagrams of CU Vir; a and b: one constant period was used; c, d: fit with two periods. Filled circles indicate photometric observations obtained before 1985 (2446000), open circles those obtained after 1985 (2446000). In a and b the dashed lines mark the 99% confidence level, while in c and d the upper and lower lines represent light and spectrum minima and maxima, respectively. Spectroscopic observations are represented by asterisks, where in (a,c) $W_\lambda(\text{Si II } 6347)$ and in (b,d) $W_\lambda(\text{Si II } 4128-31, 4201)$ are plotted. Figure taken from Pyper et al. 1998;

α Circini

α Cir (HD 128898, HR 5463) is a very bright ($V=3.19$ mag) member of the pulsating subgroup of the Ap stars (roAp) and was discovered to have a period of 6.83 min in 1987 by Kurtz & Cropper.

With a $v_e \sin i=12.5 \text{ km s}^{-1}$ and a rotational period of $P=4.4790(1) \text{ d}$ this star is an ideal candidate to determine the stellar surface structure and probe the influence of the magnetic field on pulsation.

Another prominent member of the roAp stars, HD 24172 (HR 1217) has been observed and analysed spectroscopically (Ryabchikova et al. 2006, Lüftinger et al. 2007) and photometrically (by the MOST space photometer, Cameron et al. 2006). The MOST-campaign revealed, in addition to pulsational frequencies detected already during ground based observing campaigns additional frequencies that are shifted due to the influence of the magnetic field.

Similar investigations for α Cir with BRITE Constellation have the potential to reveal comparable effects of another prototypical member of this group of stars and to test observational and recent theoretical investigations (Cunha et al. 2006, Saio et. al. 2005) that try to explain the correlation and interaction of the various astrophysically crucial processes present in these stars.

α Andromedae

HgMn (CP3) stars and their prominent member α Andromedae have recently come into the focus of scientific interest, as a seven-year monitoring (Kochukhov et al. 2007) of this non-magnetic star revealed a secular evolution of its mercury cloud cover. It is the first time that we observe such a dynamical structure formation process, where possibly the heavy-element clouds created by atomic diffusion (Michaud et al. 1974) are affected by a non-equilibrium dynamical evolution, possibly based on the same physical processes as weather patterns on giant planets and the earth (Kochukhov et al. 2007). With BRITE Constellation we will be able to further monitor the evolution of 'stellar weather' in α And (and its timescale) and possibly similar effects in other HgMn stars.

Summary

The unique potentials of data obtained with BRITE Constellation are:

- the ability to obtain long-term, continuous space-quality light curves, which is crucial to perform spot modeling from photometric data. In the context of DI we benefit from the fact that light curves are particularly sensitive to structure in equatorial and low-latitude bands (Unruh et al. 1995)

- besides analysing inhomogeneous stellar surface structures, we will be able to obtain precise, hitherto unknown, rotational periods for a number of stars
- the possibility to find evidence for a breaking mechanism associated with stellar magnetic fields, as already observed for e.g. the Ap star CU Vir.
- we will have the opportunity to find pulsational frequencies not detectable via ground based observations (due to a much lower noise level) and to trace the influence of magnetic fields on the frequency pattern of magnetic pulsating stars.

Thus, we will be able to provide, with the further development of theoretical aspects, new information for diffusion properties within stellar atmospheres and to obtain new insights in the atmospheric structure formation and the complex interplay of abundance variations, pulsation and magnetic fields in CP stars.

Hence, these stars provide unique access to otherwise invisible stellar interior processes and structures, making them extremely useful as stellar laboratories to explore and understand the physics of many complex, interacting phenomena, presumably also present in other types of stars.

References

- Adelman, S.J., Malanushenko, V., Ryabchikova, T.A., et al. 2001, *A&A*, 375, 982
- Babel, J. 1992, *A&A*, 258, 449
- Croll, B., Walker, G.A.H., Kuschnig, R., et al. 2006, *ApJ*, 648, 607
- Kaiser, A. 2007, these proceedings
- Cunha, M.S. 2006, *MNRAS*, 365, 153
- Kellett, B.J., Graffagnino, V., Bingham, et al. 2007, *arXiv:astro-ph/0701214v1*
- Kurtz, D.W. 1982, *MNRAS*, 200, 807
- Kurtz, D.W., Cropper, M.S. 1987, *MNRAS*, 228, 125
- Kuschnig, R., Ryabchikova, T.A., Piskunov, N.E., et al. 1999, *A&A*, 348, 924
- Kochukhov, O. 2003, PhD Thesis
- Kochukhov, O., Adelman, S.J., Gulliver, A.F., et al. 2007, *NatPh*, 3, 526
- Leone, F., Trigilio, C., Umana, G. 1994, *A&A*, 283, 908
- Lüftinger, T. 2007, PhD Thesis
- Matthews, J.M., Kuschnig, R., Guenther, D.B., et al., 2004, *Nature*, 430, 51
- Michaud G. 1974, *ApL*, 15, 143
- Michaud G. 1970, *ApJ*, 160 640
- Preston, G.W., 1974, *Ann. Rev. Astron. Astrophys.* 12, 257

- Pyper, D.M., Ryabchikova, T., Malanushenko, V., et al. 1998, A&A, 339, 822
- Ryabchikova, T., Nesvacil, N., Weiss, W.W, et al. 2004, A&A, 423, 705
- Ryabchikova, T., Sachkov, M., Weiss, W.W., et al. 2007, A&A, 462, 1103
- Saio, H. 2005, MNRAS, 360, 1022
- Unruh, Y.C., Collier C.A., Cutispoto, G. 1995, MNRAS, 277, 1145
- Vauclair, S., Dolez, N., Gough, D.O., 1991, A&A, 252, 618
- Walker, G., Matthews, G., Kuschnig, R., et al. 2003, PASP, 115, 1023
- Walker, G., Croll, B., Kuschnig, R., et al. 2007, ApJ, 659, 1611

Observing γ Doradus Stars with BRITE - an Outlook

M. Gruberbauer¹, R. Neuteufel¹, W. W. Weiss¹

¹ Institut für Astronomie, Türkenschanzstrasse 17, 1180 Vienna, Austria

Abstract

We discuss the advantages and challenges of observing γ Doradus stars with the BRITE-Constellation satellite network and how using these instruments can improve our understanding of these objects.

Introduction

γ Doradus (hereafter γ Dor) stars are a relatively new class of pulsating stars and have been defined in Kaye et al. (1999). These stars are of spectral type A7 to F5 (IV-V) and are, as such, crossing the red edge of the classical instability strip in the HR diagram, close to the much better studied class of δ Scuti stars. The pulsations are assumed to be due to high-order, low-degree g-modes, which results in periods ranging from about 8 to 80 hours. Their g-mode nature is what makes γ Dor stars very interesting asteroseismic targets, since these modes probe the interiors of stars. While the driving mechanism, attributed to the blocking of radiative energy transport by convection at the base of the convective envelope, is not yet completely understood, models are already able to reproduce basic characteristics of γ Dor stars (Dupret et al. 2006). Since their initial discovery, the number of known γ Dor pulsators has increased and is now probably close to about 100 stars.

Previous observations show moderate amplitudes of light variation, clustering at about 0.04 mag. However, data from current satellite missions like MOST (Microvariability and Oscillation of STars, Walker et al. 2003) yield evidence for much lower amplitudes (e.g. King et al., *in preparation*) which are hard to detect with ground-based observations. Thus, with current space missions and the advent of even more advanced instruments like COROT (Baglin et al. 2002), a dramatic boost in γ Dor discoveries can be expected.

Aside from “normal” γ Dor stars also four hybrid pulsators, showing also characteristic frequencies of δ Scuti stars, have been found as of yet. Two of these discoveries have been made from space (Rowe et al. 2006, King et al. 2006). These are especially interesting, since the presence of g- and p-modes

allows to probe not only the deep interior but also the outer envelope of the star. An overview of the state of asteroseismology of γ Dor stars can be found in Handler (2005).

BRITE (BRiGht Target Explorer)-Constellation (hereafter BRITE-C) is a network of nanosatellite pairs designed for asteroseismic observations of the brightest stars ($m_V < 6$). The satellites will operate in low-Earth orbit (LEO) and as a network, they will be able to observe stars over very long time bases in the order of weeks or months, depending on the position of the target. Each pair will be able to deliver colour information, since each of its satellites is equipped with a different filter. For more information on BRITE-C we refer to other papers in these proceedings.

γ Dor stars and Space Missions

For every type of pulsating stars, mode identification is the primary goal of frequency analysis and in most cases a necessary step for fitting model frequencies to test pulsation theory. Alas, γ Dor stars have several properties which make mode identification a very delicate problem. Since γ Dor stars have periods which are of the same order as their rotation periods, the impact of rotational effects on the frequency spectrum has to be considered. Even more fundamental, the time-scale of their oscillations can lead to misinterpretation of other types of variability (e.g. binarity, rotational modulation) or instrumental trends as g-mode pulsation. It is therefore very important that each newly proposed member of the γ Dor class is unambiguously identified as a pulsating star. For white light photometry as in the case of MOST or the SISMO field of COROT (for a COROT-specific summary on γ Dor observations see Mathias et al. 2006), additional colour information or spectroscopy should be taken into consideration, unless the frequency spectrum is dense enough to rule out any other source of variability than stellar oscillations.

Advantages of Observing γ Dor Stars with BRITE-C

As stated in the introduction, BRITE-C is planned to be composed of nanosatellites with different optical filters. Consequently, it will be the only space mission designed for asteroseismology which is able to deliver well-defined colour information. In case of serendipitous discoveries of new γ Dor stars, which could not be identified as variable from ground, this will be a very useful tool to assess the nature of their frequencies. Also, the phase differences and amplitude ratios between the different filters will help to put constraints on the mode identification.

BRITE-C is designed to look at stars over a very long time-base and without daily gaps and hence avoiding $1\ d^{-1}$ aliasing, which is common to single-site observations from ground. The merit is a much cleaner window function, compared to ground-based observations.

Long time-bases are very important for increasing the frequency resolution which is proportional to $1/\Delta T$, where ΔT is the length of the time series. The same proportionality also applies to the frequency uncertainty. Thus, longer time-bases deliver smaller upper limits for the error bars of the actual frequency values (Kallinger et al. 2007). Both, the clean window function and the increase in frequency resolution are needed in order for the dense but narrow frequency spectrum of multi-mode γ Dor stars to be clearly resolved. Eventually, also the precision of about 1 mmag per data point, which the designers of BRITE-C are aiming for, is well suited for γ Dor stars.

Challenges

The biggest challenge when employing satellites for highly precise time-series measurements is the stability of the instruments. Satellites in a LEO are subject to scattered earthshine, which produces artificial signal at the satellite's orbital frequency (and harmonics). Additionally, long-term trends and daily modulation of the earthshine intensity, produced by albedo changes due to the Earth's rotation, can show up in the low-frequency part of the spectrum (see Reegen et al. 2006 for a discussion of these effects for the case of the MOST satellite). Constant monitoring and correction for these effects is very important, especially for slowly pulsating stars, whose periods are in the order of several orbit periods. Consequently, we propose that several comparison stars should be observed together with programme stars. This condition will be fulfilled due to the large field of view of 24 degrees where typically 4 bright stars can be observed simultaneously. Having multiple satellites observing the same targets will also be beneficial, due to the fact that purely instrumental trends will have different characteristics for each instrument.

Observing strategy for γ Dor stars

The BRITE-C satellites will most likely not be suitable for extensive variability surveys, since the faintest stars BRITE-C will be able to observe with the required minimum accuracy are at $m_V \sim 6$. Also, the stars should not lie in crowded fields to ensure that overlapping point spread functions (PSF) of other stars do not introduce parasitic signal. A list of proposed candidates is shown in Table 1. Also, the search for hybrid pulsators amongst these γ Dor

HD	sp. t.	V	reference	comments
218396	A5V	5.964	Rodriguez et al. 2006	multi-mode γ Dor
206043	F2V	5.783	Henry et al. 2001	multi-mode γ Dor
147787	F4IV	5.27	de Cat et al. 2006	SB, γ Dor cand.
166114	F2V	5.858	Handler 1999	γ Dor cand.
153580	F6V	5.285	Baade & Kjeldsen 1997	B, γ Dor cand.

Table 1: Promising BRITE-C γ Dor targets; SB : spectroscopic binary; B : star in binary system

stars/candidates or targets of the BRITE-C δ Scuti-programme should be pursued. Ground-based spectroscopy and Adaptive Optics imaging should further help to optimize the target selection.

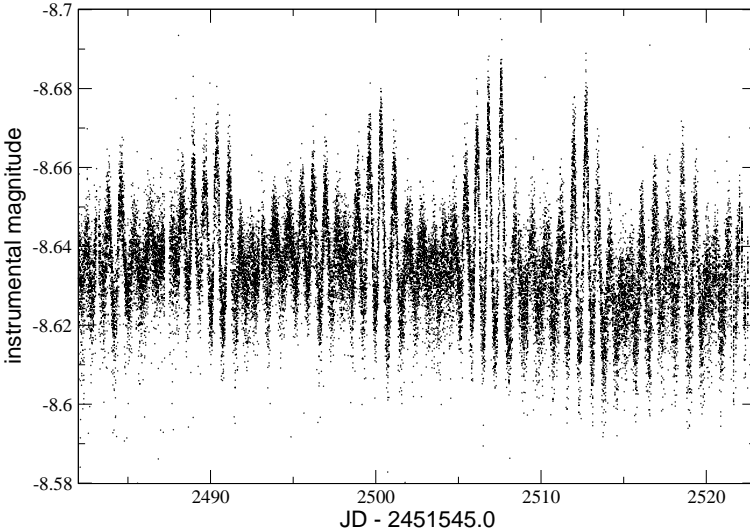


Figure 1: The time series of a recently discovered γ Dor star, as observed by the MOST satellite. BRITE-C will be able to deliver similarly exciting results due to the long time-bases and colour information.

Conclusions

In order to progress with the study of γ Dor stars, to improve and test theory (e.g. modelling of eigenfrequencies, driving mechanism, rotational effects) unambiguous detections with optimized instruments are needed. Furthermore,

it is crucial that the frequency spectra of multi-mode γ Dor stars are better understood BRITE-C will be an ideal contributor in this field by delivering data sets of excellent quality. The long time-bases will help to resolve the frequencies in which the most complex γ Dor stars pulsate, while the colour information, which no other current or soon-to-be-launched space mission except for BRITE-C is able to deliver, can be used for mode identification. Figure 1 shows a light curve of a γ Dor star, recently discovered by the MOST satellite (King et al., *in preparation*), with a beating signature clearly hinting at multi-mode pulsation. We hope that it is also an outlook on what can be achieved with BRITE-C.

Acknowledgments. The authors would like to thank Gerald Handler for his contribution to the discussion. WWW is supported by the Austrian Science Promotion Agency (FFG - MOST). MG, RN and WWW are supported by the Austrian Science Funds (FWF - P17580).

References

- Baade, D., Kjeldsen, H. 1997, A&A, 323, 429
Baglin, A., Auvergne, M., Barge, P., et al. 2002, ESA-SP, 485, 17
de Cat, P., Eyer, L., Cuypers, J., et al. 2006, A&A, 449, 281
Dupret, M.-A., Grigahcène, A., Garrido, R., et al. 2006, MmSAI, 77, 366
Handler, G. 2005, JApA, 26, 24
Handler, G. 1999, MNRAS, 309, 19
Henry, G.W., Fekel, F.C., Kaye, A.B., et al. 2001, AJ, 122, 3383
Kallinger, T., Reegen, P., Weiss, W.W. 2007, A&A, submitted
Kaye, A.B., Handler, G., Krisciunas, K., et al. 1999, PASP, 111, 840
King, H., Matthews, J.M., Rowe, J.F., et al. 2006, CoAst, 148, 28
Mathias, P., Matar, E., Jankov, S., et al. 2006, MmSAI, 77, 470
Reegen, P., Kallinger, T., Frast, D., et al. 2006, MNRAS, 367, 1417
Rodriguez, E., Costa, V., Zhou, A.-Y., et al. 2006, A&A, 456, 261
Rowe, J.F., Matthews, J.M., Cameron, C., et al. 2006, CoAst, 148, 34
Walker, G., Matthews, J., Kuschnig, R., et al. 2003, PASP, 115, 1023

β Pictoris: Planets and Pulsations

K. Zwintz¹

¹ Institut für Astronomie, Türkenschanzstrasse 17, 1180 Vienna, Austria

Abstract

The A5 dwarf star β Pictoris has been subject of numerous studies because it addresses several questions of stellar astrophysics, like stellar evolution, circumstellar disks, planet formation and pulsations.

With $V = 3.86$ mag, it falls within the observable magnitude range of BRITE and is a promising target for this space mission.

Evolutionary stage

One of the open questions is the evolutionary stage of β Pic. Latest age determinations agree to 20 ± 10 million years (e.g., Barrado y Navascues et al. 1999), but with an upper limit of a factor of 10 more. From its position in the Hertzsprung-Russell (HR) diagram (e.g., Vidal-Madjar et al., 1998) it is right on the zero-age main sequence or slightly before. In other terms, β Pic is either a pre-main sequence (PMS) object or a young main sequence star. The debate about its evolutionary stage is still ongoing, but there are indications for the early main sequence phase: the star shows no emission lines in its spectrum, which would be characteristic for the PMS phase. Also, there is no star forming region nearby from which it could have been recently emerged, and the interstellar medium around β Pic is rather thin (e.g., Vidal-Madjar et al., 1998).

Circumstellar disk

β Pic's massive circumstellar disk was first discovered by IRAS observations in 1983 as a large and unexpected infrared excess which was then called "Vega like phenomenon". A year later Smith & Terrile discovered that the dust disk is seen edge on and that it at least extends to 400 AU around the star. As the lifetime of the dust grains is shorter than the star's age, the grains must form permanently. This can be explained by collisions among large, kilometer-sized bodies like comets or by slow evaporation (Smith & Terrile, 1984).

Vidal-Madjar et al. (1998) report that the disk around β Pic extends up to 1100 AU around the star, i.e., a size of 10 times our solar system. The disk was found to be structured, showing a cleaner, dust-free region at 35 AU from the star. The authors also discovered that the inner part of the disk is slightly warped which can only be explained by at least one giant planet.

Thanks to several, successive Hubble Space Telescope (HST) observations, the most detailed picture yet of a dust disk surrounding a nearby star is available for β Pictoris. These measurements confirmed the slightly warped disk and brought indirect evidence for a large planet orbiting the star within the inner clear zone: The suspected planet itself is too faint to be seen against the bright star, but it is gravitationally sweeping up dust and icy planetesimals from the disk.

Planet(s) around β Pictoris?

One planet at 12 AU with $2 M_{\text{Jupiter}}$ can already explain the observed warp in the disk and 2 of the 4 belt-like structures which were discovered by HST. With two additional planets the other two belts with planetesimals can be explained, where strong upper limits for those planets can be given: one planet should have $2 M_{\text{Saturn}}$ at a distance of 25 AU, the other $4 M_{\text{Neptune}}$ at 44 AU (Freistetter et al., 2007). But no planetary transits have been observed yet.

Pulsations

During the search for a planetary transit around β Pic, δ Scuti like pulsations have been discovered in the star. Koen (2003) identified three frequencies at 47.055, 38.081 & 52.724 d^{-1} with amplitudes below 1.5 mmag using photometric time series in Johnson B filter obtained within 4 nights. Using a 50-cm telescope and a classic PMT still a neutral density filter had to be used to enable the observations of such a bright star.

Spectroscopic time series observations (Koen et al., 2003b) obtained with the GIRAFFE spectrograph at the SAAO 1.9-m telescope clearly show line profile variations. The 18 frequencies inferred from these data were identified to be high-degree, non-radial pulsation modes.

β Pictoris and BRITE

Using the characteristics of BRITE and its detector, 6 unpolluted objects are lying within the field of view of 24° around β Pictoris (see Figure 1). Hence, they could be observed simultaneously.

With the photometry provided by BRITE, the pulsations of β Pic at low amplitudes could be studied in more detail. This is complicated from ground due to the relative brightness of the star. The first detection of a planetary transit lies also within reach of observations with BRITE which would finally provide observational evidence for the theory.

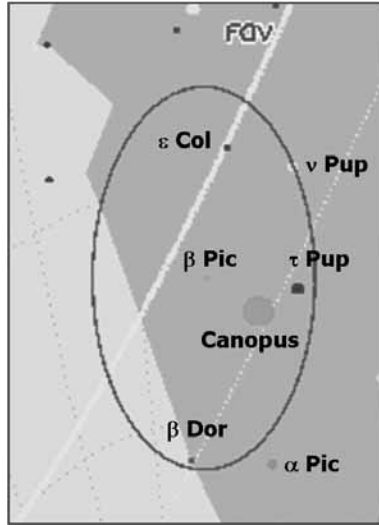


Figure 1: BRITE field of view centered on β Pictoris (Kaiser, priv. comm.).

Acknowledgments. KZ acknowledges funding through the Austrian Science Funds (FWF, project T335-N16). Use was made of the HST webpage (<http://www.stsci.edu>).

References

- Barrado y Navascués, D., Stauffer, J.R., Song, I., et al. 1999, ApJ, 520, 123
 Freistetter, F., Krivov, A.V., Lhne, T. 2007, A&A 466, 389
 Guenther, D.B., Kallinger, T., Zwintz, K., et al. 2007, ApJ, in press
 The Hipparcos and Tycho Catalogues, ESA 1997, ESA SP-1200
 Koen, C. 2003a, MNRAS, 341, 1385
 Koen, C., Balona, L.A., Khadaroo, K., et al. 2003b, MNRAS 344, 1250
 Smith, B.A., Terrile, R.J., 1984, Science, 226, 1421
 Vidal-Madjar, A., Lecavelier des Etangs, A., Ferlet, R. 1998, P&SS, 46, 629

Stellar Activity with BRITE: the “Aurigae” field

K. G. Strassmeier

Astrophysical Institute Potsdam (AIP)
An der Sternwarte 16, D-14482 Potsdam, Germany

Abstract

Photometric time series of active stars can pin down some of the ingredients that govern the stellar magnetic field, itself being the driver of all non-thermal stellar emissions. Among the most important – and least understood – astrophysical ingredients is stellar rotation and its subtle latitudinal dependence called differential rotation. Rotation switches on and maintains the internal dynamo, itself a phenomenon from the interaction of turbulent plasma motions and large-scale shearing forces in the deep stellar interior. I propose to observe the active binary Capella, made up of two giants in exposed locations in the HR-diagram. Along with Capella (α Aur), another eight stars brighter than 4th magnitude would be in the field-of-view of BRITE, among them such benchmark variables as ζ Aur or θ Aur.

Motivation

The interaction of a stellar magnetic field with its surrounding plasma appears to be the source of a large variety of atmospheric phenomena that can be used to better understand a star and its evolution itself as well as study its environment. Such magnetic-field related phenomena were collectively coined “stellar activity”. Our magnetic Sun and the many non-thermal energetic phenomena from its interaction with the outer heliosphere, also known as “space weather”, play even a central role for our own planet. Therefore, stellar-activity studies continuously moved central stage after the discovery of extra-solar planets back in the mid nineties. The reason is the many connections between the parent star’s output and the impact on its planetary system, from the time of its formation until its habitability.

Magnetic fields brake the rotation of the collapsing pre-stellar cloud enabling star formation in the first place and, later, couple the rotation of the star with its pre-planetary disk. This is a violent time for the star. But even much later, at the age of the Sun, its magnetic field still emits energetic radiation

conductive to the destruction of complex molecules in the upper Earth atmosphere. It also governs the habitability of the biosphere through this energetic particle bombardment. The Earth's magnetic field again protects us from it. Understanding solar and stellar magnetic activity likely holds the key to glimpse into the galaxy's biological evolution, if there is one. The search for Earth-like planets is part of this enterprise. Therefore, we believe that studying the rotation of (low-mass) stars that harbor significant magnetic fields, i.e. active stars, provides the physics for such illuminative questions as whether life could exist elsewhere in the universe.

Stellar activity and photometry

A magnetically-active star will show variations of its brightness because dark spots or bright plages will move in and out of view as the star rotates. It enables the observation of very precise stellar rotational periods and, coupled with knowledge of its radius, the determination of the star's specific angular momentum; for low-mass stars at certain stages in their evolution this is a rather important physical quantity. Monitoring the brightness variations over many consecutive stellar rotations can be used to infer the surface spot and plage evolution, itself being just localized magnetic flux. Modern mathematical inversion methods allow the recovery of the two-dimensional surface structure from individual light curves (e.g. Savanov & Strassmeier 2007, among others), given that they can be obtained nearly uninterrupted.

Furthermore, one can isolate the rotational period for each latitudinal strip on the surface at which a spot or a plage appears, thereby detecting and measuring differential surface rotation, one of the two main ingredients for a stellar dynamo (the other is helicity).

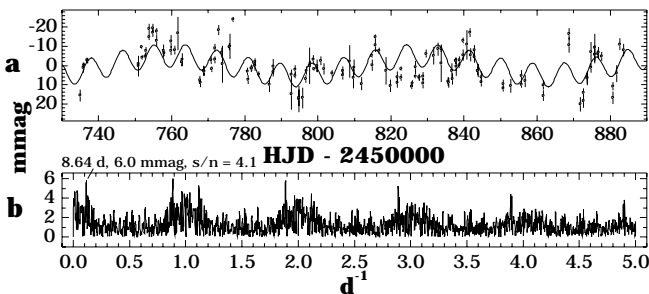


Figure 1: a The H α -light curve of Capella during the observing season 1997/98 (dots with error bars) and the fit from a two-frequency solution with a 106-day and a 8.6-day period. b The amplitude spectrum for the above data.

Is BRITE relevant for active-star photometry?

Yes, even given the brightness limit of 4th magnitude for 1-mmag precision, but being a bit generous and expanding this to 5th magnitude, we find a total of 17 active stars in the sky. All of them are evolved stars. The brightest five (all brighter than 4.2mag) are luminosity-class III giants, again all of them binaries and one even in an eclipsing system. Only two are single Hertzsprung-gap¹ giants. In this respect, BRITE’s golden bullet would be to monitor an active giant’s rotationally modulated light curve for a long duration in time.

What you usually can’t do from the ground

Observing bright stars with small amplitudes from the ground is a painstaking challenge, if possible at all. Fig. 1 shows our photometry of the brightest active star in the sky, $V=0.1$ -mag Capella (α Aurigae). This data was taken with one of the two 0.75m Vienna APTs equipped with a 5-mag neutral density filter and a narrow-band $H\alpha$ filter. We believe we have detected the rotational periods of both stellar components of Capella (Strassmeier et al. 2001). The brighter K giant appears to rotate with 106 days and the fainter but more active early-G giant with 8.6 days. However, the quality of the data is such that these periods have large error bars or can even be questioned but, what is more important, the Capella system appears to be an important laboratory for testing tidal friction theories – synchronization, circularization and coplanarity – in combination with stellar evolution theory.

The Capella system: what’s so interesting?

Astrophysical parameters of giant stars are uncertain because there are just a few such stars that can be studied in spectroscopic binary systems, and even less that are also eclipsing binaries. Roche lobe overflow and mass exchange set a limit to the stellar radius in a close binary. Non-interacting binaries with giant components have therefore mostly very long orbital periods and are difficult to observe within an astronomer’s lifetime. There are, however, a few systems that have sufficiently short orbital periods (see, e.g., Andersen 1991). Capella is such a system and consists of an active G1III and a G8-K0III component (Strassmeier & Fekel 1990) in a 104-day orbit.

The present position of the G1III component in the Hertzsprung gap, where it is approaching the base of the giant branch, indicates violent changes are taking place in its internal structure; the mass of the convection zone increases rapidly as does also the total stellar moment of inertia. We may expect that

¹When crossing the Hertzsprung gap the star quickly redistributes internal angular momentum and causes increased surface rotation for a brief period in time.

this has a profound impact on the visible surface rotation. Precise rotation periods of stars in this evolutionary stage may thus help to further understand the angular-momentum loss in late-type stars.

Shcherbakov et al. (1990) discovered a modulation of the He I $1.08\mu\text{m}$ equivalent width with the 104-day orbital period. This variation, and its periodicity, was later confirmed by Katsova & Shcherbakov (1998). The latter authors also concluded that the main He I-absorption line must originate in the chromosphere of the quiescent *cool* component, while the residual helium emission and the highly ionized iron lines are thought to be connected with a magnetized wind that originates from plages on the active *hot* component and then forms a shock wave in the corona of the cool component. Therefore, chromospheric emission is expected from both components.

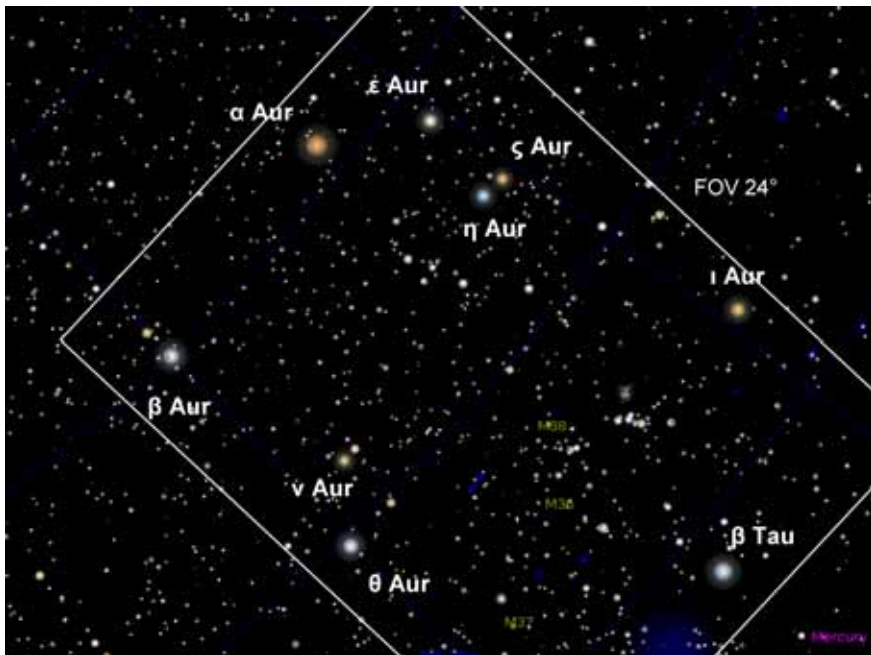


Figure 2: The proposed “Aurigae” field. It contains nine variable stars brighter than 4th magnitude. The brightest being the active binary Capella but each one represents a distinctive class of its own with a large variety of astrophysical challenges.

Conclusion: observe a 24-degree field in Aurigae

My proposal is to dedicate BRITE time to Capella. Sampling requirement would be one measurement per satellite orbit, but at least one every 1-2 hours, for a total duration of >104 days (the orbital period). Comparably short exposures and on-board coadding of many CCD frames would be required. Simultaneous Doppler imaging of the G-giant during the two quadrature phases with our ground-based facility STELLA/SES could be provided and would make up a unique data set. Additionally, the Capella position in the sky is very favorable for catching other, bright stars at the same time, some of them famous variable stars with lots of unknown astrophysics. Table 1 is a summary of these stars.

β *Aur* is a detached eclipsing binary that was used recently to determine non-linear limb-darkening coefficients for both of its components based on high-precision photometry from the WIRE satellite (Southworth et al. 2007).

ϵ *Aur* is a binary star system that eclipses once every 27.1 years. It is the star with the longest period known to date. The next eclipse is predicted to begin in 2009. The eclipse is flat-bottomed and lasts nearly two years. A mid-eclipse brightening was seen by several observers, including observations from space, and many models appeared for its explanation. Among them a neutron star with a warped semi-opaque disk. Photometry of the primary F star appears to show pulsational variability (Strassmeier et al. 2001).

ζ *Aur* is a long-period eclipsing binary with a K supergiant and a mid-B main sequence star. A recent orbit was determined by Griffin (2005) with a period of 972 days. The importance are the eclipses of the B star when it traverses the chromosphere of the K star, which lasts for some weeks either side of the eclipse. It has been used to probe the K supergiant’s atmosphere as a function of height above the limb.

η *Aur* is a chemically peculiar B3 main-sequence star. It appears to be single. Crawford et al. (1971) lists it as one of their photometric standard stars while Simbad quotes it as a Variable.

θ *Aur* is a well-known chemically peculiar Ap star whose surface elemental distribution had been spatially resolved by means of Doppler imaging. Theta Aur ($P = 3.6188$ d) exhibits large amplitude variations with two components contributing to the light minima (e.g. Adelman 1997).

ν *Aur*. Numerous photometric observations of this star exist but were mostly taken in the reference of standard-star all-sky photometry (e.g. Oja 1985, Eggen 1963). It is not conclusively known whether it is a micro variable or not. Simbad lists it as part of a wide binary.

ι *Aur*. Although a suspected variable, its light variability has not been proven so far. The star is a single K3 bright giant. Recently, Lèbre et al. (2006) determined its lithium abundance and gave a summary of its rotational

Table 1: Stars brighter than 4th magnitude in the “Aurigae” field.

Star	<i>V</i> (mag)	Sp. type	Type of variability	Notes
α Aur	0.1	G1III +K0III	Rotation	Binary with two giant stars
β Aur	1.9	A2IV+	Eclipsing	Detached eclipsing system
ϵ Aur	3.0	F0Ia	Eclipsing	Binary with longest known
			Pulsating	orbital period
ζ Aur	3.8	K4Ib +B6V	Eclipsing	Atmospheric eclipses
η Aur	3.1	B3V	Rotation	Chemically peculiar B star
θ Aur	2.6	A0p	Rotation	Magnetic chemically peculiar star
ν Aur	4.0	K0III	unknown	Binary
ι Aur	2.7	K3II	unknown	Suspected variable
β Tau	1.7	B7III	unknown	Chemically peculiar HgMn star

properties.

β *Tau*. Also known as γ Aur. Again, no continuous photometry seems to exist of this very bright binary. It has received substantial attention after it was listed among the few mercury-manganese stars (see Adelman et al. 2006).

Acknowledgments. I thank Werner Weiss and Michel Breger for inviting me to this workshop. Substantial use was made of the SIMBAD data base run by CDS Strasbourg.

References

- Adelman, S.J. 1997, PASP 109, 9
- Adelman, S.J., Caliskan, H., Gulliver, A.F., et al. 2006, A&A 447, 685
- Andersen, J. 1991, A&AR 3, 91
- Crawford, D.L., Barnes, J.V., Golson, J.C. 1971, AJ 76, 1058
- Eggen, O.J. 1963, AJ 68, 483
- Griffin, R.F. 2005, The Obs. 125, 1
- Katsova, M.M., Shcherbakov, A.G. 1998, A&A 329, 1080
- Lèbre, A., de Laverny, P., Do Nascimento, J.D., et al., 2006, A&A 450, 1173
- Oja, T. 1985, A&AS 59, 461
- Savanov, I., Strassmeier, K.G. 2007, A&A, submitted
- Shcherbakov, A.G., Tuominen, I., Jetsu, L., et al. 1990, A&A 235, 205

Southworth, J., Bruntt, H., Buzasi, D.L. 2007, A&A 467, 1215

Strassmeier, K.G., Fekel, F.C. 1990, A&A 230, 389

Strassmeier, K.G., Reegen, P., Granzer, T. 2001, AN 321, 115



R. Kuschnig, T. Kallinger and A. Kaiser discussing the workshop.

Exploring solar-type pulsation with BRITE

T. Kallinger

Institut für Astronomie, Türkenschanzstrasse 17, 1180 Vienna, Austria

Abstract

It is evident that there is still no complete picture of how pulsation works in stars with convective envelopes. In the past few years the field of observing solar-type oscillations has moved from ambiguous detections to firm measurements. However, I will demonstrate that BRITE is not an appropriate instrument to observe solar-type pulsation in sun-like stars, but rather perfectly suited to detect solar-type oscillations in stars cooler and more luminous than the Sun. Asteroseismology of red giants is still in its infancy and the few currently available high-precision data may not be adequate to answer the open questions. Using clever observing strategies, BRITE can help to significantly improve our understanding of the interaction between pulsation and convection, but also of stellar evolution during the important red giant phase in general.

Introduction

Our understanding of the Sun's structure has been revolutionised over the last three decades by helioseismology. This technique allows investigations of the solar interior by observing p -modes at the stellar surface.

Observing solar-type oscillations in other stars was for a long time not feasible due to the extremely small pulsation amplitudes. As high-precision radial velocity measurements from the ground and ultra-precise rapid photometry from space became available, detections of stochastically driven oscillations were reported for several sun-like stars. Examples include α Cen A (Bouchy & Carrier 2002) and B (Kjeldsen et al. 2005) or Procyon A (Leccia et al. 2007 for radial velocity observations, Bruntt et al. 2005 for WIRE¹ photometry or Guenther et al. 2007 for MOST² photometry). Because of the very low amplitudes (some ppm in luminosity or some ten $\text{cm}\cdot\text{s}^{-1}$ in radial velocity, respectively), it is still an extremely challenging task to observe solar-type oscillations in G- or late F-type main-sequence (or slightly evolved) stars and the number of potential

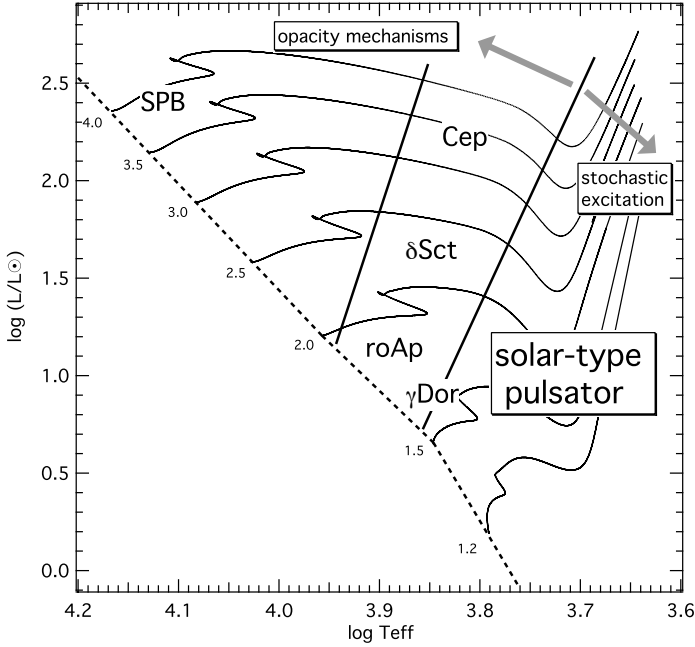


Figure 1: Theoretical HR-Diagram showing examples for regions where pulsating stars are observed.

targets in very limited.

For stars cooler and more luminous than the Sun, however, the amplitudes are greater (some hundred ppm or some $\text{m}\cdot\text{s}^{-1}$) and are more easily observable. The larger radii of red giants extend their pulsation periods from about 5 minutes in the Sun to a range of several hours to several days. This again complicates groundbased detections and frequency identifications, especially due to daily aliasing, making them perfect targets for space-based observations. Examples for pulsating red giants are ϵ Oph (De Ridder et al. 2006 for radial velocity observations and Kallinger et al. 2007 for MOST photometry) or ξ Hya (Frandsen et al. 2002). Currently about a dozen of red giants showing solar-type pulsation are known and at least three additional candidates have been discovered by MOST (not yet published).

¹ *Wide-field InfraRed Explorer* star tracker photometry

² *Microvariability and Oscillation in STars*; a Canadian micro-satellite mission with assistance from the University of Vienna, Austria

Solar-type pulsation

Looking at the HR-Diagram (Fig. 1), one can find various regions where stars tend to show variability. Intermediate mass stars ($> \sim 1.5 M_{\odot}$) cross the classical δ Scuti instability strip (in the center of the HR-Diagram) during their evolution from the main sequence towards the subgiant branch. During this evolutionary phase, stars have an appropriate internal configuration to become pulsationally unstable, presumably driven by the κ mechanism in the hydrogen and helium ionization zones.

Beyond the red edge of the instability strip, stars possess convective envelopes and can show mode instability due to perturbations of their convective flux. It is believed that the acoustic noise generated by the convection in the star's resonant cavity may drive intrinsically stable (hence damped) p -mode pulsation, resulting in damped and stochastically excited (solar-type) pulsation. Unlike p -modes in stars in the classical instability strip, which can coherently oscillate for millions of years, acoustic modes caused by turbulence in the convective envelopes have much shorter lifetimes. Pulsation of this nature can be characterized, in its simplest description, as a superposition of stochastically excited and intrinsically damped harmonic oscillations. The Fourier transform of a set of such incoherent signals produces a broadened peak in the power spectrum, a so-called Lorentzian profile, provided that the time series is infinitely long. For finite data sets, the Fourier transform enforces artificial beating frequencies, randomly distributed under the Lorentzian profile, to reproduce the amplitude (and phase) modulation of the signal.

Such a damped and re-excited mode carries, in addition to the information about the stellar interior (via its frequency), information about the convection zone via its peak envelope in the power spectrum. This can be used to test and improve convection theories as well as nonadiabatic pulsation theory. Fig. 2 (left panel) displays the noise-free synthetic time series of a mono-periodic but strongly damped (with a damping rate of 0.1 per day) and randomly re-excited signal as well as the Fourier amplitude spectrum of the same signal (right panel). The intrinsic mode lifetime (the inverse damping rate) is determined from the line width Γ of a Lorentzian profile function (grey-shaded area in Fig.2) fitted to the amplitude spectrum with $\Gamma = 1/(\pi\tau)$ where τ denotes the mode lifetime.

To date, direct measurements of mode lifetimes (via mode line widths) are available only for the Sun. However, there is the possibility to estimate mode lifetimes indirectly. For solar-type oscillation, the scatter of the largest amplitude peak under the Lorentzian profile around the real mode frequency (center of the Lorentzian profile) is a function of the intrinsic mode lifetime (and the data set length as well as signal-to-noise ratio of the mode). By comparing the observed frequency scatter with extensive simulations, Kjeldsen

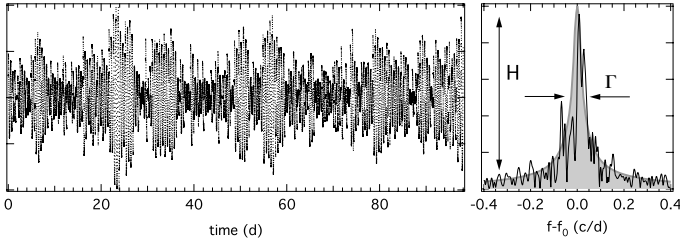


Figure 2: Synthetic light curve of a mono-periodic but strongly damped and stochastically re-excited signal. The Fourier transform enforces artificial beat frequencies, to reproduce the amplitude (and phase) modulation of the signal, causing randomly distributed peaks under a Lorentzian profile (grey-shaded area). The width and height of the profile depend on the damping rate (inverse lifetime).

et al. (2005) determined the mode lifetimes of α Cen A and B to be roughly 2 and 3 days, respectively. Using a similar approach, Kallinger et al. (2007) found a mode lifetime of about 10 to 20 days for p -modes in ϵ Oph.

Solar-type pulsation in sun-like stars

As already mentioned, solar-type oscillations in G and late F-type stars from the main sequence to the end of the hydrogen core-burning (which are generally referred to as sun-like stars) show very small amplitudes and the number of sun-like stars where solar-type oscillations have been detected is quite limited. To date, all known solar-type pulsators have been discovered using high-pressure radial velocity measurements from ground. To observe them photometrically, space instruments are needed. Unfortunately, the currently operating photometric satellite missions MOST and WIRE are not sensitive enough to *unambiguously* observe solar-type oscillations in sun-like stars, even the brightest ones (except for α Cen A). In other words, the photometric amplitudes are smaller than expected (e.g., one of the main goals of MOST was to detect solar-type oscillations in sun-like stars – and the detection limit is actually better than the requirements). The french-lead mission COROT³ should be capable to fill this lack of photometric observations.

However, some sun-like stars are bright enough to be observable with BRITE. E.g., Fig 3 shows a Fourier power spectrum of a simulated photometric time series as we would expect it for the F5 IV star Procyon A. Mode frequencies and amplitudes (scaled from radial velocity amplitudes) are taken from Leccia

³Convection, Rotation and planetary Transits

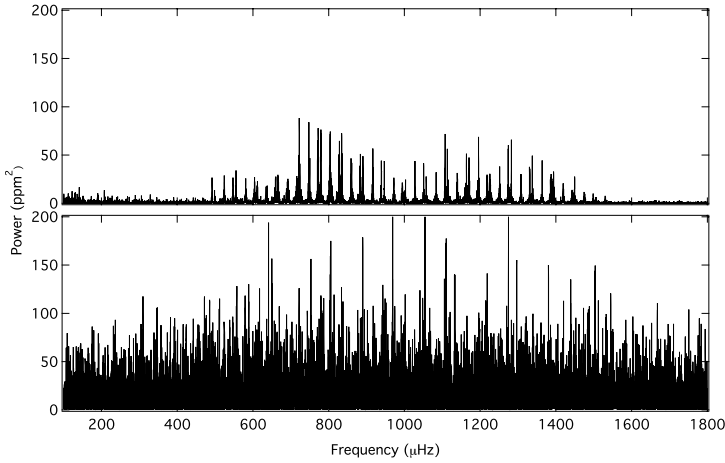


Figure 3: *Top panel:* Fourier power spectrum of a synthetic photometric time series based on radial velocity observations of Procyon A. *Bottom panel:* Same as above but as expected for typical BRITE observations (300ppm point-to-point scatter and 30% duty cycle).

et al. (2007) and have a lifetime of 2 days. The low frequency power comes from a simple granulation noise model with parameters estimated from Bruntt et al. (2005). The power spectrum given in the bottom panel of Fig.3 should illustrate what we can typically expect when observing Procyon A with BRITE. A typical point-to-point scatter of 300ppm (for a $V=0.3$ mag star) was added (A. Kaiser, private comm.), the time series was resampled to 6 sec exposures and the duty cycle was restricted to 30% (typical for a single BRITE satellite). It is obvious that the p -mode signal gets lost in the noise and instrumental signal. Even when increasing the duty cycle to 90% and decreasing the point-to-point-scatter by 50%, no clear signature of the p -mode pattern is evident. Hence, I strongly recommend not to attempt to observe solar-type oscillations in sun-like stars with BRITE.

Solar-type pulsation on the giant branch

The situation changes for more developed stars. As the amplitudes of solar-type oscillation scale with stellar luminosity the signal is more easily observable in red giants. E.g., a typical K0 giant has a luminosity of $50L_{\odot}$ and one can expect an amplitude of about 200ppm for solar-type oscillation (compared to about 4ppm for the Sun) for such a star. However, the increased stellar radius

extends the pulsation periods from about 5 minutes in the Sun to a range of some hours to days. This complicates ground based observations, especially due to daily aliasing, and calls for space observations. Besides the absence of the Earth's atmosphere, space based observations of pulsating cool giants benefit from the satellite orbit. All photometric space missions so far fly in Low Earth Orbits with an orbital period on the order of 100 minutes. Hence, uninterrupted observations with orbital gaps (as it is planned for BRITE) yield a clean spectral window function in the low frequency domain (below ~ 10 c/d) but with alias peaks at roughly 14 c/d (and multiples thereof). This is of particular interest when observing solar-type oscillation in red giant stars because the frequency regime of pulsation is well below the orbital frequency and instrumental aliases do not distort the intrinsic eigenspectrum.

It has been suggested by several authors that only radial p -modes should be observable in red giants while nonradial modes are assumed to be damped. The theoretical position is unclear. Dziembowski et al. (2001) showed the existence of strongly trapped unstable nonradial modes in the central regions of giants in between very closely spaced modes of the same degree l . These modes follow the same pattern of frequency spacing as radial acoustic waves and correspond to mixed g - and p -modes. Only in their linear stability analysis, which includes the effects of turbulent pressure based on the mixing-length formalism, they find amplitudes of the radial modes of the sub-giant star α UMa to be much smaller than observed, with the nonradial mode amplitudes predicted to be even smaller. On the observational side, Hekker et al. (2006) note that the line profile variations of several pulsating red giants suggest the existence of nonradial modes. Apart from this, Stello et al. (2006) found evidence that the mode lifetimes of oscillations in the G7 giant ξ Hya are only about 2 days which is roughly 5 to 10 times shorter than what is inferred from theoretical considerations (Houdek & Gough 2002).

Most recently, Kallinger et al. (2007) found clear evidence for radial and nonradial modes in the G9.5 giant ϵ Oph in both luminosity and radial velocity measurements based on MOST observations and spectroscopic time series (De Ridder et al. 2006), respectively. They fit 18 of the 21 most significant photometric frequencies to radial and $l=1, 2$ and 3 modes (see left panel of Fig.4). The best fitting model lies within the uncertainty of the known position in the HR-Diagram and its interferometrically determined radius (see right panel of Fig.4). The observed frequency scatter is consistent with mode lifetimes of 10 to 20 days.

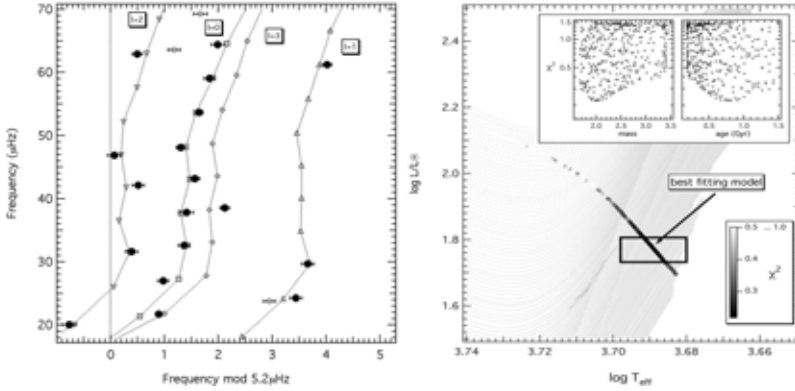


Figure 4: *Left panel:* Echelle diagram of the 21 most significant photometric modes of ϵ Oph used to constrain the best fit. Filled dots corresponds to the 18 frequencies matching model frequencies indicated by grey symbols and connected by line segments. *Right panel:* Theoretical HR-Diagram showing the uncertainty box location of ϵ Oph and a subset of the stellar model grid used for pulsation analysis (small grey dots). The grey scale (large dots) gives the χ^2 values derived from the differences between observed and model modes where the scale is limited to values smaller than 1. The location of the best fitting model is indicated by the arrow. The inserts illustrate χ^2 as a function of model mass and age, respectively.

Observing strategies

As outlined in the previous section, pulsating G and K giants are perfect candidates for photometric long-term observations with BRITe. Contrary to sun-like stars, solar-type oscillations in red giants exhibit amplitudes large enough to be clearly detectable with BRITe. The frequency regime of pulsation fits into a frequency range free from instrumental distortion. Additionally, there are many potential targets with well known fundamental parameters (even the radii are well constrained for most bright giant stars) bright enough to meet the mission requirements.

In terms of a reasonable target selection, however, it has to be mentioned that more luminous (hence larger amplitudes and in most cases also brighter) does not necessarily mean “better” targets. The acoustic cut-off frequency as well as the large frequency separation are inversely proportional to the stellar radius. In other words, for more luminous stars (with a larger radius), the frequency range of pulsation becomes narrower and moves to lower frequencies. This leads to the fact that at a certain point the Lorentzian profiles of consecutive modes start to overlap, making the identification of individual modes

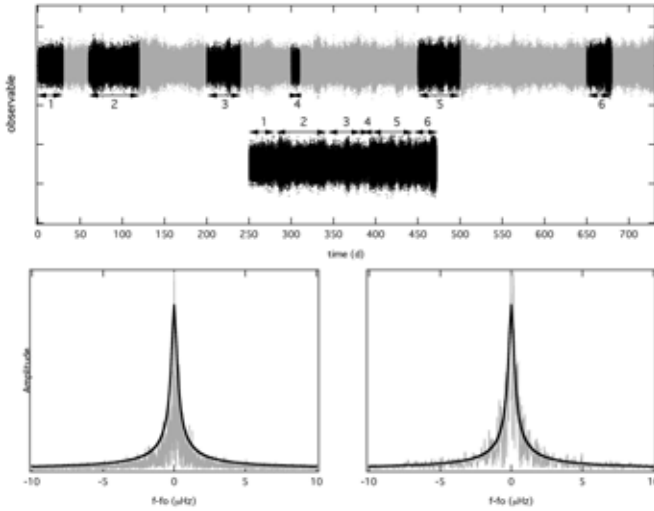


Figure 5: Synthetic time series including a stochastically excited damped signal illustrating that different observations of arbitrary length and epoch *stitched together* yield a reasonable result. The bottom left panel shows the Fourier power spectrum of the entire data set (including a Lorentzian fit). The bottom right panel gives the same but only for the black parts of the simulated time series stitched together.

nearly impossible. Hence, I propose to focus on targets filling up the undisturbed frequency range (up to about 10c/d) and having a large (but also small) frequency separation large enough to obtain clearly separated Lorentzian profiles. This sets a limit to stellar radii roughly smaller than $15 R_{\odot}$ for intermediate mass stars assuming lifetimes longer than 10 days.

To date, only relatively short data sets (on the order of some weeks) of pulsating red giants are available where the fact that the Fourier peak width due to the data set length is comparable to the width of the Lorentzian profile prevents a direct determination of the mode lifetimes (via the profile width). Hence, the current and future challenge in observing solar-type oscillation in red giants is to obtain data sets long enough to actually “see” the Lorentzian profiles in the power spectrum. Therefore, data sets 5 to 10 times as long as the mode lifetime are necessary, corresponding to more than 100 days of continuous observations. Entering a new era of red giant observations, COROT will observe several dozens of red giants for up to 150 days in the Exoplanet program. Unfortunately, only faint stars in small areas in the sky with poorly or even unknown fundamental parameters can be observed, which complicates detailed asteroseismic investigations. For the near future BRITE will be the

only instrument capable to observe *bright* red giants for more than some weeks from space.

Finally, I want to mention that observing red giants for a long time does not necessarily mean to observe them continuously. A damped and stochastically excited signal has the attribute that is not coherent. Hence it has no “phase” in a classical sense like a normal sinusoidal signal. This has the advantage that a solar-type pulsator can be observed during several time-slots and the subsets can be stitched together without paying attention to the gaps (keeping the gaps degrades the spectral window functions). Fig. 5 illustrates such an observing strategy and shows that no artificial signal distorts the power spectrum of a “pseudo-continuous” time series.

Acknowledgments. Financial support was received from the Austrian Research Promotion Agency (FFG) and the Austrian Science Fund (FWF P17580)

References

- Bouchy ,F., Carrier, F. 2002, A&A, 390, 205
Bruntt, H., Kjeldsen, H., Buzasi, D. L., et al. 2005, ApJ, 633, 440
De Ridder J., Barban C., Carrier F., et al. 2006, A&A, 448, 689
Dziembowski, W. A., Gough, D. O., Houdek, G., et al. 2001, MNRAS, 328, 601
Frandsen, S., Carrier, F., Aerts, C., et al. 2002, A&A, 394, L5
Guenther, D. B., Kallinger, T., Reegen, P., et al. 2007, CoAst, 151, 5
Hekker, S., Aerts, C., De Ridder, J., Carrier, F. 2006, A&A, 458, 931
Houdek, G., Gough, D. O. 2002, MNRAS, 336, L65
Kallinger, T., Guenther, D. B., Matthews, J. M., et al. 2007, A&A, in press
Kjeldsen, H., Bedding, T. R., Butler, P., et al. 2005, ApJ, 635, 1281
Leccia, S., Kjeldsen, H., Bonanno, A., et al. 2007, A&A, 464, 1059
Stello, D., Kjeldsen, H., Bedding, T. R., Buzasi, D. 2006, A&A, 448, 709

Identifying pulsation modes from two-passband photometry

J. Daszyńska-Daszkiewicz

Instytut Astronomiczny, Uniwersytet Wrocławski, ul. Kopernika 11, Poland

Abstract

I discuss a prospect for mode identification from two-passband photometry of forthcoming BRIDE space mission. Examples of photometric diagnostic diagrams are shown for three types of main sequence pulsating variables: β Cephei, Slowly Pulsating B-type and δ Scuti stars. I consider also taking into account the radial velocity data from simultaneous spectroscopy, which can be carried out from the ground. With such observations, much better discrimination of the spherical harmonic degree, ℓ , can be accomplished and more constraints on stellar parameters and input physics can be derived.

Introduction

Nowadays space based observations allow detecting oscillation modes with lower and lower photometric amplitudes. We are already at the detection threshold of the order of $10^{-5} - 10^{-6}$ mag, resulting in a growing number of frequency peaks. There are many examples of excellent work both observational and theoretical based on WIRE and MOST data (e.g. Bruntt et al. 2007, Walker et al. 2005, Barban et al. 2007, Saio et al. 2007). Now we expect similar results from the just initiated COROT mission.

However, for using these rich frequency data for asteroseismic modelling, mode identification is a prerequisite. In the case of main sequence pulsators, we are still far from obtaining very regular patterns in the oscillation spectra, which could help in solving the problem. We are also far from nonlinear theory, which would answer a question about mode selection mechanism. The main unresolved problem is why most of the theoretically unstable modes are not observed. Nowakowski (2005) suggested that the dominant effect of limiting the mode amplitude is a collective saturation of the opacity driving mechanism, instead of a resonant mode coupling.

In order to identify modes in β Cephei, δ Scuti or Slowly Pulsating B-type stars, we need additional observables from multicolour photometry or/and

spectroscopy. The photometric method of mode identification consists in using amplitude ratios and phase differences in different passbands; it is based on the semi-analytical formula for the light variation due to linear pulsation derived by Dziembowski (1977). Balona & Stobie (1979) showed that modes with different values of ℓ are located in different regions on the amplitude ratios *vs* phase differences diagram. Since then, the method has been applied to various types of pulsating variables by many authors (Watson 1988, Garrido et al. 1990, Heynderickx et al. 1994). The next important improvement was including nonadiabatic calculations by Cugier, Dziembowski & Pamyatnykh (1994), who applied the method to β Cep stars. Then, Balona & Evers (1999) emphasized the problem of very high sensitivity of photometric amplitudes and phases to the treatment of convection in the case of δ Sct stars. A photometric identification of ℓ for SPB stars, based on nonadiabatic calculations, was performed by Townsend (2002). All these works were done by assuming that the rotation does not influence pulsation. However, main sequence pulsators are very often rapid rotators. The next step in developing the method was its extension to close frequency modes coupled by a fast rotation by Daszyńska-Daszkiewicz et al. (2002). The photometric method in the version for long-period g-modes in rotating stars, for which perturbation approach is no longer adequate, was formulated by Townsend (2003a) and Daszyńska-Daszkiewicz et al. (2007).

A few years ago, Daszyńska-Daszkiewicz et al. (2003, 2005a) proposed a new method of the identification of ℓ , which uses the amplitudes and phases themselves and combines photometry, and radial velocity data. The method allows also to extract simultaneously a new asteroseismic probe, which yields constraints on stellar parameters and input physics, e.g., convection, opacities.

BRITE (BRiGht Target Explorer) is the first space-based mission which will perform two-colour photometry of bright stars. It will give an opportunity of not only detecting low-level oscillations but also of identifying their degrees ℓ . However, much more could be achieved, if ground-based spectroscopic observations are organized simultaneously. Then another type of information, contained in the radial velocity and line profile variations, would be supplied.

The aim of this paper is to show what can be done for mode identification from observations with the two BRITE passbands. I will recall the basic formulae and show examples of photometric diagnostic diagrams for models of β Cephei, SPB and δ Scuti stars. Then I will present diagrams which include amplitudes and phases from photometric and radial velocity variations. Finally, I will discuss uncertainties arising from effects of rotation, convection and atmospheric models. A summary and conclusions are given in the last section.

Mode identification from photometry

In order to calculate photometric amplitudes and phases, two inputs are needed. They come from

- nonadiabtic theory of stellar pulsation,
- models of stellar atmospheres.

We assume linear pulsation theory, which is adequate because of small mode amplitudes in main sequence pulsators, and we use temporally static, plane parallel atmosphere, which is justified because the eigenfunctions of the considered modes are nearly constant in the atmosphere.

Let us consider a pulsation mode in the zero-rotation approximation, the geometry of which can be described by a single spherical harmonic, Y_ℓ^m , with the degree ℓ and the azimuthal order m . The shape of the radial eigenfunctions of the mode are determined by its radial order n . Then the local radial displacement is given by

$$\frac{\delta r}{R} = \varepsilon Y_\ell^m(\theta, \phi) e^{-i\omega t}, \quad (1)$$

where ε is the intrinsic mode amplitude, ω is the angular pulsation frequency, which of course depends on (n, ℓ, m) ; other symbols have their usual meanings. The corresponding changes of the bolometric flux, \mathcal{F}_{bol} , and the local gravity, g , are given by

$$\frac{\delta \mathcal{F}_{\text{bol}}}{\mathcal{F}_{\text{bol}}} = \varepsilon f Y_\ell^m(\theta, \phi) e^{-i\omega t}, \quad (2)$$

and

$$\frac{\delta g_{\text{eff}}}{g_{\text{eff}}} = -\varepsilon \left(2 + \frac{\omega^2 R^3}{GM} \right) Y_\ell^m(\theta, \phi) e^{-i\omega t}. \quad (3)$$

The complex parameter, f , describes the ratio of the radiative flux perturbation to the radial displacement at the level of the photosphere and it is obtained from nonadiabatic calculations.

The complex photometric amplitudes of the light variation in the passband λ due to a pulsation mode with frequency ω can be written in the following form

$$\mathcal{A}_\lambda(i) = -1.086 \varepsilon Y_\ell^m(i, 0) b_\ell^\lambda (D_{1,\ell}^\lambda + D_{2,\ell} + D_{3,\ell}^\lambda) \quad (4)$$

where

$$D_{1,\ell}^\lambda = \frac{1}{4} f \frac{\partial \log(\mathcal{F}_\lambda | b_\ell^\lambda |)}{\partial \log T_{\text{eff}}}, \quad (5a)$$

$$D_{2,\ell} = (2 + \ell)(1 - \ell), \quad (5b)$$

$$D_{3,\ell}^\lambda = - \left(2 + \frac{\omega^2 R^3}{GM} \right) \frac{\partial \log(\mathcal{F}_\lambda |b_\ell^\lambda|)}{\partial \log g_{\text{eff}}^0} \quad (5c)$$

and i is the inclination angle. The partial derivatives of $\log(\mathcal{F}_\lambda |b_\ell^\lambda|)$ over effective temperature and gravity are derived from atmospheric models and

$$b_\ell^\lambda = \int_0^1 h_\lambda(\mu) \mu P_\ell(\mu) d\mu, \quad (6)$$

is the disc-averaging factor, containing the information about the visibility of the mode with a given degree ℓ . The integrals b_ℓ^λ are weighted by the limb-darkening law, $h_\lambda(\mu)$. The term $D_{1,\ell}^\lambda$ describes the temperature effects, the term $D_{2,\ell}$ stands for the geometrical effects, and the influence of gravity changes is contained in the term $D_{3,\ell}^\lambda$. The terms $D_{1,\ell}^\lambda$ and $D_{3,\ell}^\lambda$ include the perturbation of the limb-darkening, and their ℓ -dependence arises from the nonlinearity of the limb-darkening law.

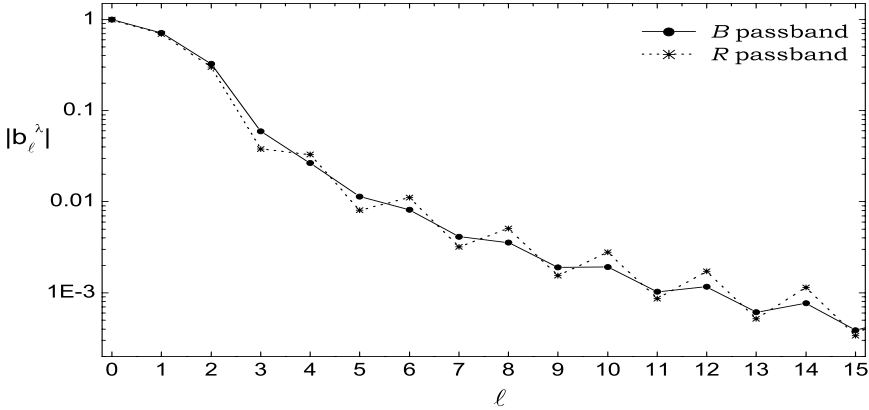


Figure 1: The disc-averaging factor, b_ℓ^λ , as a function of the spherical harmonic degree, ℓ , for the BR Johnson filters. The adopted stellar parameters are $\log T_{\text{eff}} = 3.875$ and $\log g = 4.0$.

The amplitudes and phases of the light variation are given by $|A_\lambda|$ and $\arg(A_\lambda)$, respectively. Having these numbers, we can construct photometric diagnostic diagrams in the form A_x/A_y vs. $\varphi_x - \varphi_y$, where x and y denote passbands. These observables are independent of the intrinsic amplitude, ε , inclination angle, i , and azimuthal order, m , because the product εY_ℓ^m drops out. These is an advantage for the identification of ℓ but also a disadvantage because the order m is beyond of the reach of the photometric method.

In this section I will give examples of photometric diagrams in the BR Johnson filters which are not very different from the BRITE passbands: BT1 (390-460 nm) and BT2 (550-700 nm). The well known property of the factor b_ℓ^λ is that it decreases very rapidly with growing degree ℓ ; this can be seen from Fig. 1. In this paper I will consider modes with degrees up to $\ell = 6$. All calculations were done with the Warsaw-New Jersey evolutionary code and nonadiabatic pulsation code of Dziembowski (1977). I used OPAL opacity tables of Iglesias & Rogers (1996) and the solar chemical composition of Grevesse & Noels (1993), assuming the metallicity $Z = 0.02$. I adopted Kurucz atmospheric models in the NOVER-ODFNEW version (Castelli & Kurucz 2004), which have more smooth flux derivatives than the standard Kurucz models, and the Claret nonlinear formula for the limb-darkening law. The standard atmospheric metallicity, $[m/H]=0.0$, and the microturbulence velocity, $\xi_t = 2$ km/s, were assumed.

β Cephei pulsators

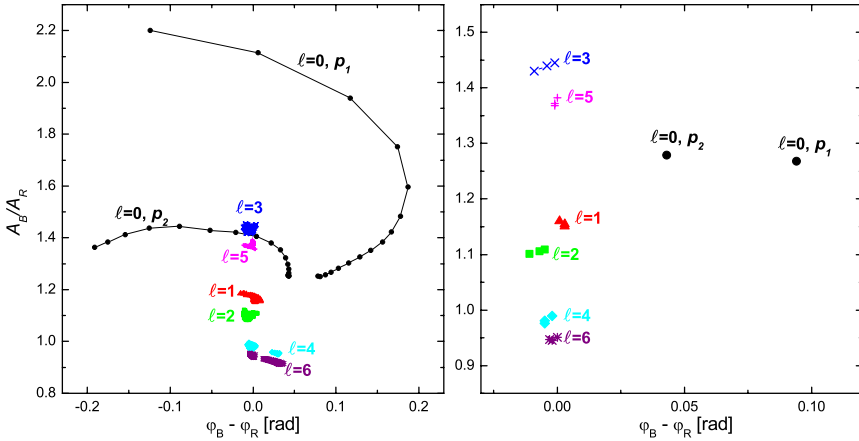


Figure 2: The locations of unstable modes with degrees ℓ up to 6 for β Cephei star models of $12 M_\odot$ on the diagnostic diagrams involving Johnson B and R filters. The left panel contains all models in the main sequence evolutionary phase, and the right panel, the model with $\log T_{\text{eff}} = 4.400$ and $\log g = 3.89$.

I considered stellar models with a mass of $M = 12 M_\odot$ during main sequence phase of evolution, corresponding to the temperature range of $\log T_{\text{eff}} = 4.445 - 4.347$. In Fig. 2, the photometric diagram in the BR passband is presented. The left panel shows all modes which become unstable between ZAMS and

TAMS and the right panel shows unstable modes for only one stellar model with $\log T_{\text{eff}} = 4.400$ and $\log g = 3.89$. Modes with different degrees ℓ are located in separated regions. The radial modes are spread over a wide range of the amplitude ratios and phase differences, whereas the nonradial modes are concentrated in small areas. This behaviour results from different contributions of the temperature ($D_{1,\ell}^\lambda f$) and the geometrical effects ($D_{2,\ell}$) to the light variation (Daszyńska-Daszkiewicz et al. 2002)

Slowly Pulsating B-type stars

In order to calculate SPB oscillation, I chose the models with $M = 5M_\odot$ on the main sequence, which include $\log T_{\text{eff}}$ from 4.235 to 4.134. Positions of modes with different values of ℓ on the photometric BR diagram are shown in Fig. 3. Again, the left panel contains all unstable modes, and the right panel, one model with $\log T_{\text{eff}} = 4.195$ and $\log g = 4.02$. The well-known property of this type of diagrams is the zero phase difference and the same amplitude ratio for all modes with $\ell = 1$. This is because the light variation of the $\ell = 1$ mode in SPB models is totally dominated by the temperature effects. We can see an overlapping of domains with different values of ℓ . This can be partly removed by considering only one model (the right panel). Another instructive

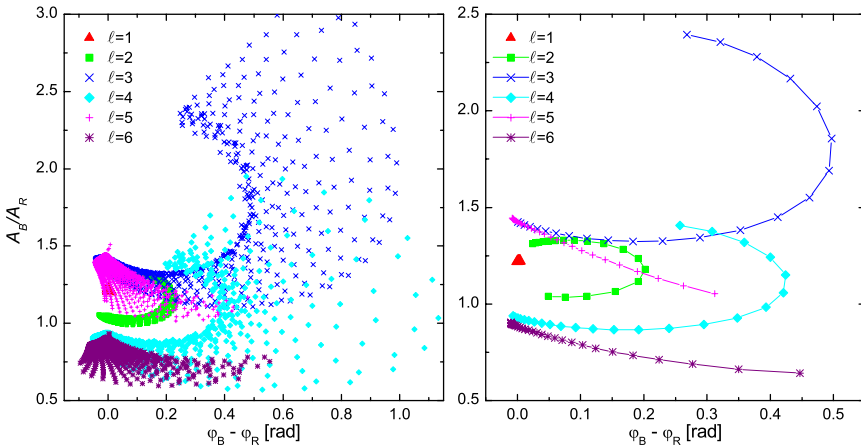


Figure 3: The same as in Fig. 2 but for Slowly Pulsating B-type star models of $5 M_\odot$. The left panel contains all models in the main sequence evolutionary phase and the right panel, the model with $\log T_{\text{eff}} = 4.195$ and $\log g = 4.02$.

information can be drawn from instability conditions. Fig.4 shows the amplitude ratio and the phase difference as a function of frequency for the model with

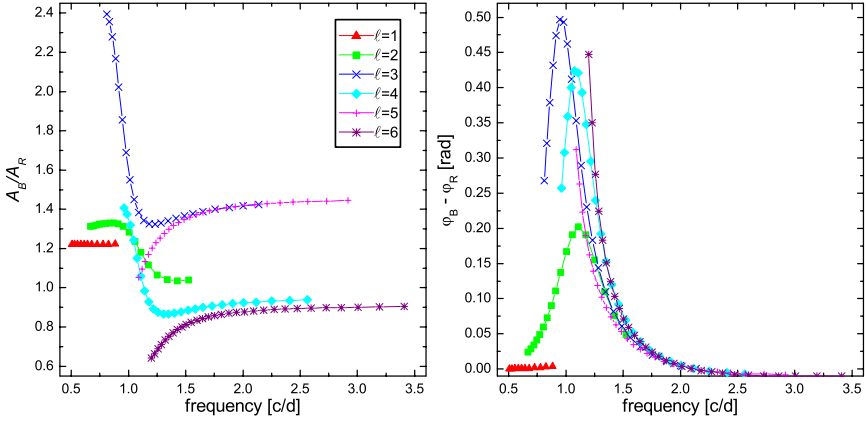


Figure 4: Amplitude ratios (on the left) and phase differences (on the right) in the BR bands as a function of oscillation frequency for the SPB model with $\log T_{\text{eff}} = 4.195$ and $\log g = 4.02$.

$\log T_{\text{eff}} = 4.195$ and $\log g = 4.02$. As one can see, modes with $\ell = 1$ are unstable only for the lowest frequencies ($\nu < 0.9$ c/d). The instability is shifted to the higher frequencies for higher ℓ -modes, e.g., the $\ell = 5$ modes become unstable for $\nu > 1.1$ c/d.

δ Scuti pulsators

As representatives of δ Sct pulsator, I took models with $M = 2M_{\odot}$ in the main sequence phase. The corresponding $\log T_{\text{eff}}$ range is (3.963, 3.854). All calculations were made under assumptions of the mixing length theory and the convective flux freezing approximation. The mixing length parameter was $\alpha_{\text{conv}} = 0.0$, i.e., an assumption of inefficient convective transport. The photometric BR diagram for this type of pulsators is presented in Fig. 5. All unstable modes of $M = 2M_{\odot}$ models are shown on the left hand side, and modes in the ($\log T_{\text{eff}} = 3.909$, $\log g = 4.02$) model on the right hand side. As we can see, there is some overlap, especially for the $\ell \leq 2$ modes. Fixing the model parameters helps in removing this ambiguity.

The common opinion about δ Sct pulsation modes is that the main information about the ℓ values is contained in the phase differences. In fact, this is true only for low degree modes with $\ell \leq 2$, but for higher ℓ 's we can learn much also from the amplitude ratios. In Fig. 6, the amplitude ratio (the left panel) and phase difference (the right panel) as a function of oscillation frequency are depicted. As we can see, not much can be achieved for low degree modes

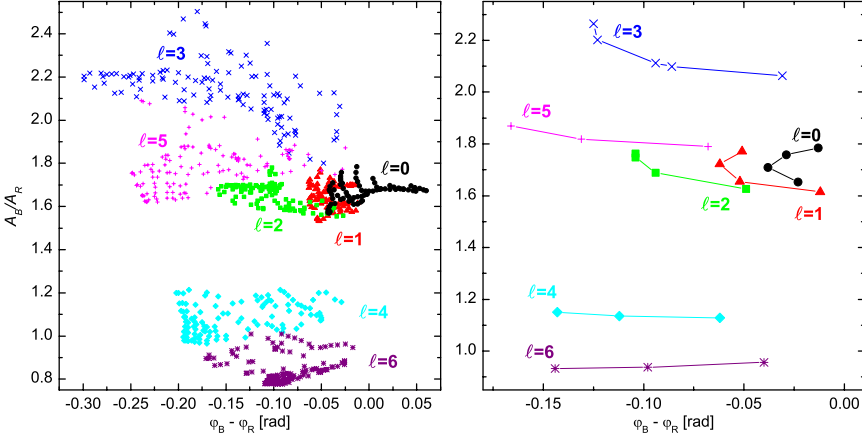


Figure 5: The same as in Fig. 2 but for δ Scuti star models of $2 M_{\odot}$. The left panel contains all models in the main sequence evolutionary phase, and the right panel, the model with $\log T_{\text{eff}} = 3.909$ and $\log g = 4.02$.

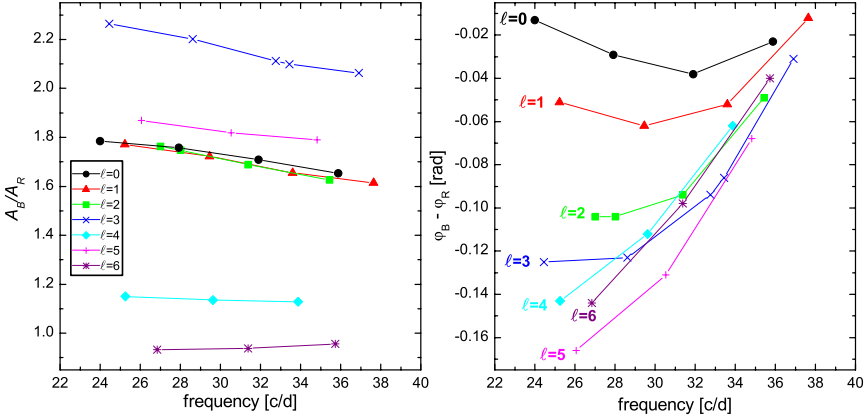


Figure 6: Amplitude ratios (on the left) and phase differences (on the right) in the BR bands as a function of oscillation frequency for the δ Sct model with $\log T_{\text{eff}} = 3.909$ and $\log g = 4.02$.

also from the A_B/A_B vs. frequency plot because the $\ell \leq 2$ modes are excited with very close frequencies. Another interesting property to note is that for very high frequency mode ($\nu > 35$ c/d), the phase differences are almost the same for all degrees ℓ .

Adding radial velocity measurements

The radial velocity variation averaged over stellar disc is expressed by the well-known Dziembowski's (1977) formula

$$V_{rad}(i) = i\omega R\varepsilon Y_\ell^m(i, 0) \left(u_\ell^\lambda + \frac{GM}{R^3\omega^2} v_\ell^\lambda \right), \quad (7)$$

where

$$u_\ell^\lambda = \int_0^1 h_\lambda(\mu) \mu^2 P_\ell(\mu) d\mu, \quad (8a)$$

and

$$v_\ell^\lambda = \ell \int_0^1 h_\lambda(\mu) \mu (P_{\ell-1}(\mu) - \mu P_\ell(\mu)) d\mu. \quad (8b)$$

From observations, the radial velocity variations are determined by calculating the first moment, \mathcal{M}_1^λ , of a well isolated spectral line.

In this section, I show examples of diagnostic diagrams constructed from the radial velocity variation and the light variation in the Johnson R filter. Unstable oscillation modes for β Cep, SPB and δ Sct star models considered in the previous section are presented in Fig 7, 8 and 9, respectively. As we can

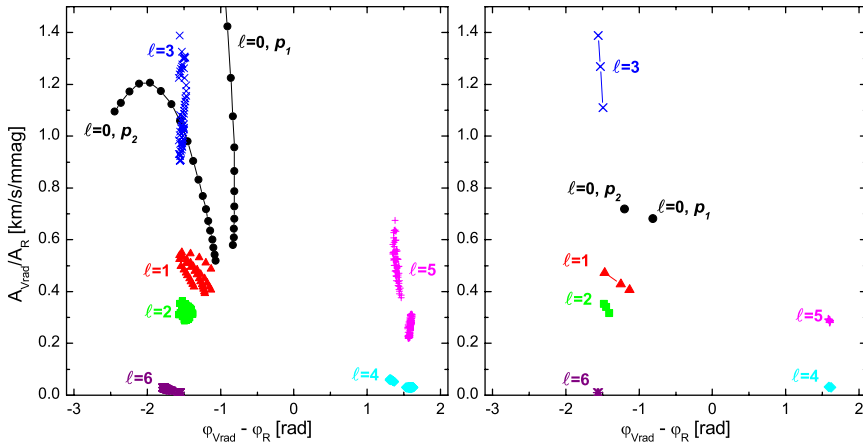


Figure 7: The location of unstable modes with degrees ℓ up to 6 for β Cep models of $12 M_\odot$ on the diagnostic diagrams constructed with amplitudes and phases for the R passband and the radial velocity variations. As in Fig. 2, the left panel shows all main sequence models, and the right panel, one model with $\log T_{\text{eff}} = 4.400$ and $\log g = 3.89$.

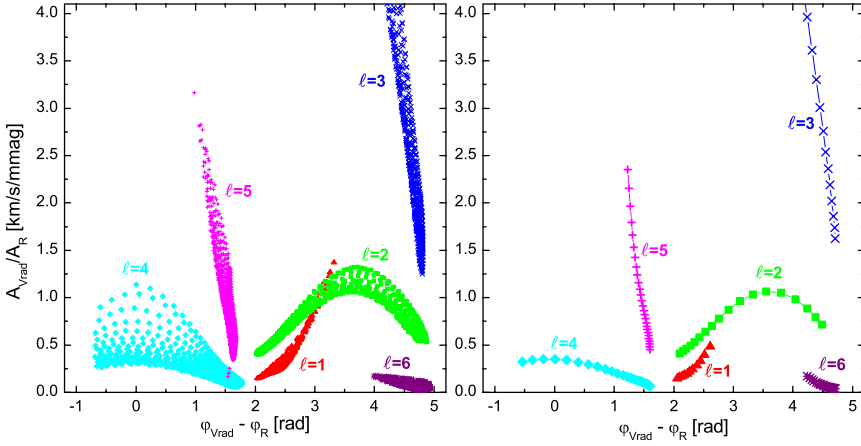


Figure 8: The same as in Fig. 7 but for SPB models of $5 M_{\odot}$. In the right panel unstable modes for the model with $\log T_{\text{eff}} = 4.195$ and $\log g = 4.02$ are plotted.

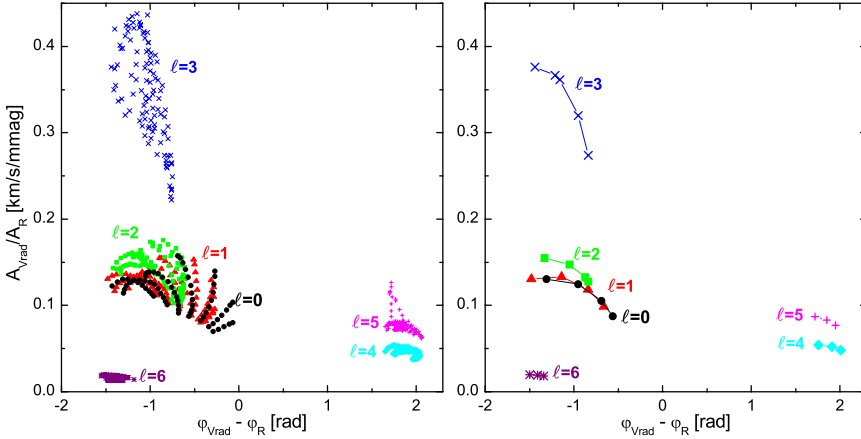


Figure 9: The same as in Fig. 7 but for δ Sct models of $2 M_{\odot}$. In the right panel unstable modes for the model with $\log T_{\text{eff}} = 3.909$ and $\log g = 4.02$ are plotted.

see, the configuration of ℓ modes domains differs from that in the photometric diagrams. In particular, there are larger phase differences between light and radial velocity variation than between two passbands.

Moreover, with two photometric passbands and the radial velocity data, one can apply the method of simultaneous extracting from observations the

degree ℓ and the nonadiabatic parameter f . Determination of the empirical value of f allows to avoid, in the process of the ℓ -identification, the input from pulsation models, which still needs many improvements, for example the pulsation-convection interaction, opacity tables, effects of diffusion, mixing etc. On the other hand, the parameter f constitutes a new asteroseismic probe, giving information on subphotospheric layers and is complementary to oscillation frequencies determined by stellar interior. Comparing empirical and theoretical values of f , one can draw conclusions about the efficiency of convection in δ Sct stars (Daszyńska-Daszkiewicz et al 2003, 2005b) or about opacities in β Cep stars (Daszyńska-Daszkiewicz et al. 2005a).

Uncertainties

There are many sources of uncertainties in all results presented in this paper. Firstly, all calculation were done assuming the zero rotation approximation. Effects of rotation can spoil the nice mode separation in the diagnostic diagrams, making them dependent on the inclination, rotation rate and the azimuthal order m . One such effect is rotational mode coupling. It takes place if the frequency distance between modes, with the degrees ℓ differing by 2 and the same m , is of the order of the rotation frequency. In such a situation, the photometric amplitude for the coupled mode has to be calculated as superposition of all mode amplitudes satisfying the conditions $\ell_k = \ell_j + 2$ and $m_k = m_j$. The effect of rotational mode coupling on the photometric diagrams for β Cep star was studied by Daszyńska-Daszkiewicz et al. (2002). Examples for δ Sct stars can be found in Daszyńska-Daszkiewicz (2007). Another case when the rotation has to be included is when the pulsational frequency, ω , is of the order of the rotational frequency, Ω , so that the perturbation approach fails. It happens often in the case of the rapidly rotating SPB stars, in which high order gravity modes are excited. Such slow modes are no longer described by the spherical harmonics, and more complicated formalisms are needed. One possibility is the use of the traditional approximation which allows expressing the angular dependence of eigenfunctions by the Hough functions (e.g. Lee & Saio 1997, Townsend 2003b). The formula for the light variation due to low frequency oscillation was given by Townsend (2003a). Daszyńska-Daszkiewicz et al. (2007) discussed a prospect for mode identification from diagnostic diagrams and derived the expression for the radial velocity variation.

Another uncertainty comes from the input physics and atmospheric models. The effect of metallicity parameter, Z , and opacities on the diagnostic diagrams for β Cep star models was considered by Cugier et al. (1994). For a higher value of Z , the separation of modes with different ℓ 's is much better. Similarly, computations with the OP tables, instead of OPAL, lead to a little better ℓ dis-

crimination, especially the radial modes are much more spread. Then, Cugier & Daszyńska (2001) checked the effect of the atmospheric metallicity parameter, $[m/H]$, and the microturbulence velocity, ξ_t , on the diagnostic properties of photometric diagrams. For β Cep stars these parameters have negligible impact.

The main problem in applying the method of diagnostic diagrams to δ Sct modes is that photometric amplitudes and phases exhibit a strong dependence on the treatment of convection (Balona & Evers 1999). To circumvent this problem, Daszyńska-Daszkiewicz et al. (2003, 2005b) invented the method of simultaneous determination of degree ℓ and the nonadiabatic parameter f from observations. Then we can identify the ℓ -value independently of the pulsation models and, by comparing empirical and theoretical f values, constraints on convection can be inferred. The result was that the convective transport in δ Sct stars studied by us is rather inefficient. The progress in modelling δ Sct pulsation with time-dependent convection treatment was achieved e.g. Grigahčene et al. (2005), Dupret et al. (2005a) and Dupret et al. (2005b).

In the case of δ Sct models, the uncertainties in atmospheric models can play much more important role than in the B-type pulsators. In Kurucz standard models, the flux derivatives over effective temperature and gravity are not smooth at the temperature where convective transport becomes important. This is because of using an overshooting approximation that moves the flux higher in the atmosphere, above the top of the nominal convection zone. In the NOVER-ODFNEW models computed by F. Castelli the problem of non-smooth derivatives does not exist. There are also NEMO models (New Model Grid of Stellar Atmospheres) which include different treatment of convection. The models were computed by the Vienna group with modified versions of the Kurucz ATLAS9 code. The grids have smaller steps in T_{eff} and $\log g$ than in Kurucz's computations, and the flux derivatives are perfectly smooth. The effect of using various atmospheric models in the calculation of δ Sct observables was discussed by Daszyńska-Daszkiewicz et al. (2004) and Daszyńska-Daszkiewicz (2007).

Conclusions

There is a potential for mode identification from the BRITE photometry. As we could see, two-colour information can yield some constraints on the spherical harmonic degree, ℓ , of the oscillation modes excited in main sequence pulsators.

However, space observations should be followed up by simultaneous ground-based spectroscopy. The advantages of adding the spectroscopic variations is obvious. By combining photometry and the radial velocity data, we will improve significantly the discrimination of ℓ and infer better seismic constraints on stel-

lar parameters and input physics. Moreover, from the line profile variations the identification of the azimuthal order, m , becomes possible. With such unprecedented data, we can hope for a great step in asteroseismology of main sequence pulsators with the BRITE-Constellation.

Acknowledgments. The author thanks Werner Weiss for inviting her to participate in the BRITE Workshop and Mikołaj Jerzykiewicz for carefully reading the manuscript. This work was supported by the Polish MNiSW grant No. 1 P03D 021 28.

References

- Balona, L.A., Evers, E.A. 1999, MNRAS 302, 349
- Balona, L.A., Stobie, R.S. 1979, MNRAS 189, 649
- Barban, C., Matthews, J.M., De Ridder, J. 2007, A&A 468, 1033
- Bruntt, H., Suárez, J.C., Bedding, T.R., et al. 2007, A&A 461, 619
- Castelli, F., Kurucz, R.L. 2004, in Proceedings of the IAU Symp. No 210, Modelling of Stellar Atmospheres, eds. N. Piskunov et al., poster A20
- Cugier, H., Daszyńska, J. 2001, A&A 377, 113
- Cugier, H., Dziembowski, W.A., Pamyatnykh, A.A., 1994, A&A 291, 143
- Daszyńska-Daszkiewicz, J., Dziembowski, W.A., Pamyatnykh, A.A., et al. 2002, A&A 392, 151
- Daszyńska-Daszkiewicz, J., Dziembowski, W.A., Pamyatnykh, A.A. 2003, A&A 407, 999
- Daszyńska-Daszkiewicz, J., Dziembowski, W.A., Pamyatnykh, A.A., et al. 2004, in Proceedings of the IAU Symp. No. 224, The A-Star Puzzle, eds. J. Zverko, J. Ziznovsky, S.J. Adelman, and W.W. Weiss, p. 853
- Daszyńska-Daszkiewicz, J., Dziembowski, W.A., Pamyatnykh, A.A., 2005a, A&A 441, 641
- Daszyńska-Daszkiewicz, J., Dziembowski, W.A., Pamyatnykh, A.A., et al. 2005b, A&A 438, 653
- Daszyńska-Daszkiewicz, J., 2007, CoAst 150, 32
- Daszyńska-Daszkiewicz, J., Dziembowski, W.A., Pamyatnykh, A.A. 2007, Acta Astron. 57, 11
- Dziembowski, W.A. 1977, Acta Astron. 27, 203
- Dupret, M.-A., Grigahcène, A., Garrido, R., et al. 2005a, A&A 435, 927
- Dupret, M.-A., Grigahcène, A., Garrido, R., et al. 2005b, MNRAS 361, 476
- Garrido, R., Garcia-Lobo, E., Rodriguez, E. 1990, A&A 234, 262
- Grigahcène, A., Dupret, M.-A., Gabriel, M., et al. 2005, A&A 434, 1055

- Heynderickx, D., Waelkens, C., Smeyers, P. 1994, *A&AS* 105, 447
- Iglesias, C.A., Rogers, F.J. 1996, *ApJ* 464, 943
- Nowakowski, R. 2005, *Acta Astron.* 55, 1
- Saio, H., Cameron, C., Kuschnig, R., et al. 2007, *CoAst* 150, 215
- Townsend, R.H.D. 2002, *MNRAS* 330, 855
- Townsend, R.H.D. 2003a, *MNRAS* 343, 125
- Townsend, R.H.D. 2003b, *MNRAS*, 340, 1020
- Walker, G.A.H., Kuschnig, R., Matthews, J.M., et al. 2005, *ApJ*, 635, L77
- Watson, R.D. 1988, *Ap&SS* 140, 255

Theoretical Aspects of Massive Stars

E.A. Dorfi¹, A. Stökl²

¹ Institut für Astronomie, Türkenschanzstrasse 17, 1180 Vienna, Austria

² École Normale Supérieure de Lyon – CRAL, 46 allée d'Italie, F-69364 Lyon
Cedex 07, France

Abstract

From numerical simulations of massive and luminous stars, we often find regular radial pulsations for a large variety of stellar parameters. The pulsation periods are typically around one day. Such pulsations are encountered during the core hydrogen burning as well as during the early core helium burning stage of evolution. The numerical results are discussed with the aim to guide observations to identify and monitor such regularly pulsating variable massive stars in nature. We emphasise that mass loss events generating circumstellar shells, complex atmospherical motions and angular variations due to stellar rotation can strongly modify the actually observable light curves.

Introduction

The properties of the most luminous stars are often rather poorly determined. Detailed observations are needed to reveal the physical parameters like age, evolutionary status, chemical composition, rotation rate and mass loss. Based on stellar wind models depending on an assumed clumping mass loss rate of $\dot{M} \simeq 10^{-4} M_{\odot}/\text{yr}$, terminal velocities up to 1000 km/s seem to be typical. From the observational point of view, the nature of LBV (Luminous Blue Variable) variability is still not well understood. Small amplitude quasi-regular photometric variations have been detected on time scales of several days while eruption-like outbursts show time scales from months to years (see e.g. Nota & Lamers, 1997, for a detailed summary on LBV properties).

Motivated by theoretical predication of LBV pulsations (Dorfi & Gautschy, 2000) as well as observations of small amplitude light variations of the Wolf-Rayet star WR123 by the MOST satellite (Lefèvre et al. 2005), we have performed a small survey on theoretical models around the stellar parameters of WR123 as discussed in the literature (e.g. Hamann & Koesterke 1998). The models were assumed to have $X = 0.35$ and $Z = 0.02$, an abundance choice which seems to be in accordance with average WN8-type stars. Based on such

Table 1: Theoretical pulsationally unstable WR123 models

Name	M [M_{\odot}]	L [$10^5 L_{\odot}$]	T_{eff} [K]	R_p [R_{\odot}]	P [days]	$\Delta R_p/R_p$	Δu [km/s]	Δm_{bol} [mag]
WR123A	22	3.16	38 000	12.97	0.517	0.23	375	0.49
WR123B	22	3.16	39 000	12.31	0.482	0.29	386	0.51
WR123C	20	3.16	38 000	13.97	0.768	0.65	669	1.64
WR123D	23	3.16	38 000	12.97	0.499	0.22	385	0.50
WR123E	23	3.16	36 000	14.45	0.594	0.22	364	0.46
WR123F	23	3.16	40 000	11.70	0.423	0.22	408	0.54
WR123G	22	3.16	40 000	11.70	0.446	0.23	403	0.54
WR123H	25	3.16	38 000	12.97	0.427	0.19	425	0.72
WR123I	25	3.16	28 000	23.88	1.295	0.24	340	0.47
WR123J	25	3.00	28 000	23.26	1.183	0.22	329	0.52
WR123L	27	3.16	38 000	12.97	0.344	0.02	58	0.10
WR123M	26	3.16	38 000	12.97	0.391	0.07	158	0.27
WR123N	25	3.00	38 000	12.63	0.377	0.10	288	0.46
WR123P	23	3.00	38 000	12.63	0.457	0.21	406	0.61
WR123Q	27	4.00	38 000	14.48	0.766	0.43	551	1.17
WR123R	25	3.16	33 000	17.19	0.719	0.22	377	0.56
WR123S	25	3.16	31 000	19.48	0.901	0.22	358	0.51
WR123U	25	2.82	33 900	15.38	0.502	0.10	261	0.39

assumptions the observed pulsation frequency of WR123 can easily be obtained from theoretical models showing strange mode pulsations (Dorfi et al. 2006).

Wolf-Rayet Models

Representing rather typical examples for pulsational variability of massive luminous stars, we summarise in Table 1 a number of radial non-linear pulsation computations of Wolf-Rayet stars. The full set of equations of radiation hydrodynamics (RHD, e.g. Mihalas & Mihalas 1984) and the numerical method used for the non-linear pulsation simulations have been described in detail by Dorfi (1998). The initial models are taken from stellar evolution calculations (Schaller et al. 1992), and are plotted in Fig. 1 for initial masses of $20 M_{\odot}$, $25 M_{\odot}$ and $40 M_{\odot}$. The mass loss rates have been calculated according to the standard CAK-theory (Castor, Abbot & Klein, 1975) of optically thick radiative-driven winds. We emphasise that due to this mass loss prescription the total mass of the pulsationally unstable stars can be significantly lower than their initial values. In Fig. 1 we have plotted the evolutionary path of the model with an initial mass of $40 M_{\odot}$ starting with a solid line followed by a dashed line where the remaining total mass of this star has been decreased to less than $25 M_{\odot}$.

The pulsational models investigated belong to massive stars at the stage of either core hydrogen burning or early core helium burning. In the dynamical computations, the radiative transfer is performed using the Rosseland-mean OPAL92-opacity for the radiative flux and the Planck-mean for the corresponding radiation energy equation.

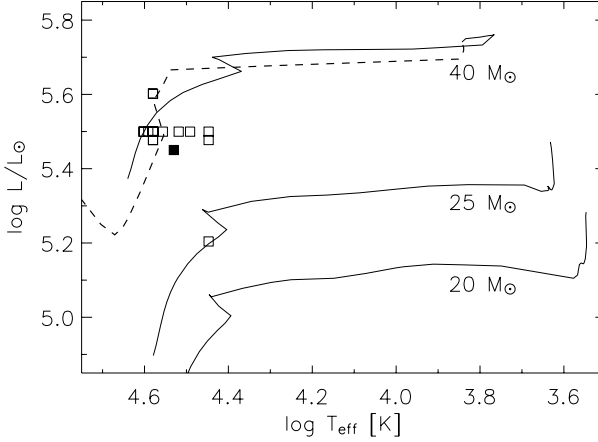


Figure 1: Evolutionary tracks of Schaller et al. (1992) with mass loss for initial masses of $20 M_{\odot}$, $25 M_{\odot}$ and $40 M_{\odot}$. The dashed line of a model with an initial mass of $40 M_{\odot}$ shows the evolution where the remaining mass has dropped below $25 M_{\odot}$. The open squares exhibit our non-linear pulsation models of Wolf-Rayet stars. The full square corresponds to model WR123U adopted to simulate the MOST observations of WR123.

In Fig. 1 we have also included model WR123K with $M = 22 M_{\odot}$, $L = 1.6 \cdot 10^4 L_{\odot}$ and $T_{\text{eff}} = 28000 \text{ K}$ located at the $25 M_{\odot}$ track which is pulsationally stable. To get this kind of WR variability, as found, e.g., by the MOST satellite for WR123 (Lefèvre et al. 2005), the luminosity has to be large enough for a given mass, in particular stellar evolutionary models without a significant mass loss could hardly develop such pulsations. As seen in Fig. 1 our pulsationally unstable models (cf. Table 1) are located around the $40 M_{\odot}$ track but due to the radiation-driven mass loss (see Schaller et al. 1992) the remaining stellar mass is around $20 M_{\odot}$.

Figure 2 displays the motion of several mass shells over 4 interior pulsational cycles with $P = 0.766$ days to illustrate the internal properties of model WR123Q as well as the atmospheric dynamics. The period of the outer layers can be determined to be 1.140 days which is about $2/3$ of the internal period. It becomes clearly visible how the interior period triggers the large scale at-

mospheric motions. At every pulsational cycle, waves are travelling outwards and, depending on the phase of the outer layers, these waves can grow up to large amplitudes, generating shock waves at different strengths which then propagate through the rest of the stellar layers. These effects are illustrated by the concentration of mass shells still showing a regular pattern. The nature of these non-linear pulsations is different from classical linear pulsations where the whole atmosphere is displaced in- and outwards while essentially retaining its structure and thickness. Here, a notable portion of the stellar atmosphere is stretched and moves in a ballistic way which is controlled by its own dynamical time scale and not by the interior pulsation time scale. Although we still find a quite regular pulsation in the deeper envelope regions with periods in agreement with a linear stability analysis, the outer layers can produce less regular external light variations. By increasing the luminosity we get more and more erratic and violent motions and the interior pulsation can become entirely obscured beneath an almost irregular flickering. The very large radial velocities encountered in these pulsations can also lead to pulsationally induced mass-loss.

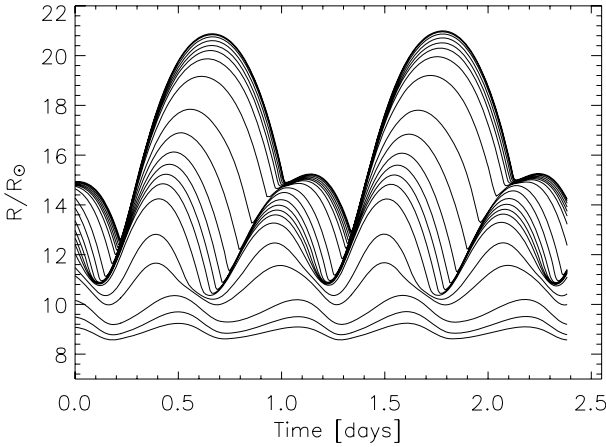


Figure 2: Mass shells of model WR123Q depicting the development of shock waves and the changes of the interior pulsational motions. The inner period correspond to 0.768 days, the external luminosity changes in a regular way every 1.140 days.

In Fig. 3, pulsation periods (in days) of Wolf-Rayet models, as given in Table 1, are plotted against the effective temperature. The shapes of the symbols correspond to the different luminosities adopted for our models. Related to mass loss occurring during stellar evolution and to initial conditions like chemical composition or rotational velocity, stars with different stellar masses can have similar luminosities, allowing for a broader range of observable pulsational

periods, in our models between 0.344 and 1.295 days. Velocity variations up to more than $\Delta u \simeq 500$ km/s are found in the stellar atmospheres. The radial pulsations give rise to relative radius changes of up to 40% and the photospherical temperature variations can exhibit a range of $\Delta T \simeq 9000$ K in the case of large spatial amplitudes. Nonetheless, the luminosity variability is rather moderate due to the comparatively low optical thickness of the most dynamic outer regions.

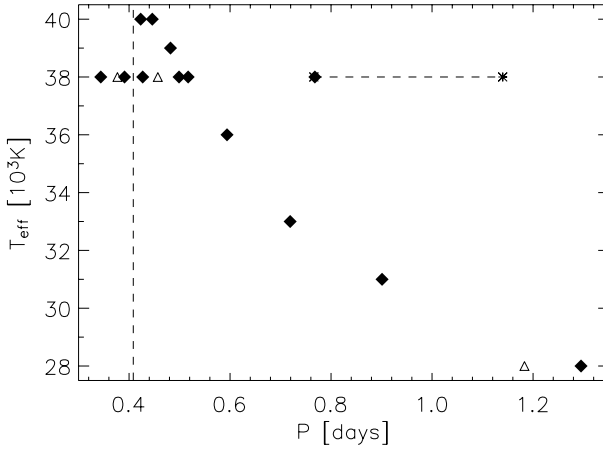


Figure 3: Internal pulsation periods for the models of Table 1. The full rhombuses correspond to a luminosity of $L = 3.16 \cdot 10^5 L_{\odot}$, the open triangles to $L = 3 \cdot 10^5 L_{\odot}$ and the crosses join both (internal and external) pulsational periods of model WR123Q with a luminosity of $L = 4 \cdot 10^5 L_{\odot}$. The vertical dashed line shows the period of $9.8 \text{ h} = 0.408 \text{ d}$ of WR123 as found in the MOST data (Lefèvre et al. 2005).

Conclusions

Summarising this large number of non-linear pulsation computations of Wolf-Rayet stars, we note that in general the observations of variable stars with large amplitude pulsations should not be interpreted by simple hydrostatic model atmospheres. The stratification of the outer stellar layers can be strongly modified by shock waves, which heat and accelerate the atmospheric material. Hence, the stellar parameters of such stars with large amplitude pulsations can only be deduced consistently from dynamical atmospheres.

Although the small number of galactic WR stars makes it more unlikely that such stars will be observed within the BRITE-mission, stars that luminous will be undoubtedly vastly overrepresented in any limited brightness sample.

According to our theoretical models, all luminous stars with $L[L_{\odot}]/M[M_{\odot}] > 10^4$, somewhat depending on the chemical composition, exhibit strange modes (see e.g. the review by Gautschy & Saio 1995) located at the outer stellar layers and the MOST observations of WR123 can serve as a particular example where pulsations with a period of 9.8 h have been detected. Following this argument, all stars in the range of $10^6 L_{\odot}$ should be unstable, but we do not expect simple light curves because of non-linear dynamical stellar atmospheres. Hence long time series of observations are required to estimate the stellar parameters of such variable sources. It will be rather cumbersome to detect regular pulsations due to shock induced light variations and further irregularities caused by non-radial effects and mass loss, in particular effects related to rotation. Since such massive stars are still young when they explode as supernovae, their initial rotation rate is usually not significantly reduced during their stellar life. This rotation will generate an angle-dependent mass loss which again can interfere with observations of an underlying regular stellar pulsation.

In general, observations of these massive stars are necessary to understand the Pre-SN-evolution of stars, the interaction of mass loss and pulsational dynamics as well as the detailed physical processes leading to radiation-driven winds and to outflow instabilities arising in these winds. Better observational constraints derived from time-resolved observations over longer periods, in close interplay with theory, are essentially needed to disentangle physical effects like radiation pressure in lines, rotation, stellar pulsations and propagating shock waves.

References

- Castor, J.I., Abbott, D.C., Klein, R.I. 1975, *ApJ*195, 157
- Dorfi, E.A. 1998, 27th Saas Fee Course, Springer, Berlin, p.263
- Dorfi, E.A., Gautschy, A. 2000, *ApJ*545, 982
- Dorfi, E.A.; Gautschy, A., Saio, H. 2006, *A&A*453, L35
- Gautschy, A., Saio, H. 1995, *ARA&A* 33, 75
- Hamann, W.-R., Koesterke, L. 1998, *A&A*335, 1003
- Lefèvre, L., Marchenko, S.V., Moffat, A.F.J., et al. 2005, *ApJ*634, L109
- Mihalas, D., Mihalas, B.W. 1984, *Foundations of Radiation Hydrodynamics*, Oxford University Press, New York
- Nota, A., Lamers, H.G.L.M.(Eds.) 1997, *Luminous Blue Variables: Massive Stars in Transition*, ASP Conf. Series Vol. 120
- Schaller, G., Schaerer, D., Meynet, G., et al. 1992, *A&ASuppl.* 96, 269

β Cephei and Slowly Pulsating B stars as targets for BRITE-Constellation

G. Handler

Institut für Astronomie, Türkenschanzstrasse 17, 1180 Vienna, Austria

Abstract

We discuss the potential of BRITE-Constellation for asteroseismology of main sequence B-type pulsators. We briefly review previous asteroseismic work on these oscillators and point out the importance of these stars for astrophysics in general. We find that BRITE-Constellation is ideally suited for studying B-type pulsators, and we identify several interesting regions in the sky that may be observed.

Introduction

This workshop has seen many interesting presentations of proposed targets that were better understood through observational data from BRITE-Constellation. Obviously, realizing the potential of a new instrument for the study of the object one is interested in, is probably any scientist's initial reaction. However, in only a few cases it was stated what the general impact of the proposed studies on astrophysics would be. Perhaps it is worth considering a different viewpoint.

During the Vienna Workshop on the Future of Asteroseismology in September 2006 (Handler & Houdek 2007), Kjeldsen (2007) made an important statement. "We promised to do asteroseismology but if you look on where we really changed the understanding of the evolution of the universe, we haven't gone where we promised yet, but we hope that space missions can do that. We have to make sure that the whole community can use all these space data. If we make another effort to spread all these data to students around the whole world, they will all learn the way seismologists study stars. Then we will have a much better chance to fund the next mission."

In other words, we first have to see how we can most efficiently use the resources we have been given, to obtain a scientific output that has the maximum possible impact on astrophysics in general, and to ensure the existence of our scientific field in the future. Only after we have found out what we can do for BRITE-Constellation to have as much scientific impact as possible, we should think about what BRITE-Constellation can do for us.

β Cephei and SPB stars

These two types of pulsating variables are main-sequence objects of spectral type B. Both have relatively simple interior structures, with convective cores and (mostly) radiative envelopes, but their pulsational behaviour is clearly distinct. Whereas the β Cephei stars pulsate in pressure and gravity modes of low radial order, with corresponding periods of 2 - 8 hours, the SPB stars exhibit gravity modes of high radial order in the period range of 0.5 - 6 days. The β Cephei stars are the most massive known main sequence pulsators ($9 < M < 17M_{\odot}$, Stankov & Handler 2005) and they are progenitors of supernovae of type II. The locations of both types of variables in the HR diagram are shown schematically in Fig. 1.

Asteroseismic results for β Cephei stars

Asteroseismology is the study of the interior of (non-radially) pulsating stars by means of their normal mode spectrum. This technique is analogous to the determination of the Earth's inner structure using earthquakes: we use stellar pulsations as "starquakes" or, more scientifically, we use stellar pulsation modes as seismic waves.

Many types of pulsating stars have been investigated with seismic methods, but real insights into their interior structures have rarely been obtained so far. The only exceptions are the Sun and some solar-like pulsators, pulsating white dwarf stars and the β Cephei stars. It is out of the scope of this paper to give an overview of the prospects and problems of asteroseismology, which is why we refer to Handler (2006) for a summary of these issues.

Why has asteroseismology been successful for the β Cephei stars? The answer seems trivial: they are simple enough that the pulsation modes can be identified, yet complicated enough to reveal effects of interior structure. At the time of this writing, there are four stars that have unique mode identifications and sufficiently rich pulsation spectra for seismic modelling, HD 129929 (Aerts et al. 2004), ν Eridani (e.g. Handler et al. 2004, Pamyatnykh et al. 2004, Jerzykiewicz et al. 2005), θ Ophiuchi (Handler et al. 2005, Briquet et al. 2005) and 12 Lacertae (Handler et al. 2006, Desmet et al., in preparation).

The seismic results obtained from these studies can be summarized as follows: the presence of differential interior rotation and the need of a small convective overshooting parameter ($\alpha_{\text{ov}} < 0.15$) have been proven for HD 129929 and ν Eri. For the latter star, the mean interior metallicity has been determined as well. For the stars θ Oph and 12 Lac, which rotate somewhat faster than HD 129929 and ν Eri, the interaction between pulsation and rotation can be studied.

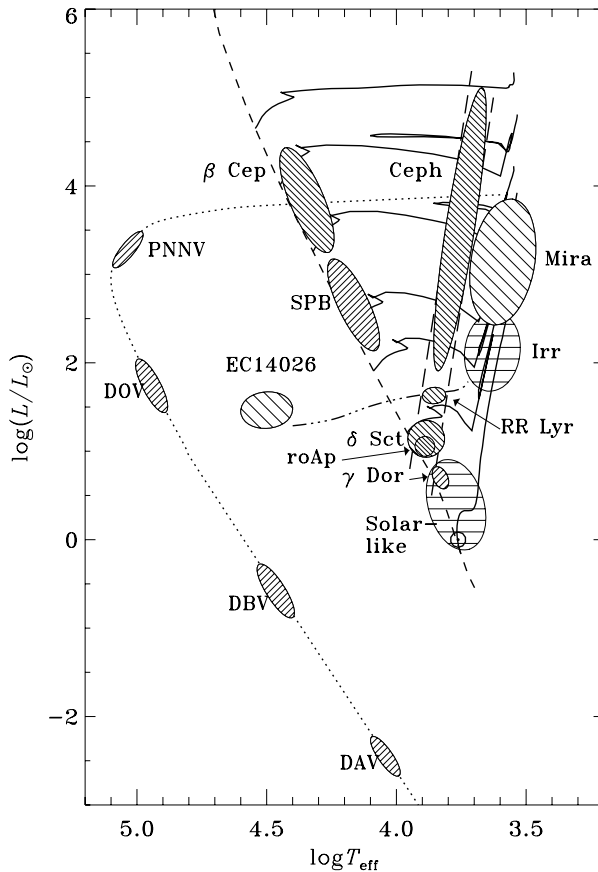


Figure 1: A theoretical HR diagram containing the locations of most of the known pulsating variables. The β Cephei and SPB stars can be found near the high-luminosity end of the main sequence. Reproduced with permission from J. Christensen-Dalsgaard.

However, some problems with the theoretical description of pulsational driving still remain, as the observed frequency spectra have a larger range than predicted. The obvious prime suspects in this context are the stellar opacities (e.g., Pamyatnykh & Ziomek 2007), or possible effects of diffusion.

Asteroseismology of SPB stars

Because these stars pulsate in high-order gravity modes, they may facilitate the application of asymptotic theory, greatly enhancing the prospects of mode identification and stellar modelling. This potential asset is also a difficulty because it follows from the long pulsation periods that only few pulsation modes have so far been detected (e.g., De Cat & Aerts 2002). In addition, the theoretical treatment of pulsation becomes difficult even at moderate rotation rates, as the pulsation and rotation periods are of the same order and a treatment of rotation as a perturbation is no longer possible. However, recent MOST satellite data may have revealed much larger numbers of pulsation frequencies for some SPB stars (e.g., Aerts et al. 2006), although data sets with a longer time base would be desirable for purposes of confirmation.

Another interesting possibility is the co-existence of stars that have both SPB star-like gravity modes and shorter-period β Cephei-type pulsation modes excited. Evidence is mounting that several such stars exist (e.g., De Cat et al. 2007 and references therein, Pigulski & Pojmanski 2007). It will be of tremendous help for the seismic application of the SPB star pulsations if some of these "hybrid" stars have pulsation spectra sufficiently rich to utilize both sets of modes.

BRITE-Constellation and B-type main sequence pulsators

A check of the latest catalogues of β Cep and SPB stars (Stankov & Handler 2005, De Cat 2002) for variables with $V < 4$ reveals a large number of possible candidates observable by BRITE-Constellation. We find 17 known and 12 candidate β Cep stars under these constraints, with another 35 stars inside the β Cep instability strip. In addition, there are three known SPB pulsators plus three more candidates among these brightest stars in the sky.

Still, this is not the whole story. As both types of stars have short main sequence lifetimes, they are all young objects and therefore occur in stellar clusters and associations. Investigating the distribution of these stars in the sky, and comparing it with the field of view of BRITE-Constellation, several interesting 25×25 -degree regions in the sky can be located; they are summarized in Table 1.

These seven fields contain a total of eleven known pulsators (some of which have already been studied from the ground, which means they have pulsational mode identifications) plus 42 other possible targets. We note that O-type stars in the BRITE-Constellation fields are also interesting from the asteroseismic point of view because theory predicts oscillations in such stars (Pamyatnykh 1999), but observations have rarely detected them.

Table 1: 25×25 -degree regions in the sky containing large numbers of β Cep and SPB stars and candidates ($V < 4$)

Region	Stellar content
Cen/Cru/Mus	1 β Cep star, 9 β Cep candidates, 1 SPB candidate
Cen/Lup	2 β Cep stars, 5 β Cep candidates, 2 SPB candidates
Upper Sco	1 β Cep star, 7 β Cep candidates, 1 O-type star
Orion	1 β Cep star, 3 β Cep candidates, 5 O-type stars
Centaurus	2 β Cep stars, 5 β Cep candidates
Lower Sco/Oph	3 β Cep stars, 2 β Cep candidates
CMa OB1	1 β Cep star, 2 β Cep candidates

How can the science output of BRITE-Constellation benefit from observing these stars? It will be possible to perform asteroseismology of supernova progenitor stars; supernovae largely determine the ecology of the universe. We also expect a general improvement in our understanding of stellar structure and evolution, such as angular momentum transport (i.e. differential interior rotation) and the size of the convective cores of massive stars, and we expect constraints on stellar opacities and diffusion from studies of mode excitation.

Why is BRITE-Constellation not only suitable, but even required for studying massive main sequence pulsators? It simply can perform efficient observations of regions densely populated with bright stars. If we compare the quantity and quality of the data to be delivered by BRITE-Constellation to that of classical ground-based observations of bright stars, we find that the efficiency of the space mission is a factor of about 100 higher. To put it short: the future of asteroseismology is BRITE!

Acknowledgments. GH is supported by the Austrian Fonds zur Förderung der wissenschaftlichen Forschung under grant P18339-N08.

References

- Aerts, C., Waelkens, C., Daszyńska-Daszkiewicz, J., et al., 2004, A&A 415, 241
Aerts, C., de Cat, P., Kuschnig, R., et al., 2006, ApJ 642, L165
Briquet, M., Lefever, K., Uytterhoeven, K., et al. 2005, MNRAS 362, 619
De Cat, P., 2002, <http://www.ster.kuleuven.ac.be/~peter/Bstars/>
De Cat, P., Aerts C. 2002, A&A 393, 965
De Cat, P., Briquet, M., Aerts, C., et al. 2007, A&A 463, 243
Handler, G., 2006, CoAst 147, 31
Handler, G., Houdek, G. 2007, CoAst Vol. 150

- Handler, G., Shobbrook, R.R., Jerzykiewicz, M., et al. 2004, MNRAS 347, 454
- Handler, G., Shobbrook, R.R., Mokgwetsi, T. 2005, MNRAS 362, 612
- Handler, G., Jerzykiewicz, M., Rodr´ıguez, E., et al. 2006, MNRAS 365, 327
- Jerzykiewicz, M., Handler, G., Shobbrook, R.R., et al. 2005, MNRAS 360, 619
- Kjeldsen, H. 2007, CoAst 150, 375
- Pamyatnykh, A.A. 1999, Acta Astron. 49, 119
- Pamyatnykh, A.A., Ziomek, W. 2007, CoAst 150, 207
- Pamyatnykh, A.A., Handler, G., Dziembowski, W.A. 2004, MNRAS 350, 1022
- Pigulski, A., Pojmanski, G. 2007, A&A, in press
- Stankov, A., Handler, G. 2005, ApJS 158, 193

The search for extrasolar planets with BRITE

R. Dvorak¹, Á. Bzszó¹

¹ Institut für Astronomie, Türkenschanzstrasse 17, 1180 Vienna, Austria

Abstract

We summarize in this report the possibilities of observing the reflecting light of a close by giant planet. BRITE could do these kind of observations only for very bright stars, but the chances that such a bright star with a close by large planet, a hot Jupiter, exists in the Solar environment are rather small. We discuss our present knowledge of analyzing reflecting light in light curves of stars.

Introduction

Since more than ten years an increasing number of extrasolar planets (exoplanets) around main sequence stars has been detected. By November 2007 264 planets are known in 215 extrasolar planetary systems (EPS) ¹. The predominant detection method is by radial-velocity measurement of the Doppler-shift in the spectrum of the star, an indirect method.

For BRITE, which will make photometric observations, light-curves and their interpretation, it is necessary to develop tools and methods to study them, and to have working models for a great class of possible observations.

Several problems arise for the direct detection and imaging of an exoplanet, among them (i) the problem of angular separation of the planet from the star, and (ii) the planet/star flux ratio are the main limiting factors. Take for instance a main sequence star of type G2V at a distance of 10pc and a planet with semi-major axis of $a = 0.4$ AU, then the angular separation is as low as 0.4 arcseconds, and the planet/star flux ratio at optical wavelengths is below 10^{-9} .

The reflection off an exoplanet's surface cannot be modeled by assuming simple reflection models or by extrapolating solar-system data. One has to consider the planet's orbital distance due to effects on its composition, as well as the constituents of its atmosphere, also the particles and their sizes play an important role.

¹according to the internet site (exoplanet.eu) provided by Jean Schneider from the Paris observatory

We plan to give an overview of the different effects acting on the light-curves of exoplanets, as described by Sudarsky et al. (2005), whom we follow closely in this article. For further literature we refer to Hubbard et al. (2001), Burrows et al. (2004), Rowe et al. (2006) and also Burrows et al. (2007).

We consider only Jupiter-type giant planets—from now on referred to as extrasolar giant planets (EGP)—with one Jupiter mass ($1M_J$) and an age of 5 Gyrs (neglecting evolutionary effects). Furthermore the planet is assumed to be at orbital distances ranging from 0.2 to 15 AU (in order that the angular separation of the planet from the star is possible), and it orbits a main-sequence star of type G2V with solar metallicity.

First we give an overview of the necessary notions, then we describe the variation of the light-curve for different orbital elements. Following that the form of the light-curve at different wavelengths will be investigated, as well as the impact of clouds and small particles in the atmosphere.

Basic notions

The *phase angle* α is the angle in the plane observer-star-planet, whose vertex lies at the planet. This angle determines the brightness of an EGP, since the *planet/star flux ratio*

$$F_P/F_S = A_g \left(\frac{r}{a}\right)^2 \phi(\alpha) \quad (1)$$

depends on it via the *phase function* $\phi(\alpha) = E(\alpha)/E(0)$, where r is the planet's radius, a its orbital distance (semi-major axis), and

$$A_g = \frac{E(0)d^2}{\pi r^2 S} \quad (2)$$

the geometrical albedo (reflectivity of the planet at full phase $\alpha = 0$ compared to the incident flux S from the star onto a perfect disc of the same radius r).

For a light-curve over one orbital period of the planet one must solve the planet/star flux ratio for both A_g and $\phi(\alpha)$, which contain the function $E(\alpha)$ —the energy per second per unit area per unit solid angle received at phase α —which itself contains an integral over the reflection coefficient ρ that is depending on many parameters (e.g. temperature, pressure, wavelength, etc.). If we need the spherical albedo $A_s = qA_g$ one has to calculate the *phase integral*

$$q = 2 \int_0^\pi d\alpha \phi(\alpha) \sin \alpha \quad (3)$$

Variation of the Orbital Elements

The relation of the phase angle to the orbital elements is given by

$$\cos \alpha = \sin(\varphi + \omega) \sin(i) \sin(\Omega) - \cos(\Omega) \cos(\varphi + \omega) \quad (4)$$

where φ is the planet's orbital angle (or "true anomaly"), i the orbital inclination, ω the argument of periastron, and Ω the longitude of the ascending node.

By default Sudarsky et al. chose a highly inclined orbit of $i \geq 80^\circ$ ($i = 0^\circ$ means face-on, and $i = 90^\circ$ is edge-on), and $\Omega = 90^\circ$.

Most of the discovered exoplanets have non-vanishing eccentricities, and there are even some planets in highly eccentric orbits. In contrast to a light-curve for zero eccentricity ($e = 0$), the light-curves differ for an eccentric orbit, the symmetric shape is distorted to a sharp peak around the pericenter position. The maximum of the planet/star flux ratio does not appear for full-phase ($\alpha = 0$), as in the circular case. For a high eccentricity the planet appears to be brighter, due to the higher incident stellar flux, for $e = 0.6$ the planet appears three times brighter compared to $e = 0$.

Variation of the orbital inclination does affect the flux ratio, it is highest for nearly edge-on orbits, and the peak value is approximately three times higher than for face-on orbits. It is remarkable that for $i = 0$ and non-vanishing eccentricity there is still a variation in the flux ratio, because the planet's distance to the star changes.

The form of the light-curve and the position of the maximum for an elliptical orbit is shifted with varying Ω . The optimal value for this parameter would be $\Omega = 90^\circ$, for then the line of nodes would be perpendicular to the line of sight.

The value of the argument of periastron ω plays an important role for the maximum of the light-curve, since for $\omega = 90^\circ$ and not edge-on orientation the opposition of the planet takes place in the perihelion when its distance from the star is smallest, for $\omega = 270^\circ$ it is exactly the other way round.

Light-curves at different wavelengths

For a fixed value of $i = 80^\circ$ and circular orbits Sudarsky et al. (2005) investigated the change in the light-curve for different values of the semi-major axis and for different wavelengths. They included the formation of clouds by condensation if the atmospheric temperature drops below a certain value. They found that especially water and ammonia clouds play important roles for EGPs that are farther out than 2 AU, while for EGPs nearer than 1 AU these clouds cannot form, and all atmospheric constituents remain in gaseous form.

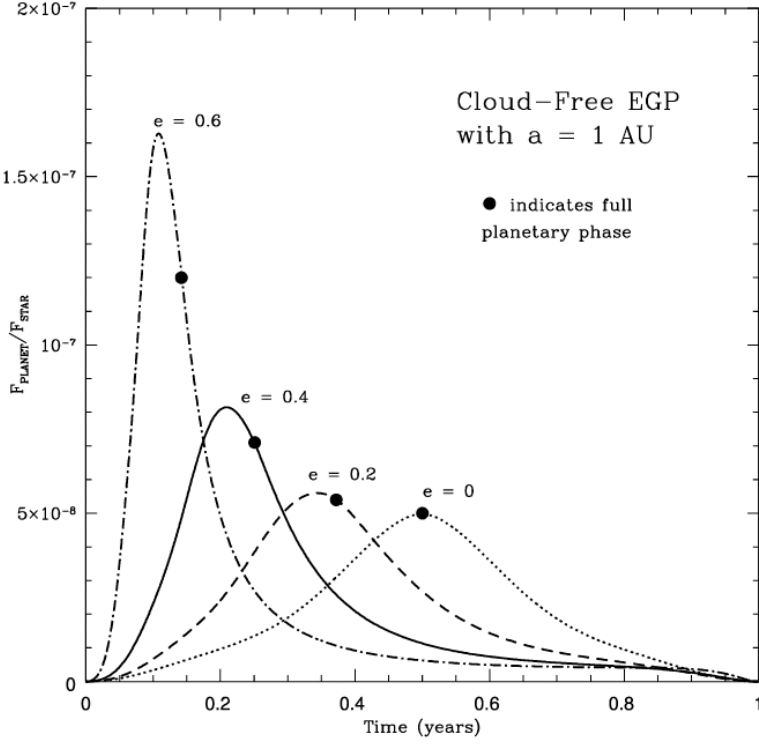


Figure 1: Variation of the light-curve for different values of the eccentricity (after Sudarsky et al. (2005), Figure 17).

In the simplest case the planet/star flux ratio would follow the $1/a^2$ law, that means that the flux ratio decreases with increasing orbital distance. In the models the behavior is different from that, the flux ratio is governed by different wavelengths at different distances. For close-in EGPs the near-infrared flux at $\lambda = 1.25\mu m$ dominates with a flux ratio of approximately 10^{-6} , partly due to thermal re-emission of the starlight, so that according to this the search of near but separable exoplanets should concentrate to the IR.

At a distance of 1 AU there is a change and the visible wavelengths become and remain predominant for all considered values up to $a = 15$ AU. Near EGPs around 1 AU are more luminous at $\lambda = 0.55\mu m$ than in the near infrared. In total there is a factor of nearly five between $\lambda = 0.55\mu m$ and $\lambda = 1.0\mu m$ for 1 AU; while this gap is smaller for a more distant EGP. With increasing

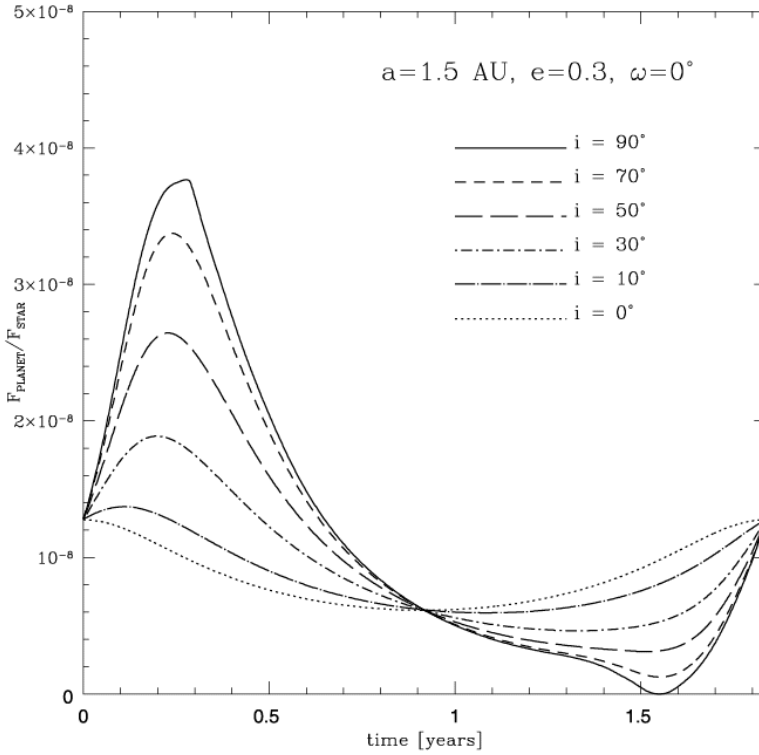


Figure 2: Variation of the light-curve for different orbital inclinations (after Sudarsky et al. (2005), Figure 20).

distance from the star the atmosphere of an EGP can undergo a change, and the formation of clouds—at first only water ice clouds in the upper atmosphere—brightens the EGP in the optical region. An EGP at 2 AU shows a planet/star flux that is about 50% of the corresponding flux for $\lambda = 0.55\mu m$ of the 1 AU planet, this is more than to expect for it without the effect of the clouds.

For even higher distances beyond $a > 6$ AU still the smaller wavelengths around $\lambda = 0.55\mu m$ dominate, and eventually ammonia ice clouds can form, with a deeper water ice cloud. The maximum planet/star flux is below 10^{-9} for $\lambda = 0.55\mu m$, and can be as low as 10^{-10} for very distant planets ($a = 10$ AU) in the IR ($\lambda = 1.0\mu m$). In general one has to expect that the IR-brightness is only about 20-40% of the optical brightness.

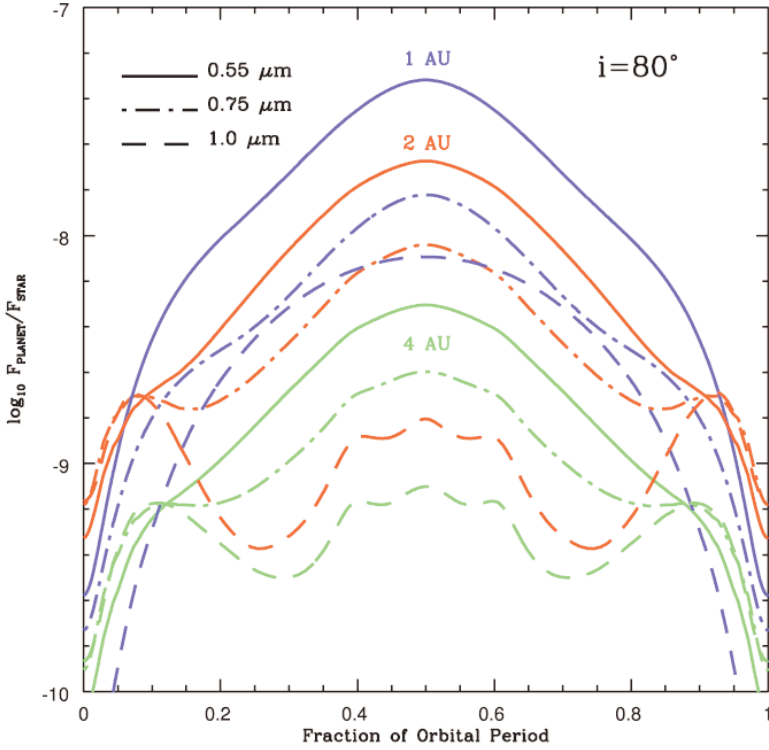


Figure 3: Variation of the light-curve for planets with different orbital distances, the dependence of the light-curve on the wavelength is also included (after Sudarsky et al. (2005), Figure 10).

Effect of particles and clouds

An EGP having clouds in its atmosphere is brighter in the optical spectral region, because of reflective Rayleigh scattering, an effect we also encounter in our Solar System.

Sometimes clouds can be a transient phenomena, provided that the EGP is on a highly eccentric orbit, it is possible that clouds form and dissolve whenever the EGP leaves the vicinity of the star or approaches it, respectively. The type of clouds (water, ammonia) plays an important role, too, as described above.

Grains and ice particles of different sizes can form at suitably low temperatures, but not at orbital distances below 2 AU, as found in the paper. From

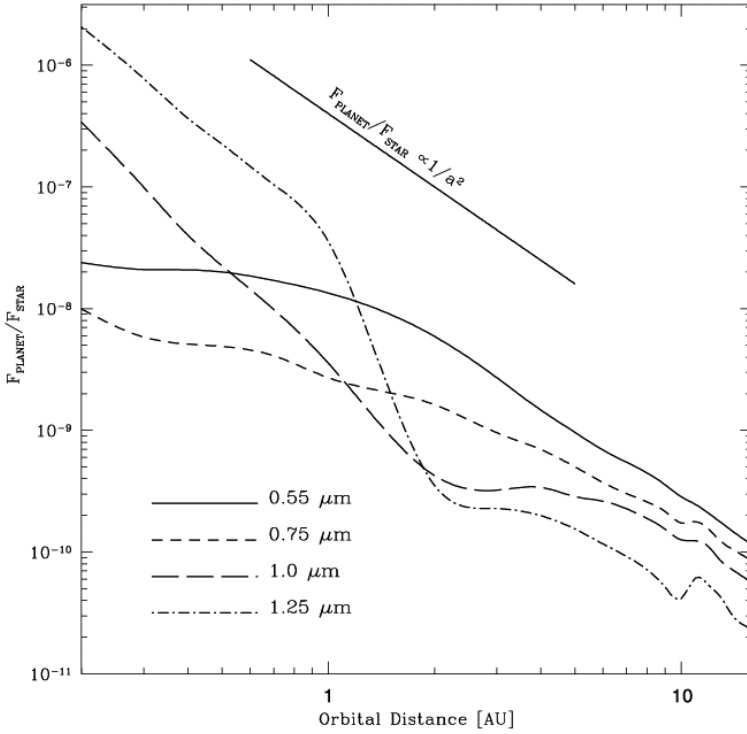


Figure 4: At different orbital distances the planet/star flux ratio is dominated by the near-IR wavelengths for close-in planets, while the flux in the visible region is increased by reflection and scattering for distances greater than 1 AU (after Sudarsky et al. (2005), Figure 12).

the viewpoint of scattering the smallest particles with diameters of about $1\mu\text{m}$ have the strongest effect on the light-curve, the planet/star flux ratio is increased by a factor of 2-4 compared to a cloudless planet (for λ in the range $0.55 - 0.75\mu\text{m}$), bigger particles up to $100\mu\text{m}$ diameter have less effect.

Summary and Conclusions

The main conclusions are the following

- The phase function of an EGP is strongly wavelength dependent, as well as the (geometrical or spherical) albedo and the phase integral, that rely

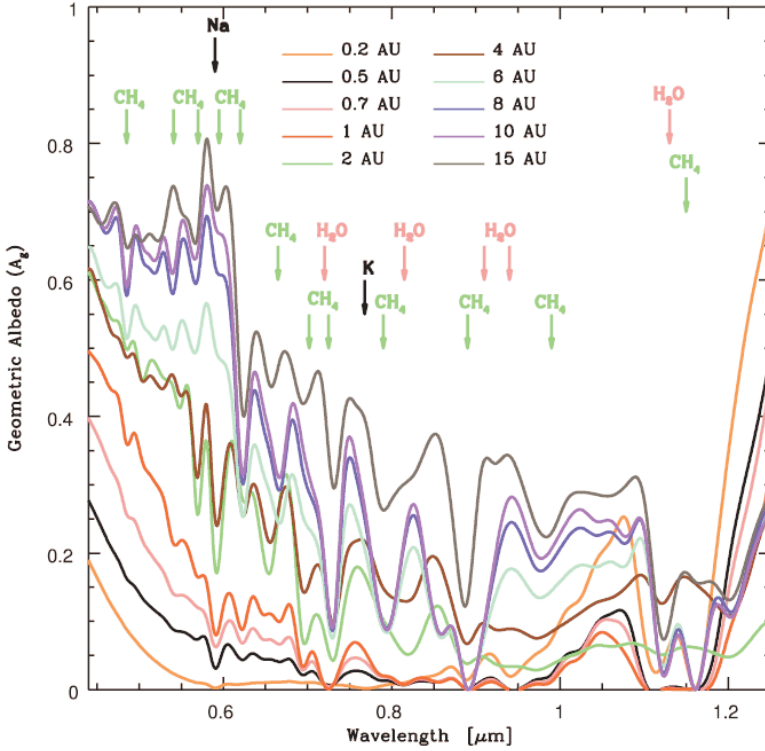


Figure 5: Geometric albedo in the region considered for wavelengths between $0.55 \mu\text{m}$ and $1.25 \mu\text{m}$. The maximum planet/star flux is below 10^{-9} for $\lambda = 0.55 \mu\text{m}$, and can be as low as 10^{-10} for very distant planets ($a = 10 \text{ AU}$) in the IR ($\lambda = 1.0 \mu\text{m}$). In general one has to expect that the IR-brightness is only about 20-40% of the optical brightness. (after Sudarsky et al. (2005), Figure 9).

on it. EGP's like those considered reflect more light in the optical than in the near infrared.

- Clouds consisting of small particles increase the planet/star flux ratio relative to that of EGP's with bigger particles or cloudless EGP's.
- In elliptical orbits EGP's exhibit higher flux ratios than for circular orbits, and the maximum of the light-curve does not coincide with full phase. Additionally for strongly eccentric orbits the atmospheric composition might change periodically, having an effect on the light-curve.

- EGPs with highly inclined orbits are generally brighter at full phase, and they should be best visible at full phase rather than at their greatest elongation, provided that the planet's orbit is not fully edge-on.
- For BRITE it will be difficult to observe a bright star surrounded by a close Gasgiant, because the number of bright stars in the Sun's vicinity with such a planet is – as far as we can estimate – quite small.

References

- Burrows, A., Budaj, J., Hubeny, I. 2007, astro-ph 0709.4080
Burrows, A., Sudarsky, D., Hubeny, I. 2004, ApJ, 609, 407
Hubbard, W.B., Fortney, J.J., Lunine, J.I., et al. 2001, ApJ, 560, 413
Rowe, J.F., Matthews, J.M., Seager, S. et al. 2006, ApJ, 646, 1241
Sudarsky, D., Burrows, A., Hubeny, I., et al. 2005, ApJ, 627, 520



The BRITE nanosatellite model.

Cluster and Association Members

E. Paunzen¹

¹ Institut für Astronomie, Türkenschanzstrasse 17, 1180 Vienna, Austria

Abstract

The selection of known members of star clusters as BRITE targets is highly preferable. The given apparent visual magnitude limit for the targets, can be immediately transformed into a distance limit of about 750 pc around the Sun depending on the absolute magnitude. For a spectral type of A0, we are, for example, limited to about 65 pc only.

With the help of WEBDA (<http://www.univie.ac.at/webda>), we have found 60 possible candidates which are true members of star clusters (including associations). The membership offers the opportunity to use the results from a detailed cluster analysis “for free”. This includes the determination of the age, the distance, the reddening, the overall metallicity and thus the mass with a high accuracy. These are very valuable starting parameters for any detailed astrophysical study of an individual object.

Star clusters - Why are they unique?

Open clusters and associations (denoted as “star clusters” in the following) are physically related groups of stars held together by mutual gravitational attraction. Therefore, they populate a limited region of space, which is typically much smaller than their distance from the Sun, so that the members are all approximately at the same distance. They are believed to originate from large cosmic gas and dust clouds (diffuse nebulae) in the Milky Way, and to continue to orbit the galaxy through the disk. In many clouds visible as bright diffuse nebulae, star formation still takes place, so that we can observe the birth of new young star clusters. This process of formation takes only a considerably short time (a few Myrs) compared to the lifetime of the cluster, so that all member stars are of similar age. Also, as all the stars in a cluster formed from the same diffuse nebula, they all have similar initial chemical composition. Hence, star clusters are of great interest for scientists:

- The cluster members are all at about the same distance from the Sun.

- They have the same age - within approximately a few million years - compared to the cluster age (up to a few billion years).
- The chemical composition of cluster members is quite homogeneous. Open cluster metallicities range from about -1.0 to $+0.6$ dex compared to the Sun.

The determination of distance, age and metallicity is, in general, not straightforward for galactic field stars. Star clusters on the other hand represent samples of stars of constant age and homogeneous chemical composition, suited for the study of processes linked to stellar structure and evolution. They allow to fix lines or loci in several important astrophysical diagrams such as the color-magnitude diagram (CMD), or the Hertzsprung-Russell diagram (HRD). Comparing the “standard” HRD, derived from nearby stars with sufficiently well known distances, or the theory of stellar evolution with the measured CMD of star clusters, provides a considerably good method to determine the distance of star clusters. Comparing their HRDs with stellar theory provides a reasonable way to estimate the age of star clusters.

BRITE target stars as members of star clusters

For a given apparent magnitude limit of targets stars ($V = 4$ mag) we can immediately calculate the distance limit for different absolute magnitudes. At maximum (not taking reddening into account) $M_V = -6$ mag (early O) we can reach 1000 pc whereas the distance significantly decreases to 65 pc for a star with $M_V = +0$ mag (A0).

With the help of WEBDA (<http://www.univie.ac.at/webda>), a highly efficient and successful database for the study of star clusters in the Milky Way and the Small Magellanic Cloud, it is possible to extract and retrieve all needed information. The database includes about 3.4 million individual measurements in most photometric systems in which cluster stars have been observed, spectroscopic observations, astrometric data, various kinds of supplementary information, and an extensive bibliography.

Taking a distance limit of 750 pc, we find in WEBDA about 220 star clusters which are closer than this value. Including the members of associations, we find about 60 *potential BRITE target stars* which are members of a star cluster.

Why to observe members of star clusters?

From kinematic (proper motions as well as radial velocities) and photometric studies we are able to establish the membership of a star to a corresponding

cluster quite accurately, especially if we take the rather close distance of our given regime into account. The proper motions, for example, are significant and can be measured with high accuracy. Several new catalogues on this topic are now available (e.g., Dias et al. 2006).

If we are able to establish the cluster membership of a BRITE target star, we get its age, distance, reddening as well as (to some extent) the overall metallicity and thus its mass “for free” from the cluster analysis. Such an analysis is always based on the isochrone fitting technique (Jørgensen & Lindegren 2005). Extensive grids of stellar tracks covering the most important evolutionary phases and a large metallicity range are available. This method is based on the knowledge of all members of the cluster making it statistically significant.

Recently, Paunzen & Netopil (2006) have summarized our current knowledge of the published cluster parameters (age, distance and reddening) on the basis of a statistical analysis. Taking their data set and restricting it to our sample volume, we find the following approximate accuracy limits according to the absolute values: $\Delta \log t \leq 15\%$, $\Delta d \leq 10\%$ and $\Delta E(B - V) \leq 5\%$. These errors can be still significantly decreased by an independent isochrone fitting procedure for each star cluster using all published and newly observed data.

Conclusions

It is preferable to observe members of star clusters (open clusters and associations) because we are able to a-priori determine their age, distance, reddening, overall metallicity and thus the mass with a high accuracy.

WEBDA, the database for star clusters will provide the already published data and an extensive number of tools to derive and extract all data and parameters.

Acknowledgments. This work was supported by the Fonds zur Förderung der wissenschaftlichen Forschung (P17580 and P17920) as well as by the Hochschuljubiläumsstiftung der Stadt Wien (H-1749/2006 WEBDA - Die Datenbank für offene Sternhaufen“)

References

- Dias, W.S., Assafin, M., Flório, V., et al. 2006, A&A 446, 949
- Jørgensen, B.R., Lindegren, L. 2005, A&A 436, 127
- Paunzen, E., Netopil, M. 2006, MNRAS 371, 1641

BRITE stars on the AGB

T. Lebzelter¹, J. Hron¹

¹ Institut für Astronomie, Türkenschanzstrasse 17, 1180 Vienna, Austria

Abstract

In this paper we evaluate the potential of the BRITE mission for investigations in the field of AGB stars.

Introduction

The Asymptotic Giant Branch (AGB) phase is a decisive step in final stellar evolution for stars of low and intermediate mass. It is characterized by low surface temperatures, huge stellar radii, high luminosity, variability of various origins and pronounced mass loss. These stars play an important role in the production of heavy elements and in the enrichment of the interstellar medium with these elements by effective mass loss. Their circumstellar environments are also the site of the production and growth of solid particles (dust). The complex nature of AGB stars requires several observational approaches in a broad wavelength range from visual photometry to mm interferometry and laboratory studies, e.g. of solid particles. A comprehensive review on AGB stars can be found in Habing & Olofsson (2003) or Kerschbaum et al. (2007).

At a first glance we would expect that AGB variables provide perfect targets for BRITE as they are among the intrinsically most luminous stars and are significantly more numerous than blue supergiants. Unfortunately the possibilities and needs are in fact limited as revealed by a more detailed look on their characteristics.

AGB stars and BRITE

AGB stars are cool, dusty and very unstable. They are thus not that bright in V , while they are the most luminous stellar sources in the infrared sky. Due to the dominant role of molecular features in their spectra the flux is strongly dependent on wavelength, so that for a description of the origin and nature of any observed variability several narrow passbands would be the preferred tool (e.g. Wing 1992 and references therein).

Table 1: List of potential targets from the General Catalogue of Variable Stars (Kholopov et al. 1985-88). Variability classes: M...mira, SRV...semiregular variable, Lb...irregular variable.

GCVS Name	V_{max}	V_{min}	Spectral type	Variability class
λ Aqr	3.70	3.80	M2	Lb
R Car	3.90	10.50	M6/M7	M
o Cet	2.00	10.10	M5-M9	M
χ Cyg	3.30	14.20	S7,1	M
τ^4 Eri	3.57	3.72	M3/M4	Lb
μ Gem	2.75	3.02	M3	Lb
R Hya	3.50	10.90	M6/M7	M
σ Lib	3.20	3.46	M3/M4	SRV
R Lyr	3.88	5.00	M5	SRV
β Peg	2.31	2.74	M2	Lb
ρ Per	3.30	4.00	M3	SRV
L ² Pup	2.60	6.20	M5	SRV

Variability of AGB stars is a phenomenon known since 400 years when the star o Cet (Mira) was discovered to be the first periodic variable star at all. The AGB variables are typically summarized in the class of long period variables, characterized by variability time scales from 30 to 1000 days and visual light amplitudes between 0.1 and 8 mag. Three subclasses were defined, namely miras (M), semiregular (SR) and irregular (L) variables, respectively. Recently, attempts can be seen to replace this old system of subclassification by a more meaningful classification according to the dominant pulsation mode (e.g. Wood 2000).

While the rather long time scales involved seem not to require a dense photometric coverage as provided by BRITE, the typical light amplitude limits the possibilities to study these stars with BRITE more severely. A typical mira with a light amplitude of several magnitudes becomes – at most – visible to BRITE only during a short phase around its maximum, most of the light cycle the star remains below the satellite's brightness limit. Miras are thus certainly not primary targets for BRITE. Table 1 gives a list of potential targets among the AGB stars applying a lower brightness limit of $V = 4$ mag. Note that all miras and some of the SRVs are clearly below this limit during minimum light.

Semi- and irregular variables are certainly a more interesting group of stars for a study with BRITE. Typical light curves can be seen e.g. in Kerschbaum et al. (2001). A proper description of the variability behaviour, which is essential for a complete understanding of the origin of the instability, requires a contin-

uous monitoring over a large number of light cycles (compare Lebzelter et al. 1995, Lebzelter & Kiss 2001). In this case the observing mode of BRITE can be extremely useful, filling also the seasonal gaps in photometric time series from automatic telescopes on the ground (Kerschbaum et al. 2001).

Another aspect of AGB star research may profit from BRITE. It is expected that only a few very large convective cells should cover the whole surface of an AGB star. Opposite to the small cells on the sun the rising and falling of these large cells should lead to clearly visible (up to 30%), irregular brightness variations on time scales between 0.3 and 1.5 years. First 3D simulations (e.g. Freytag et al. 2002) give results comparable to the irregular light variations observed in red supergiants. Variability due to convective cells may also be hidden in the light change of AGB variables. A second indication for surface inhomogeneities that should become visible in a high precision, continuous study comes from the observed asymmetric shapes of planetary nebulae, the product of an AGB star's heavy mass loss. It is suspected that these asymmetries result from spots, deviations from spherical symmetry of the AGB star or binarity (e.g. Soker & Hadar 2002).

Conclusions

We find that AGB stars as representatives of the intrinsically bright stellar objects are interesting targets for BRITE. However, the number of possible targets is rather small, including only about 10 SRVs/Lbs with the current brightness limit (including the two bright red supergiants – variability class SRC – α Ori and α Sco). To improve the situation and to increase the scientific outcome of the mission in the field of AGB stars we would favour the use of a redder (e.g. R , I) and more narrow pass band for the observations.

For the science cases we find first that the typical timescales of SRVs do not necessarily require a high sampling rate or high photometric precision. In principle the required monitoring could also be done from the ground. For irregular variables with their variations occurring partly on shorter time scales and with smaller light amplitudes a monitoring with BRITE may resolve the origin of their irregularity. Furthermore, in all AGB stars asymmetries and convective cells at the surface may leave signatures detectable with high precision, long time photometry. A synergy with ground based parallel interferometric imaging, which typically goes for the brightest objects, too, can be expected. For all these aspects BRITE can contribute significantly to our knowledge of the late evolutionary stages of solar like stars. However, as mentioned above, it will be critical to achieve a time series with a length of at least the length of the variability period, i.e. a few ten to a few hundred days of continuous measurements (with only a few data points per day). Finally, the COROT mission,

which also monitors a few AGB stars, may suggest further interesting aspects not considered up to now.

Acknowledgments. This work has been supported by the FWF through projects P18171-N02, P20046-N16 and P19503-N13, respectively.

References

- Freytag, B., Steffen, M., Dorch, B. 2002, AN, 323, 213
- Habing, H.J., Olofsson, H. (eds.) 2003, "Asymptotic Giant Branch Stars", Springer
- Kerschbaum, F., Lebzelter, T., Lazaro, C. 2001, A&A, 375, 527
- Kerschbaum, F., Charbonnel, C., Wing, R.F. (eds.) 2007, "Why Galaxies Care About AGB Stars", ASPC in press
- Kholopov, P.N., Samus, N.N., Frolov, M.S., et al. 1985-88, "General Catalogue of Variable Stars. 4th edition", Nauka Publishing House, Moscow
- Lebzelter, T., Kerschbaum, F., Hron, J. 1995, A&A, 298, 159
- Lebzelter, T., Kiss, L.L. 2001, A&A, 380, 388
- Soker, N., Hadar, R. 2002, MNRAS, 331, 731
- Wing, R.F. 1992, JAVSO, 21, 42
- Wood, P.R. 2000, PASA, 17, 18

List of Participants

Angela **Baier**, University of Vienna, Austria
baier@astro.univie.ac.at

Paul **Beck**, University of Vienna, Austria
beck@astro.univie.ac.at

Michel **Breger**, University of Vienna, Austria
breger@astro.univie.ac.at

Dieter **Breitschwerdt**, University of Vienna, Austria
breitschwerdt@astro.univie.ac.at

Jadwiga **Daszyńska-Daszkiewicz**, Wroclaw University, Poland
daszynska@astro.uni.wroc.pl

Ernst **Dorfi**, University of Vienna, Austria
dorfi@astro.univie.ac.at

Rudolf **Dvorak**, University of Vienna, Austria
dvorak@astro.univie.ac.at

Robert **Finsterbusch**, Technical University Graz, Austria
robert.finsterbusch@joanneum.at

Michael **Fischer**, Technical University Vienna, Austria
michael.fischer@tuwien.ac.at

Barbara **Funk**, University of Vienna, Austria
funk@astro.univie.ac.at

Michaela **Gitsch**, FFG /ALR, Austria
michaela.gitsch@ffg.at

Cordell **Grant**, University of Toronto, Canada
cgrant@utias-sfl.net

Michael **Gruberbauer**, University of Vienna, Austria
gruberbauer@astro.univie.ac.at

Elisabeth **Guggenberger**, University of Vienna, Austria
guggenberger@astro.univie.ac.at

Gerald **Handler**, University of Vienna, Austria
handler@astro.univie.ac.at

Markus **Hareter**, University of Vienna, Austria
hareter@astro.univie.ac.at

Josef **Hron**, University of Vienna, Austria
hron@astro.univie.ac.at

Daniel **Huber**, University of Vienna, Austria
huber@astro.univie.ac.at

Bruno **Josseck**, University of Graz, Austria
bruno.josseck@tugraz.at

Alexander **Kaiser**, University of Vienna, Austria
kaiser@astro.univie.ac.at

Thomas **Kallinger**, University of Vienna, Austria
kallinger@astro.univie.ac.at

Werner **Keim**, Siemens Austria
keim.werner@siemens.com

Otto **Koudelka**, University of Graz, Austria
koudelka@TUGraz.at

Viktor **Kudielka**, Technical University Vienna, Austria
viktor.kudielka@ieee.org

Rainer **Kuschnig**, University of British Columbia, Canada
kuschnig@astro.ubc.ca

Thomas **Lebzelter**, University of Vienna, Austria
lebzelter@astro.univie.ac.at

Christoph **Lhotka**, University of Vienna, Austria
lhotka@astro.univie.ac.at

Theresa **Lüftinger**, University of Vienna, Austria
lueftinger@astro.univie.ac.at

Andreas **Merdonig**, Technical University Graz, Austria
andreas.merdonig@TUGraz.at

Stefan **Mochnacki**, University of Toronto, Canada
stefan@lepus.astro.utoronto.ca

Richard **Neuteufel**, University of Vienna, Austria
neuteufel@astro.univie.ac.at

Marlene **Obbrugger**, University of Vienna, Austria
obbrugger@astro.univie.ac.at

Jürgen **Öhlinger**, University of Vienna, Austria
oehlinger@astro.univie.ac.at

Ernst **Paunzen**, University of Vienna, Austria
ernst.paunzen@univie.ac.at

Lena **Schneider**, University of Vienna, Austria
schneider@astro.univie.ac.at

Arpad **Scholtz**, Technical University Vienna, Austria
arpad.scholtz@tuwien.ac.at

Peter **Schrotter**, Technical University Graz, Austria
peter.schrotter@tugraz.at

Alexander **Stökl**, École Normale Supérieure de Lyon, France
stoekl@astro.univie.ac.at

Klaus G. **Strassmeier**, Astrophys. Institute Potsdam, Germany
kstrassmeier@aip.de

Manuela **Unterberger**, University of Graz, Austria
manuela.unterberger@tugraz.at

Nicolas **Valavanoglou**, Technical University Graz, Austria
valavanoglou@tugraz.at

Werner W. **Weiss**, University of Vienna, Austria
weiss@astro.univie.ac.at

Konstanze **Zwintz**, University of Vienna, Austria
zwintz@astro.univie.ac.at



The audience during the BRITE Workshop.